CalVal altimétrie/marégraphie

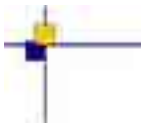

Validation of altimetric data by comparison with tide gauge measurements

for TOPEX/Poseidon, Jason-1 and Envisat

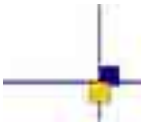

Reference : CLS.DOS/NT/09-115

Nomenclature : SALP-NT-MA-EA-21691-CLS

Issue : 1rev 1

Date : 15 juin 2010

SALP Service Altimetrie & Localisation Precise

CLS Collecte Localisation Satellites

cnes Centre National d'Études Spatiales

CLS - 8-10 Rue Hermès - Parc Technologique du Canal - 31520 Ramonville St-Agne - FRANCE
Telephone 33 5 61 39 47 00 / Fax 33 5 61 75 10 14

Chronology Issues :		
Issue :	Date :	Reason for change :
1.0	22 January 2010	Creation
1.1	15 June 2010	Update

People involved in this issue :		
Written by :	G. Valladeau M. Ablain	CLS CLS
Checked by :	DT/AQM	CLS
Approved by :	JP. Dumont	CLS
Application authorized by :		

Index Sheet :	
Context :	
Keywords :	
Hyperlink :	

Proprietary information : no part of this document may be reproduced divulged or used in any form without prior permission from CLS and CNES.

Distribution :		
Company	Means of distribution	Names
CLS/DOS	1 electronic copy	G.DIBARBOURE
	1 electronic copy	B.SOUSSI
	1 electronic copy	F.LEFEVRE
	1 electronic copy	V.ROSMORDUC
	1 electronic copy	P.ESCUDIER
	1 electronic copy	J.DORANDEU
DOC/CLS	1 electronic copy	DOCUMENTATION
CNES	1 cd-rom	T.GUINLE
CNES	1 cd-rom	T.AL ARISS
CNES	1 cd-rom	T.CORREALE
CNES	1 electronic copy	E.BRONNER
CNES	1 electronic copy	J.LAMBIN
CNES	1 electronic copy	A.LOMBARD
CNES	1 electronic copy	N.PICOT
ESA	1 electronic copy	P.FEMENIAS

Proprietary information : no part of this document may be reproduced divulged or used in any form without prior permission from CLS and CNES.

List of tables and figures

Liste des tableaux

1 *Corrections applied for altimetric SSH calculation* . . . 36

Table des figures

1 *Location of the tide gauges. Top left : GLOSS/CLIVAR. Top right : SONEL (green) , OPPE (blue) and BODC (red). Bottom : IMEDEA* . . . 3
2 *Bias estimation between RA-2 and in-situ measurement* . . . 7
3 *Monitoring of altimeter/in-situ SSH differences with both methods of reference bias calculation. Top left : Jason-1, top right : T/P, bottom : Envisat.* . . . 9
4 *Altimeter/in-situ SSH differences standard deviation with both methods of reference bias calculation. Top left : Jason-1, top right : T/P, bottom : Envisat* . . . 10
5 *Cycle by cycle monitoring of raw mean SLA differences between TOPEX/Poseidon and tide gauge measurements. Left : with Poseidon cycles. Right : Poseidon data have been removed* . . . 13
6 *Cycle by cycle monitoring of standard deviation SLA differences between TOPEX and tide gauge measurements* . . . 14
7 *Cycle by cycle monitoring of number of tide gauges considered on the whole TOPEX/Poseidon space mission* . . . 15
8 *Cycle by cycle monitoring of mean SLA differences between Jason-1 and tide gauge measurements* . . . 16
9 *Cycle by cycle monitoring of standard deviation SLA differences between Jason-1 and tide gauge measurements* . . . 17
10 *Left : cycle by cycle monitoring of mean SLA differences between Envisat and tide gauge measurements. Right : variance differences between SSHs using the coastal editing flag and basic editing flag with regard to tide gauge measurements* . . . 18
11 *Cycle by cycle monitoring of colocated mean of altimeter SLA for Jason-1 and Envisat* 19
12 *Cycle by cycle monitoring of standard deviation SLA differences between Envisat and tide gauge measurements* . . . 19
13 *Histograms of SLA variance differences between altimeter and in-situ data using successively GOT4.7 and GOT00V2 tide models. Top left : TOPEX/Poseidon, top right : Jason-1, bottom : Envisat* . . . 22
14 *Differences of SLA variance differences between altimeter and in-situ data using successively basic and coastal editing flag. Left : Jason-1, right : Envisat* . . . 23
15 *Monitoring of SSH variance differences computed with GDR-C and GDR-B for Jason-1 (cm^2)* . . . 24
16 *Impact of the new 2-parameters Sea State Bias computed with Gourrion's wind on the monitoring of the mean altimeter/in-situ tide gauge differences. Left : Old SSB (Chelton's wind). Right : New SSB (Gourrion's wind)* . . . 25
17 *Monitoring of SSH variance differences computed with GDR-C and GDR-B for TOPEX/Poseidon (cm^2)* . . . 25
18 *Example of an information card for the Kwajalei tide gauge* . . . 27
19 *Availability on tide gauge information cards on the AVISO website* . . . 28
20 *General operating diagram of the tide gauge data processing sequence* . . . 32

Proprietary information : no part of this document may be reproduced divulged or used in any form without prior permission from CLS and CNES.

List of items to be defined or to be confirmed

Applicable documents / reference documents

Proprietary information : no part of this document may be reproduced divulged or used in any form without prior permission from CLS and CNES.

Table des matières

1. Introduction - Document overview **1**

2. Presentation of the tidal database **2**
2.1. **Overview** . . . 2
2.2. **Origin** . . . 2
2.3. **Data availability** . . . 4
2.4. **Developments and improvements of the current release** . . . 5
2.4.1. Selection of relevant time series . . . 5

3. Description of the altimeter/tide gauges comparison procedure **6**
3.1. **Overview** . . . 6
3.2. **Pre-processing of the altimetric and in-situ tide gauge sea surface heights** 6
3.2.1. Calculation of the altimetric sea surface height . . . 6
3.2.2. Calculation of the in-situ sea surface height . . . 7
3.3. **Computation of the potential relative bias** . . . 7
3.4. **Sequence of the altimeter/tide gauges comparison procedure** . . . 8
3.4.1. Selection of altimetric and tide gauges data . . . 8
3.4.2. Editing of altimetric and in-situ data . . . 8
3.4.3. Improvement of the computation of the global reference bias . . . 8
3.4.4. Correction of vertical movements on tide gauges . . . 10
3.4.5. Monitorings of SSH bias between altimetric and in-situ-data . . . 11

4. Analysis of potential drifts or jumps in altimeter MSL **12**
4.1. **Overview** . . . 12
4.2. **Analyses for each altimetric mission** . . . 12
4.2.1. TOPEX/Poseidon . . . 12
4.2.2. Jason-1 . . . 15
4.2.3. Envisat . . . 17

5. Estimation of altimetric SSH improvements **20**
5.1. **Overview** . . . 20
5.2. **Impact of new GOT4.7 tidal model correction** . . . 21
5.3. **Impact of the coastal editing flag on altimeter/in-situ SLA consistency** . . 22
5.4. **Impact of the GDR-C reprocessing on altimeter/in-situ SLA consistency** 23
5.5. **Impact of new Sea State Bias (SSB) correction on TOPEX/Poseidon** . . . 24

6. Quality assessment of in-situ tide gauge time series **26**
6.1. **Presentation of the tide gauge information cards** . . . 26
6.2. **Availability of tide gauge information cards** . . . 28

7. Conclusion **29**

8. References **31**

9. Annexes **32**
9.1. **Annex : General operating diagram** . . . 32
9.2. **Annex : OceanObs'09 poster** . . . 33
9.3. **Annex : Corrections applied for altimetric SSH calculation** . . . 35
9.4. **Annex : Information cards for the Rodrigue and Cocos Island tide gauges** 37

Proprietary information : no part of this document may be reproduced divulged or used in any form without prior permission from CLS and CNES.

9.5. **Annex : Jason-1 global monitoring report** 40

Proprietary information : no part of this document may be reproduced divulged or used in any form without prior permission from CLS and CNES.

1. Introduction - Document overview

This document is the synthesis report for 2009 concerning altimeter/in-situ validation activities which aims at comparing altimetric data with measurements provided by tide gauges. This activity is supported by the CNES in the frame of the SALP contract (package 2-C) for the whole altimeter missions but also by the ESA as a support for the ESA EOM-ADQ RA-2 and MWR activities in the frame of the ENVISAT Phase E.

The interest of using in-situ measurements to validate altimetric data is on the one hand a way to detect potential jumps or drifts in the Mean Seal Level (MSL) evolutions, which is one of the main indicators for climate warming studies. On the other hand, the comparison of altimetric data with external and independent measurements is useful to measure the sea surface height (SSH) consistency in order to detect anomalies or to measure improvements of new altimeter standards (correction, orbit, ...).
A third purpose of this activity has been developed during this year and concerns the quality control of the in-situ measurements used thanks to the whole altimetric time series available on each tide gauge time period.

Results presented in this document are thus a synthesis of the different goals that have been reached during 2009. Firstly, the document describes the tide gauges database used for this study and the way they are computed in order to make them comparable to altimetric SSH. The tide gauge networks used and the data availability are precisely described, especially for the new networks added in the database in 2009. New corrections used in the in-situ SSH calculation is also specified.

Then the document details the method developed to compare altimetric data and tide gauge measurements. Some improvements have been developed in 2009 and the method will present the way of using the quality control performed on in-situ measurements to remove spurious tide gauges. Basically, this method is based on a multi-cross-calibration between tide gauge measurements and all altimeter time series available in order to detect potential jumps or abnormal drifts in tide gauge SSH evolutions.

The third part of the report points out the main results concerning the detection of altimeter MSL drift. It gets onto multi-mission analysis for the three main altimetric missions TOPEX/Poseidon, Jason-1 and Envisat. The analyses are performed taking into account the in-situ quality control flag improved this year. The accuracy of this method to estimate the altimeter MSL trend is then discussed.

As mentioned, an other objective of this method is the analysis of the SSH consistency in order to evaluate the new altimetric standard improvements for the SSH calculation. In 2009, the comparison procedure of new altimetric standards has been completed with spatial diagnostics, especially through variance differences histograms. Some studies performed in the frame of the SLOOP project, the Jason-1 GDR-C reprocessing or the TOPEX/Poseidon SSH computation have been performed in order to measure these improvements. They concern the improvements of the coastal editing flag, the Jason-1 GDR-B/GDR-C data, the ionospheric correction and the sea state bias correction.

Proprietary information : no part of this document may be reproduced divulged or used in any form without prior permission from CLS and CNES.

2. Presentation of the tidal database

2.1. Overview

The tidal database consists in records of tide gauge Sea Surface Height (SSH) from independent networks. Several types of geophysical corrections such as tide, pressure and wind effects are then applied on these raw data so as to deduce filtered Sea Level Anomalies (SLA) from high frequency phenomena in order to be consistent with altimetric data. The comparison between altimetric data and tide gauge measurements is thus made possible thanks to this tidal database and softwares dedicated to its computation. This section details the way of manipulating tide gauge measurements.

2.2. Origin

Last year, the tidal database consisted in 4 different tide gauge networks (GLOSS/CLIVAR, SONEL, OPPE and BODC) which resulted from different collaborations. During 2009, in the frame of the SLOOP project, the CLS in-situ database has been enhanced thanks to the IMEDEA institute tide gauge network, which consists in 48 tide gauges in the Mediterranean Sea. The goal of such tide gauges is not only to improve the in-situ spatial sampling to detect altimetric drifts or jumps but the interest of a dense network to study impacts of new altimeter standards locally, such as in the Mediterranean Sea.

Here are the details of the networks computed in the CLS database (figure 1) :

- GLOSS/CLIVAR (Global Sea Level Observing System/Climate Variability and Predictability) "fast" sea level data : this network provides 257 tide gauges gathered by the University of Hawaii Sea Level Center (USHLC) and updated within a few weeks or a few months (*ilikai.soest.hawaii.edu/uhslc*), which is 37 more tide gauges comparing to 2008.

- SONEL (Système d'Observation du Niveau des Eaux Littorales) : this network consists in 30 tide gauges which major part is set on the french shoreline (*www.sonel.org*)

- BODC (British Oceanographic Data Centre) : 42 UK tide gauges of this network, which are held by the Permanent Service for Mean Sea Level (PSMSL), are computed in the tidal database (*www.bodc.ac.uk*)

- OPPE (Organismo Público de Puertos del Estado) : 19 of these tide gauges are built in the CLS database, which uniformly samples spanish coasts (*www.puertos.es*)

- IMEDEA (Mediterranean Institute for Advanced Studies) : 48 tide gauges widespread in the Mediterranean Sea are routinely computed in the CLS in-situ tide gauge database (*www.imedea.uib.es*)

Proprietary information : no part of this document may be reproduced divulged or used in any form without prior permission from CLS and CNES.

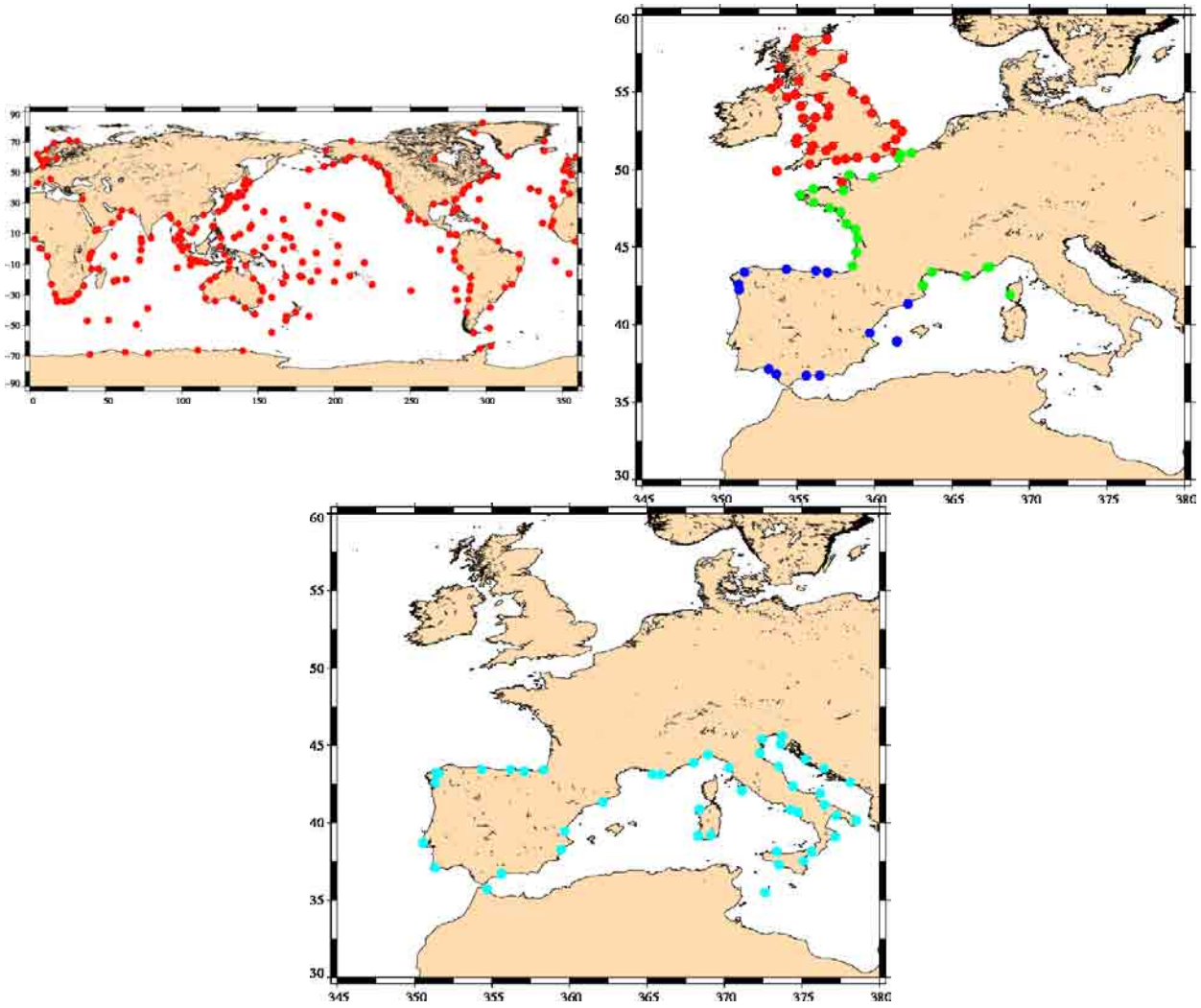

FIG. 1 – *Location of the tide gauges. Top left : GLOSS/CLIVAR. Top right : SONEL (green) , OPPE (blue) and BODC (red). Bottom : IMEDEA*

Proprietary information : no part of this document may be reproduced divulged or used in any form without prior permission from CLS and CNES.

2.3. Data availability

For the whole tidal networks, hourly data are computed and archived according to a linear procedure :

- 1. Weekly download of the updated data
- 2. Conversion from the original-sized data to the CLS-sized data (in-situ measurements tables) with several steps of validations
- 3. High frequency tidal waves filtering (diurnal and semi-diurnal tides) by a specific algorithm based on the Demerliac low-pass filter [Bessero, 1985]
- 4. Long-time tidal waves filtering by a specific algorithm based on well-balanced tide tables [Cartwright and Eden, 1973]
- 5. Withdrawal of the high frequency Dynamical Atmospheric Correction (DAC) [Dorandeu and Le Traon, 1999, Carrere and Lyard, 2003]

By the means of "in-situ measurements tables" specific format, SSH measured by tide gauges can be filtered from high frequency phenomena quoted above.

Here are the main fields recorded into in-situ measurements tables :

- 1. raw data
- 2. tide filtered data (semi-diurnal, diurnal and long period constituent)
- 3. tide filtered and improved inverse barometer corrected data
- 4. tide filtered and high frequency MOG2D corrected data

The tidal database is updated every week according to the availability of new tide gauge measurements. Note that in 2009 the high resolution MOG2D correction has been introduced in the in-situ measurements tables. This correction was studied with regard to the low resolution itself and improves results at tide gauge locations (not shown).

Proprietary information : no part of this document may be reproduced divulged or used in any form without prior permission from CLS and CNES.

2.4. Developments and improvements of the current release

2.4.1. Selection of relevant time series

Another major improvement in the tidal database is related to the in-situ time series themselves. Thanks to recent studies on in-situ datasets, we discovered that some tide gauge time series don't provide the physical state of the ocean. This can originate in works or fixes on tide gauges or non-material phenomena like animal actions. Several tide gauge time series are thus not used in the data processing sequence and solutions are being looked to compute the whole tidal database in the process.
To detect these potential problems on tide gauges :

- a cross-comparison with each altimeter time series is performed for each tide gauge. The multi-cross-calibration is necessary to determine which instrument (altimeter or beacon) is the most reliable on each time period at each tide gauge location. Thus, when altimeter data are consistent with each other, this means that there may be a problem on the in-situ measurement. The cross-comparison is able to provide a quality control on each tide gauge used for each altimeter mission.

- tide gauges are removed if a jump or a strong drift is clearly observed only.

In order to automate the detection of these anomalies, we performed tide gauge identification cards, which 2 examples are following (see annex) :

- For the Pohnpei tide gauge, no abnormal anomalies is detected. This tide gauge can thus be used in the process.

- For the Valparaiso tide gauge, a jump is detected at the end of the time period thanks to Jason-1 and Envisat altimeter data. Thus this tide gauge is not used in the cross-comparison.

During this year numerous improvements have been performed on the tide gauge quality control as it is useful for different projects such as the Altika space mission to determine an absolute calibration site. In the future, the aim will be to look for and correct jumps detected in tide gauges time series (thanks to all altimeter time series available) in order to increase the valid tide gauge number used in the altimeter/tide gauge cross-comparison. As these part of this activity has been improved this year, investigations about monitorings and correlations are further discussed in part 6.

Proprietary information : no part of this document may be reproduced divulged or used in any form without prior permission from CLS and CNES.

3. Description of the altimeter/tide gauges comparison procedure

3.1. Overview

The main goal of this activity is to compare altimetric and in-situ tide gauge sea level anomalies. To make this comparison possible, sea surface height measurements have first to be processed (annex). The physical content of tide gauge and altimetric measurements are not completely equivalent. Both datasets have thus to be pre-processed before comparing each other. The physical principle of tide gauge/altimetric comparison is displayed in figure 2. It highlights 3 sources of discrepancies between both datasets :

- The SSH reference is not the same since tide gauge measurements have been already referenced to a mean sea surface (MSS). Thus the MSS has to be removed from altimetric SSH.
- Oceanic tidal effects have to be corrected on altimetric and tide gauge data since measurements are not located exactly in the same place. Concerning altimetric measurements, an ocean tide model is applied (GOT00 for instance), whereas dedicated filters are applied for tide gauge data in order to remove the short and long tide wavelengths (diurnal, semi-diurnal and long period tides).
- Atmospheric effects have also to be corrected for the same reason applying on the first hand a dynamical atmospheric correction (MOG2D model) for altimetric measurements and on the second hand a dedicated filter for tide gauge data in order to remove high frequency signals.
- Finally, sea level anomalies are compared between altimetric and in-situ data.

3.2. Pre-processing of the altimetric and in-situ tide gauge sea surface heights

A pre-processing is thus performed on altimetric and in-situ tide gauge sea surface heights so as to compare each other.

3.2.1. Calculation of the altimetric sea surface height

The sea surface height (SSH) calculation is defined below :

$$SSH = Orbit - Altimeter\ Range - \sum_{i=1}^{n} Correction_i - Mean\ Sea\ Surface$$

The mean sea surface used is the CLS2001 Mean Sea Surface model [Hernandez and Schaeffer, 2001] and the usual corrections are the following :

$$\begin{aligned}\sum_{i=1}^{n} Correction_i \;=\; & Dry\ troposphere\ correction : new\ S1\ and\ S2\ atmospheric\ tides\ applied \\ + \; & Combined\ atmospheric\ correction :\ MOG2D\ and\ inverse\ barometer \\ + \; & wet\ troposphere\ correction\ coming\ from\ ECMWF\ model \\ + \; & Filtered\ dual\ frequency\ ionospheric\ correction \\ + \; & Non\ parametric\ sea\ state\ bias\ correction\end{aligned}$$

Proprietary information : no part of this document may be reproduced divulged or used in any form without prior permission from CLS and CNES.

+ *Geocentric ocean tide height, GOT* 2000 : *S*1 *atmospheric tide is applied*[*Ray*, 1999]
+ *Solid earth tide height*
+ *Geocentric pole tide height*

Generally, the same corrections are applied for each mission but there are some exceptions due to instrumental anomalies on satellites or the unavailability of geophysical models (at the beginning of TOPEX/Poseidon for instance). The different SSH formula used for each altimetric mission are presented in annex for TOPEX/Poseidon, Jason-1, Envisat, Geosat Follow-On and ERS-2.

3.2.2. Calculation of the in-situ sea surface height

The assessment of in-situ sea surface height is almost the same one as previously. However, since potential bias are searched out, there's no need to have an absolute reference frame for tide gauges. It is simply necessary to remove geophysical and atmospheric effects from in-situ measurements in order to stay consistent with altimetric data. This is almost immediate starting from in-situ time series :

- By developing specific tide filters so as to remove short wavelengths phenomena (diurnal, semi diurnal tides and short-time atmospheric effects)
- By carrying out an algorithm of long period time series or low frequency tide withdrawal (from one week to one year in term of wavelength)

3.3. Computation of the potential relative bias

From all these corrections, the altimetric drift can be calculated as presented below :

Bias = ΔAltimeter - ΔTide Gauge (+/- errors on models, corrections and measurements)

Figure 2 presents the general diagram used for the Envisat RA-2 altimeter.

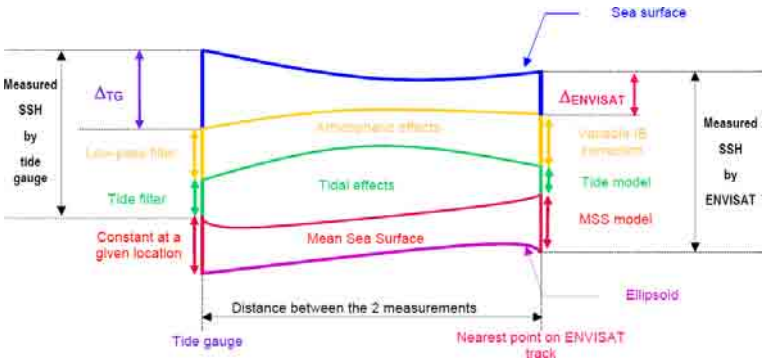

FIG. 2 – *Bias estimation between RA-2 and in-situ measurement*

Since relative bias between altimetric and tide gauges data are searched out, there is no use mastering the Mean Sea Surface (MSS) at the location of the tide gauge. Indeed, whereas the MSS differs on the four closest altimeter tracks at each cycle (as the selected altimeter points are different), this one is constant considering the tide gauge.

Proprietary information : no part of this document may be reproduced divulged or used in any form without prior permission from CLS and CNES.

3.4. Sequence of the altimeter/tide gauges comparison procedure

The method consists in estimating sea level on altimetric tracks at the closest locations of a given tide gauge. It is composed of several steps which are described here.

3.4.1. Selection of altimetric and tide gauges data

The first step of the comparison procedure is related to the space and time altimetric and tide gauges data selection. Tide gauges are first selected in relation to the period studied. They have to cover the altimetric data period over 2 years at least. All quality controlled tide gauges which don't check this criteria are not used. Then altimetric data with a valid SSH content are selected over each satellite pass close to the selected tide gauges. Only closest measurements according to a distance criteria of 160 km are stored, which enables to get at least one measurement on the closest altimeter track for each space mission.
The associated SSH is computed for the selected altimetric measurements. In order to be able to compute differences between altimetric and in-situ tide gauge measurements, a linear interpolation is then realised on in-situ data at the altimetric dates.

3.4.2. Editing of altimetric and in-situ data

The following step is the editing of altimetric and in-situ data. The purpose of this editing procedure is to perform some additional "quality" controls on each altimetric and in-situ dataset.

These controls are directed around two main axes : the consistency and the relevance of the following statistics performed on results. Concerning the consistency, criteria used are the minimum of correlation between tide gauges and altimetric track time series (Mitchum specified it to 0.3) and the maximum RMS of the bias from the linear regression straight line.
As regards to the relevance of the statistics, two criteria are also defined : the minimum number of points of an altimetric track to take it in account (in percentage of the number of cycles to be computed) and the number of the closest tracks to a given tide gauge selected. Indeed, the closest the tracks are, the better the estimate of the bias between altimetric and in-situ tide gauge data will be.

Statistics on these "valid" results are then performed so as to determine potential drifts between altimetric data and in-situ tide gauge measurements.

3.4.3. Improvement of the computation of the global reference bias

As explained in previous annual reports, tide gauges are not referenced to the same mean sea surface. Investigations on altimeter/tide gauges SSH comparisons have leaded this year to consider the global reference bias for each tide gauge with regard to the colocated altimeter data. Indeed, in the frame of altimetric/in-situ difference monitoring, tide gauge measurements can be offset on the Mean Sea Surface (MSS) used in the altimeter SSH computation. The main effect of the computation of this reference bias is to improve the consistency between both SSH and thus to better estimate potential drifts or jumps in the altimetric measurements.

In this way, for each tide gauge time series both altimeter and in-situ time series which cover the

Proprietary information : no part of this document may be reproduced divulged or used in any form without prior permission from CLS and CNES.

whole studied period are averaged on the latter. The difference between these two values lead to a specific reference bias for the tide gauge considered. Thus, the reference bias is computed with regard to the corresponding altimeter/in-situ time period, which make it precise and allow us to get an accurate estimate of the SSH differences.

Figure 3 displays drifts of SSH differences for Jason-1, T/P and Envisat missions with the old and new reference bias.
Thanks to such method, the differences SSH trends seems to be more accurate and the formal adjustment error is weaker. In particular, this is underlined in the three main missions Jason-1, TOPEX,Poseidon and Envisat, which latter trend is reduced from 0.7 mm/year and its formal adjustment error of 0.07 mm/year.

Second point, the standard deviation of SSH differences is also improved thanks to the new computation of the global reference bias, which seems to be consistent with the fact that both SSHs are now compared from the same reference.Thus, figure 4 displays means of SSH differences standard deviation for Jason-1, TOPEX/Poseidon and Envisat missions with the old and new reference bias. As we can see, the standard deviation of SSH differences is enhanced by 1.3 cm for Jason-1 and Envisat while it is 0.4 cm for TOPEX/Poseidon. As measurements are more consistent, this argues in more reliable results when detecting trends in altimetric data thanks to tide gauge measurements.

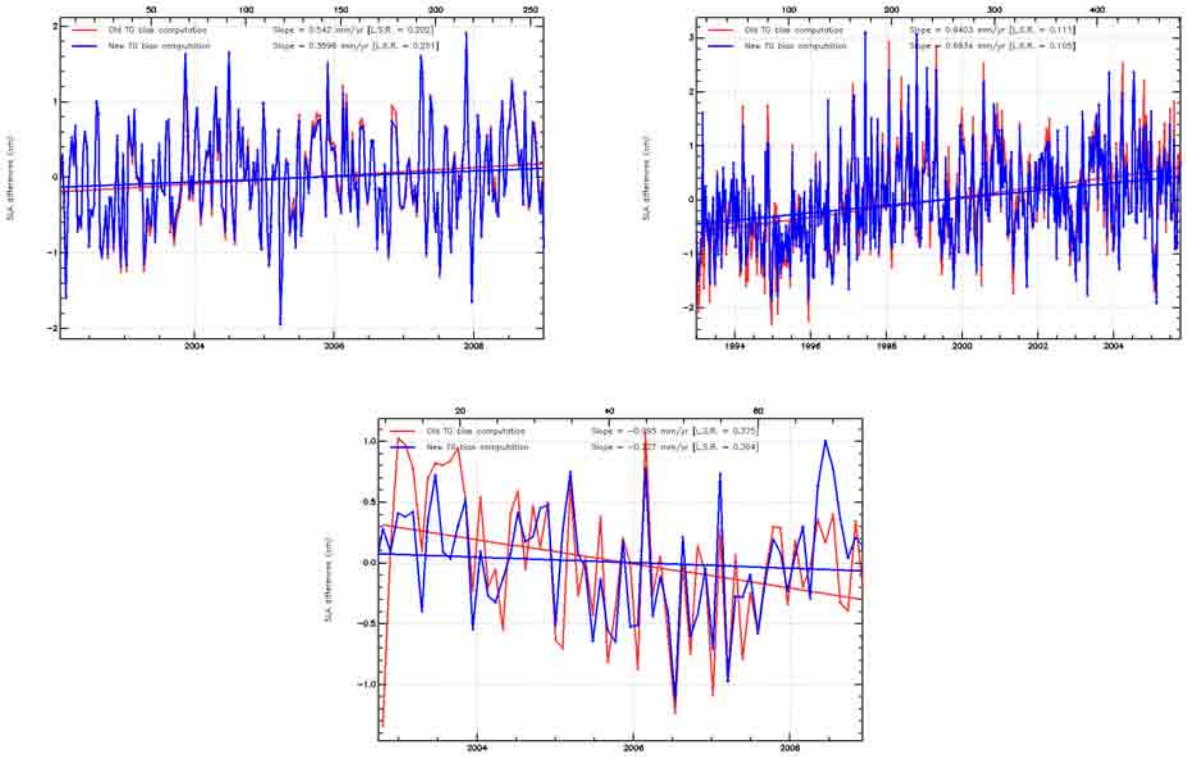

FIG. 3 – *Monitoring of altimeter/in-situ SSH differences with both methods of reference bias calculation. Top left : Jason-1, top right : T/P, bottom : Envisat.*

Proprietary information : no part of this document may be reproduced divulged or used in any form without prior permission from CLS and CNES.

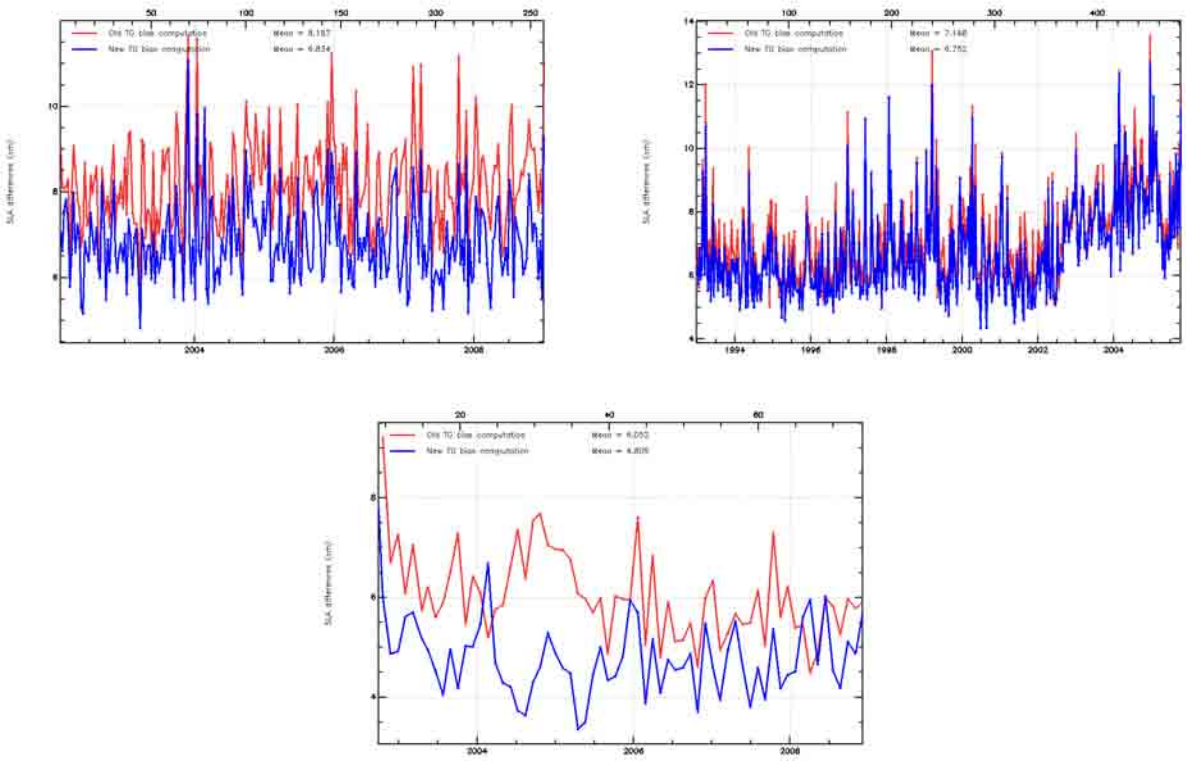

FIG. 4 – *Altimeter/in-situ SSH differences standard deviation with both methods of reference bias calculation. Top left : Jason-1, top right : T/P, bottom : Envisat*

3.4.4. Correction of vertical movements on tide gauges

Note that the main goal of the database presented above is the comparison with altimetric measurements. To estimate the rate of global sea level rise, two problems have to be taken into account when using tide gauges. The first is the fact that tide gauges measure sea level relative to a point attached to the land which can move vertically at rates comparable to the long term sea level signal. The second problem is the spatial distribution of tide gauges, in particular those with long records, which are restricted to the coastlines (Wöppelmann et al., 2007). This part of the document focuses on the first point.

The problem of correcting tide gauges records from vertical land motion upon which they are settled has only been partially solved. At best, the analyses so far have included corrections for one of the many processes that can affect the land stability, namely the Glacial Isostatic Adjustment (GIA). However, GIA models don't account for the other sources of vertical land motion that can affect tide gauges. The method presented here is an alternative approach which measures (rather than to model) the rates of vertical land motion at tide gauge locations by the means of space geodesy.

Proprietary information : no part of this document may be reproduced divulged or used in any form without prior permission from CLS and CNES.

3.4.5. Monitorings of SSH bias between altimetric and in-situ-data

The previous editing procedure presented above emphasizes the reliability of the altimeter/tide gauges comparison procedure. A monitoring report, composed of statistics results on several quantities, is then generated for each space altimetric mission.

Note that in 2009 one part of this work has consisted in routinely presenting the most important results for each mission. The monitoring report which is generated after each new cycle has thus been updated and an example of the results is presented in annex . The most important results are presented first, adding new diagnostics like hemispheric or even/odd altimeter/tide gauge SLA differences. Then, it is now possible to directly study different altimeter SSH. In the current release are studied the impact of the coastal editing flag, the ECMWF and radiometer wet troposphere correction and the influence of the orbit error. Finally, cycle per cycle statistics computed from altimetric and in-situ sea surface heights (displayed in an annex part) provide :

- The number of tide gauges used to perform the comparison procedure.
- The mean bias between altimetric data and in-situ tide gauges measurements.
- The standard deviation of the bias computed from these sea surface heights.
- The minimum and the maximum of this bias.

Thanks to such statistics can be pointed out the influence and the impact of altimeter corrections brought to sea surface heights. Thus potential altimetric drifts can be estimated from the comparison to in-situ measurements.

Proprietary information : no part of this document may be reproduced divulged or used in any form without prior permission from CLS and CNES.

4. Analysis of potential drifts or jumps in altimeter MSL

4.1. Overview

The cycle by cycle monitoring of average SLA differences between altimeter and tide gauge data provide relevant information to detect potential drifts or jumps on mean sea level trend derived from altimetric data. New assessments of these long-term comparisons until the end of 2009 are presented in this part in agreement with the MSL calculation and using an extended in-situ network. The main three altimeter missions TOPEX/Poseidon, Jason-1 and Envisat will be studied. As the method performed thanks to at least 2-years tide gauge time series, results on Jason-2 can't lead to an accurate assessment of the Jason-2/tide gauge long term difference trend. However in 2009 all the parameters have been updated for this space mission, which is ready to be computed in 2010. Moreover, trends for the SLA differences statistic monitoring are calculated from quality controlled tide gauge measurements, 60-day filtered with annual and semi-annual signals removed. As only a few tide gauges can be corrected from vertical movements (their colocation with GPS stations is effective for only 60 tide gauges), a global vertical movement correction of 0.2 mm/year, in agreement with Peltier GIA global correction, is computed from these in-situ measurements combined to GPS vertical velocities.

4.2. Analyses for each altimetric mission

4.2.1. TOPEX/Poseidon

Results presented here have been performed using new orbit standards in the TOPEX/Poseidon SSH (GSFC), the new Sea State Bias, high resolution MOG2D and the new oceanic GOT tide release 4.7. To date, this is the best SSH computed for TOPEX/Poseidon, which is moreover homogeneous with other space missions studied in the present document (Jason-1 and Envisat).

The monitoring of SLA differences between TOPEX/Poseidon and tide gauges is plotted in figure 5 (with or without Poseidon cycles). The different phases of the mission are displayed with different colors : green for TOPEX-A altimeter, blue for TOPEX-B altimeter, purple for TOPEX over its new orbit during the tandem phase with Jason-1, and Poseidon cycle in red squares.

Before analyzing the global trend, note that the Poseidon cycles are less systematically biased in comparison with TOPEX than they were to be. This is due to the new 2 parameters Sea State Bias (with Gourrion's wind) computed in the TOPEX/Poseidon SSH (see TOPEX/Poseidon annual report) in which Poseidon cycles are artificially offset on the TOPEX SSH monitoring. In order to combine data of both altimeters (TOPEX and Poseidon), a global bias is applied depending on the TOPEX period (TOPEX-A / TOPEX-B) and on the Sea State Bias correction applied (4-parameters SSB for Poseidon and 2 different non-parametric SSB for TOPEX-A and TOPEX-B). Regarding such results, this item has still to be thoroughly investigated to understand differences in TOPEX and Poseidon SSH comparison through tide gauge measurements.

After a 2-month boxcar filter results obtained as plotted in figure 5 right show a slight difference in trends comparing with previous results. The new global trend is then -0.3 mm/year $\pm$ 0.1 mm

Proprietary information : no part of this document may be reproduced divulged or used in any form without prior permission from CLS and CNES.

over the 1993-2005 while it was 0.3 mm/year in 2008. The slight adjustment formal error proves the efficiency of our method to compute the trend for these SLA differences. Separating TOPEX-A and TOPEX-B period, trends are respectively close to 1 mm/year and 0.5 mm/year. The difference with the global trend might be due to the shift which appears when moving to the TOPEX New Orbit in September 2002.

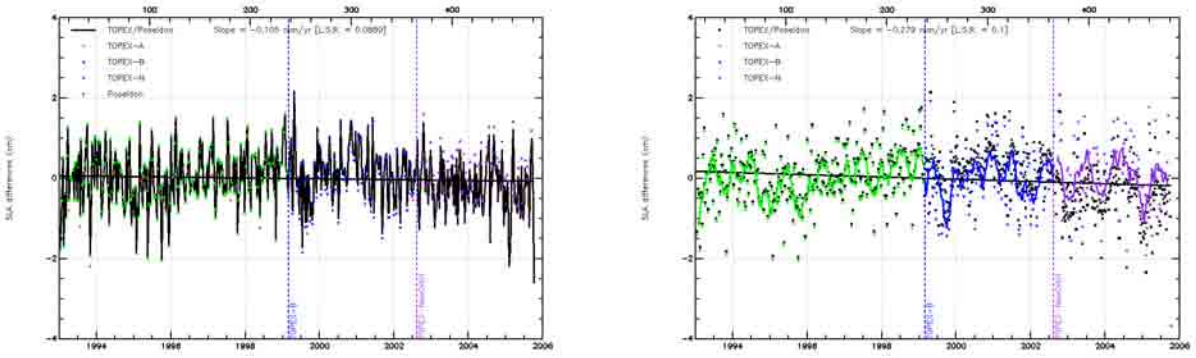

FIG. 5 – *Cycle by cycle monitoring of raw mean SLA differences between TOPEX/Poseidon and tide gauge measurements. Left : with Poseidon cycles. Right : Poseidon data have been removed*

The cycle by cycle monitoring of standard deviation SLA differences is plotted in figure 6. It highlights a standard deviation close to 7 cm in average on the TOPEX-A and TOPEX-B time period while it is 9 cm with TOPEX-N, corresponding to the TOPEX orbit change in September 2002 when the satellite moved over the Jason-1 interleaved track in order to benefit from both altimeter missions in oceanic applications (Jason-1 phase tandem). This has to be linked with differences in the previous monitoring where the global slope is influenced by the TOPEX-N shift. The standard deviation is not really homogeneous overall the T/P period. Stronger values (higher than 10 cm) are sometimes observed, which can be related to the number of colocated altimeter and in-situ measurements weaker than expected (due to altimeter or in-situ data incidents). In this way, Poseidon measurements are often statistically higher than TOPEX's one. Some studies (Vincent et al, 2004 [12]) already shown the slight increase of TOPEX SLA variance after 2002, especially due to the MSS performances lower over the new ground track. Finally, this also explains the better SSH consistency between TOPEX and tide gauges before 2002. It's interesting to notice the ability of the method to measure with independent data the altimeter SLA performances.

Proprietary information : no part of this document may be reproduced divulged or used in any form without prior permission from CLS and CNES.

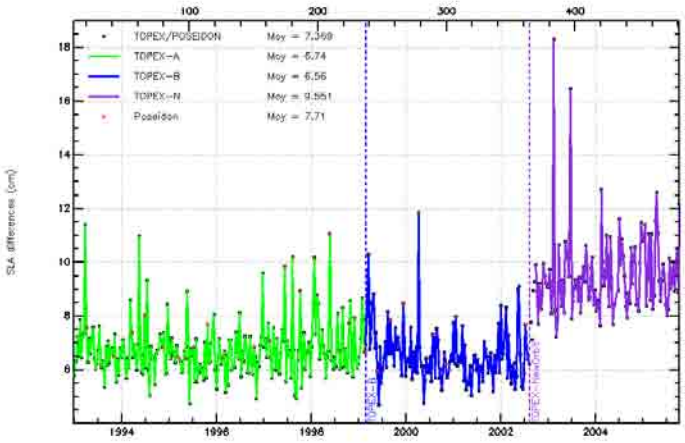

FIG. 6 – *Cycle by cycle monitoring of standard deviation SLA differences between TOPEX and tide gauge measurements*

As shown in figure 6, the standard deviation of altimeter/tide gauge SLA differences increase from about 3 cm between TOPEX-A/B and its new orbit. The number of measurements, displayed on figure 7, shows that tide gauges considered are 1/4 weaker when the satellite passed on its new orbit. The reason for this behavior could be linked to the problem on the recorder of the altimeter which caused a loss of altimeter data. Thus, 1/4 of altimeter/in-situ SSH differences could explain the 3 cm increase of the standard deviation SLA differences.
Another reason for this increase of the standard deviation differences is linked to the SLA variability with T/P on its new ground track. Indeed, because the MSS is less precise outside the nominal track, a degradation of TOPEX/Poseidon performance is observed after the orbit change. Note that this raise in the TOPEX/Poseidon standard deviation difference is not detected with T/S profiles (see annual report of the altimetry - T/S profiles comparison [13]). Contrary to our method where altimetry is directly colocated to tide gauges, the T/S processing uses the 10-day boxed-averaged altimetric SLA, which leads to smooth the effect of changing ground track. Thus, a solution in our method to free from combining both T/P time periods (the initial phase from cycles 11 to 364 and the phase tandem from cycles 369 to 481) would be to separate both phases.

Proprietary information : no part of this document may be reproduced divulged or used in any form without prior permission from CLS and CNES.

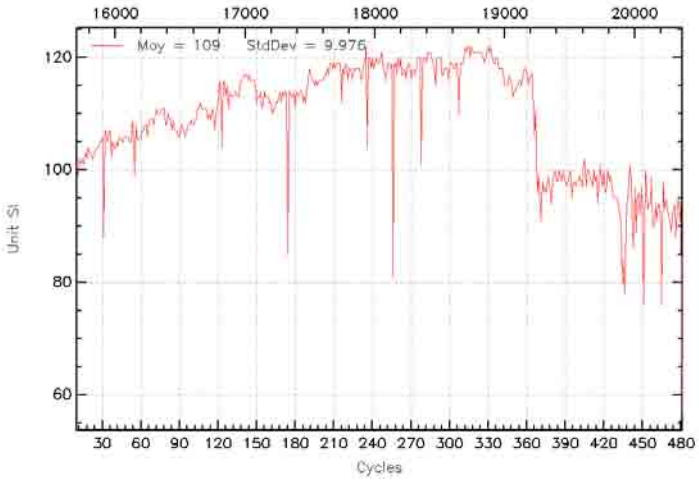

FIG. 7 – *Cycle by cycle monitoring of number of tide gauges considered on the whole TOPEX/Poseidon space mission*

4.2.2. Jason-1

Concerning Jason-1 space mission, there were two major events in 2009 : the altimeter orbit change between the 26 of January and the 10 of February and a safehold mode in September (about 10 days of data are missing). Concerning the ground processing, the new GDR-C release is effective for almost the Jason-1 mission. Main changes are the new orbit, new JMR calibration and new Sea State Bias. More details are provided in Jason-1 User Handbook document. For further information concerning the impact on the SLA performances, please refer to the OSTST poster and presentation (Commien, 2008 [6]). In consequence, note that from now on the Jason-1 data are homogeneous overall the time period.

The cycle by cycle monitoring of Jason-1 and tide gauges SLA differences is plotted in figure 8. The global trend is close to -0.05 mm/year with a slight adjustment formal error of 0.2 mm/year. Moreover, residual annual signals are displayed on this monitoring. It is important to determine the origin of such signals and know if it could result from one or several altimeter corrections. For instance, possible explanations for this signal have to be investigated through rainfall, land waters or atmospheric loading on tide gauges. Indeed such natural phenomena could affect the terrestrial crustal vertical movements at large scales and these movements may not be measured the same way by the altimeter and by tide gauges.

Proprietary information : no part of this document may be reproduced divulged or used in any form without prior permission from CLS and CNES.

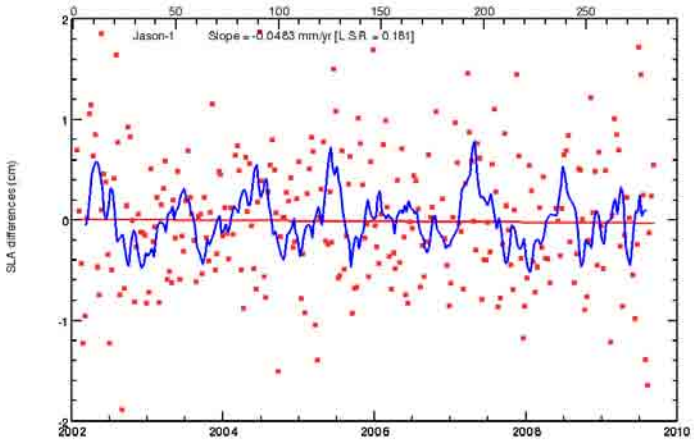

FIG. 8 – *Cycle by cycle monitoring of mean SLA differences between Jason-1 and tide gauge measurements*

The standard deviation of SLA differences between Jason-1 and tide gauge data (see figure 9) is now in agreement with the one of TOPEX/Poseidon (see figure 6) : about 6.7 cm for Jason-1 (before 2009) and 6.5/6.7 cm for TOPEX/Poseidon (before 2002). As new standards are more homogeneous between the two missions, this level of RMS differences is a good result and show a good SSH consistency between altimeter data and tide gauge measurements.

Since cycle 260, Jason-1 moves from its new interleaved orbit, raising the RMS to 10 cm. Indeed the standard deviation of the SLA differences between altimeter data and tide gauge measurements display a strong increase from cycle 260, since Jason-1 satellite moved to the Tandem Mission orbit on the new ground track spacing to the West of Jason-2. This was already the ground track of TOPEX during its Tandem Mission with Jason-1. In addition, Jason-1 is temporally shifted by 5 days. The consequence is a degradation of Jason-1 performance observed after the orbit change, indeed the MSS (necessary for SLA computation) adds errors when used outside the nominal T/P / Jason-1 / Jason-2 ground track (Dorandeu et al., 2004 [7]). Thus, figure 9 show that even with this raise of the standard deviation of SLA differences the mean of RMS differences is 6.7 cm. This increase is about 3.5 cm, from 6.5 cm to 10 cm. Note that this degradation has been pointed out in the CalVal Jason-1 and Jason-2 annual report too.

Proprietary information : no part of this document may be reproduced divulged or used in any form without prior permission from CLS and CNES.

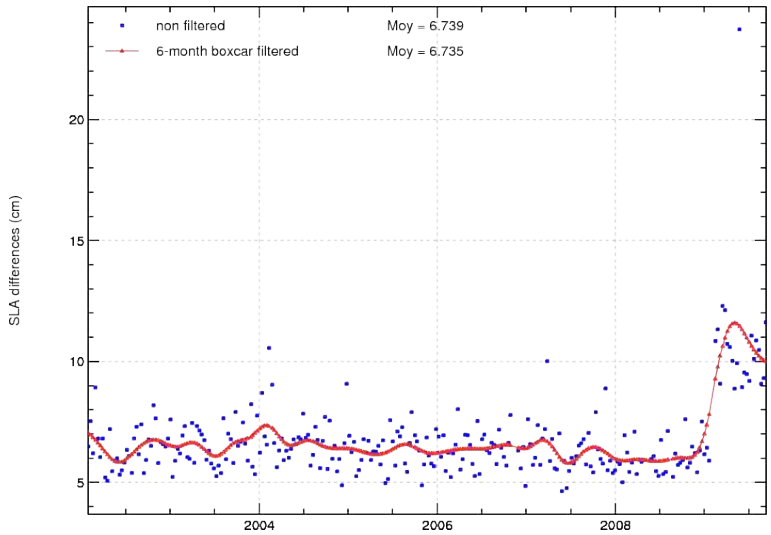

FIG. 9 – *Cycle by cycle monitoring of standard deviation SLA differences between Jason-1 and tide gauge measurements*

4.2.3. Envisat

Envisat measurements provide an accurate SSH as for Jason-1. However global MSL studies have shown until now a particular behavior of the Envisat MSL, especially at the beginning of the period where the MSL slope is not in agreement with Jason-1 and TOPEX/Poseidon ones. To date, the Envisat SSH is homogeneous enough to be compared with those of Jason-1 although its reprocessing will be performed in 2010. Indeed a new GDR-C standard orbit was computed at CNES simultaneously for Jason-1 and Envisat. This standard was/will be used for Jason-1/Envisat reprocessing. To date this orbit has been updated on Envisat between cycles 22 and 72 and the editing coastal flag (editing with relaxed thresholds to get altimeter measurements closer to the shore) has been corrected (see Envisat annual report 2009), which provides more accurate altimeter/in-situ SLA differences at tide gauge locations (see figure 10 right). On this histogram, positive values on variance differences mean that the editing coastal flag improves SLA differences at tide gauge locations. As the mean is about 1.9 cm^2, the SSH calculated on Envisat is better for this activity taken into account this flag but also all coastal geophysical correction (ionospheric, tide...).

Proprietary information : no part of this document may be reproduced divulged or used in any form without prior permission from CLS and CNES.

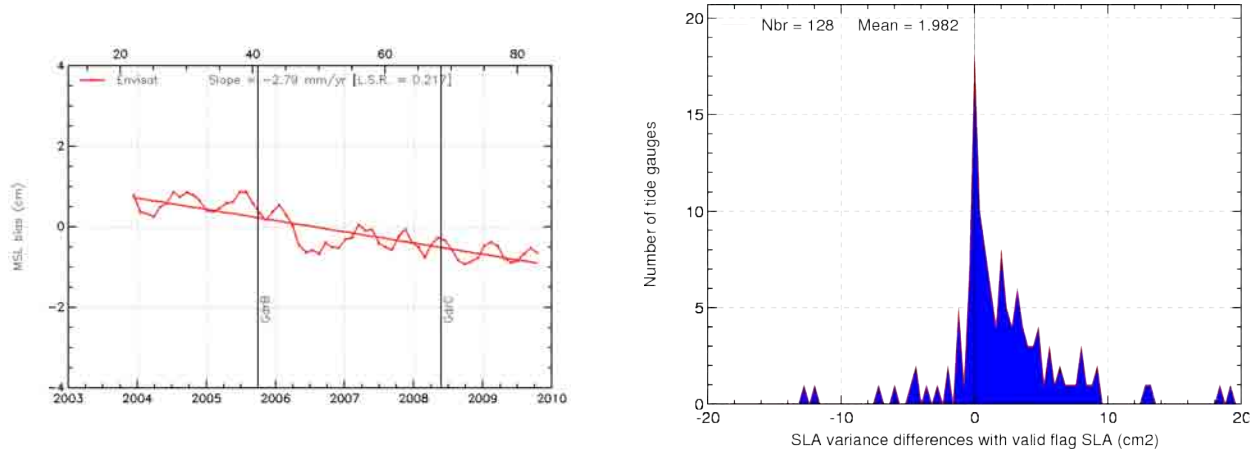

FIG. 10 – *Left : cycle by cycle monitoring of mean SLA differences between Envisat and tide gauge measurements. Right : variance differences between SSHs using the coastal editing flag and basic editing flag with regard to tide gauge measurements*

The cycle by cycle monitoring of Envisat and tide gauges SLA differences is plotted in figure 10 left. This figure highlights a strong negative global trend close to -2.8 mm/year with an adjustment formal error close to 0.2 mm/year since cycle 22 to the end of the period (cycle 82). Note that the ECMWF wet troposphere correction is here applied in the SSH calculation as a result of a drift or abnormal signal on the radiometer correction. But the associated trend for Jason-1 is very weak (see figure 8) and the global MSL trends are similar for these two missions. Hence the question why the Jason-1 / Envisat trend differences at tide gauges location is not coherent with the global MSL trends difference ? Indeed as seen on figure 11, a difference greater than 3 mm/year is detected between both trends of the mean altimeter SLA colocated to tide gauges. And this difference is of the order of the difference between Jason-1/tide gauges and Envisat/tide gauges comparisons computed previously (fig. 8 and 10). As Jason-1 and TOPEX/Poseidon coastal and global MSLs are coherent, the tide gauge spatial sampling is sufficient to assess the global trend of the MSL. This suggest that there are spatial heterogeneities of the Envisat MSL trend which are not physical but instrumental and which would explain the observed difference between the local and global MSL trends. Moreover, the SSH has been calculated with the new GDR releases over this period. A lot of evolutions in this release, associated with IPF and CMA version, were taken into account. All the geophysical corrections improved in the GDR-B release are updated on the whole period (Sea State Bias, ionospheric correction, MOG2D Dynamic Atmospheric Correction...). Therefore, the remaining differences are likely to be due to an orbit inhomogeneity and/or to instrumental updates (IF Mask, ...). This Envisat MSL behavior is under investigation and should be better understood thanks to the full reprocessing of the mission in 2010.

Proprietary information : no part of this document may be reproduced divulged or used in any form without prior permission from CLS and CNES.

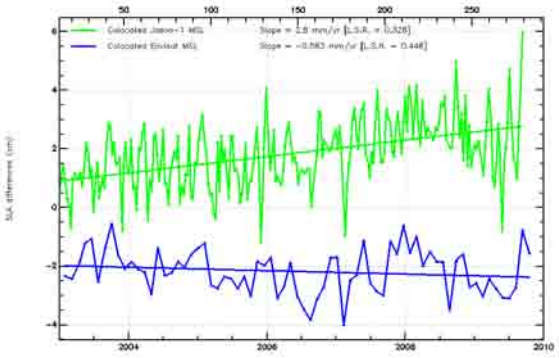

FIG. 11 – *Cycle by cycle monitoring of colocated mean of altimeter SLA for Jason-1 and Envisat*

Concerning the monitoring of the SLA differences standard deviation (figure 12), the average value (about 4.8 cm RMS) is lower than both TOPEX/Poseidon and Jason-1. In fact, the low Envisat figure is not really comparable. Indeed, the standard deviation is calculated cycle by cycle but the 35-day repetitivity for Envisat (instead of the 10-day repetitivity for Jason-1 and TOPEX/Poseidon), reduces the SLA RMS differences since there are more homogeneous measurements for each tide gauge. This monitoring should be also reprocessed in 2010 with a 10-day sub-cycle for Envisat in order to be compared with Jason-1 and TOPEX/Poseidon.

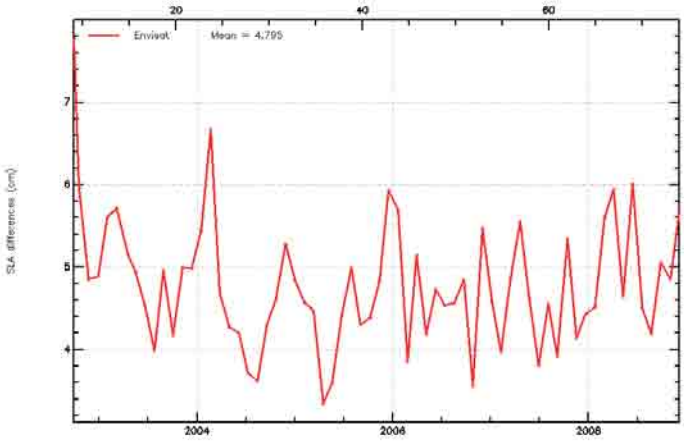

FIG. 12 – *Cycle by cycle monitoring of standard deviation SLA differences between Envisat and tide gauge measurements*

Proprietary information : no part of this document may be reproduced divulged or used in any form without prior permission from CLS and CNES.

5. Estimation of altimetric SSH improvements

5.1. Overview

As already mentioned, the second main goal of the Calval in-situ activity is to estimate improvements of altimetric data analyzing the SSH consistency between altimeter and in-situ measurements. This part aims at presenting the capability of the altimeter/tide gauges comparison procedure to measure the impact of new altimetric standards on the SSH consistency. These new altimeter standards can be new geophysical corrections (tide model correction, dynamical atmospheric correction,...), new orbits or new algorithms in ground processing. These evolutions can be contained in a new release of altimetric.

The basic principle of the method is to compare the SLA consistency between altimeter and tide gauges data using successively the old and new standards in the altimeter SSH calculation. The main criteria used is the analyse of SLA variance differences :

$$\Delta VAR(SLA)_{Alti} = VAR(SLA_{Alti(NewStandards)} - SLA_{TG}) - VAR(SLA_{Alti(OldStandards)} - SLA_{TG})$$

In addition, as the SSH provided by tide gauges uses the tidal correction and the dynamical atmospheric correction, the SSH consistency improvement can also be analyzed by a similar variance criteria (only for both corrections) at tide gauges locations without using altimeter data :

$$\Delta VAR(SLA)_{TG} = VAR(SLA_{TG(NewStandards)}) - VAR(SLA_{TG(OldStandards)})$$

If $\Delta VAR(SLA)_{Alti}$ or $\Delta VAR(SLA)_{TG}$ is negative, this argues for an improvement of new standards in the SSH calculation. The cycle by cycle monitoring of these statistics is systematically performed in order to detect change in the new standards in comparison with the former ones. Another diagnostic also developed is the histogram of the variance SLA differences as function of the tide gauge number as plotted in figure 14.

In the same idea, the correlation of altimeter and tide gauge SSHs is locally analyzed for a given tide gauge (see information cards of tide gauges in annex). The difference of correlation using old and new altimeter standards is mapped in order to detect accurately areas where the altimetric SSH is improved.

The following analyses presented here are not exhaustive. Their main objective is to illustrate and demonstrate the interest of the method.

Proprietary information : no part of this document may be reproduced divulged or used in any form without prior permission from CLS and CNES.

5.2. Impact of new GOT4.7 tidal model correction

The first study is about the enhancement of the new GOT4.7 tidal model correction in the altimetric SLA computation. This study has been performed in 2008 in relationship with the PISTACH project. As this new standard as updated in CLS altimeter tables in 2009, the comparison with in-situ tide gauge measurements has been performed with these new standard. Thus figure 13 displays histograms of SLA variance differences between altimeter and in-situ data using successively GOT4.7 and GOT00V2 tide models for the three main missions TOPEX/Poseidon, Jason-1 and Envisat. This diagnostic is a way of demonstrating the improvement of new standard at tide gauge locations.

For availability reasons of datasets, the global period is different between all these missions as the performance of the GOT4.7 tide correction is studied on their own global time period. Positive values mean that altimetric SLA using GOT00V2 tide correction is more coherent with tide gauge SLA than altimetric SLA using GOT4.7. Conversely, negative values mean that the use of the GOT4.7 tide correction makes altimetric SLA more coherent with tide gauge SLA than with GOT00V2. Negative values mean therefore that the use of GOT4.7 for altimetric SLA reduces the variance.
Results with regard to the three space missions display a mean gain value of about -1.5 cm^2 for TOPEX/Poseidon, -1.7 cm^2 for Jason-1 and -0.6 cm^2 for Envisat. As it was demonstrated in Cal-Val studies, the new tide correction is more efficient in coastal areas except in the Hudson Bay and in the north of the Bering strait. Comparisons with tide gauge measurements logically lead to good results for the space missions considered through these histograms of variance differences and confirm the improvement of the computation of altimeter SSHs with the new GOT4.7 tide correction.

Proprietary information : no part of this document may be reproduced divulged or used in any form without prior permission from CLS and CNES.

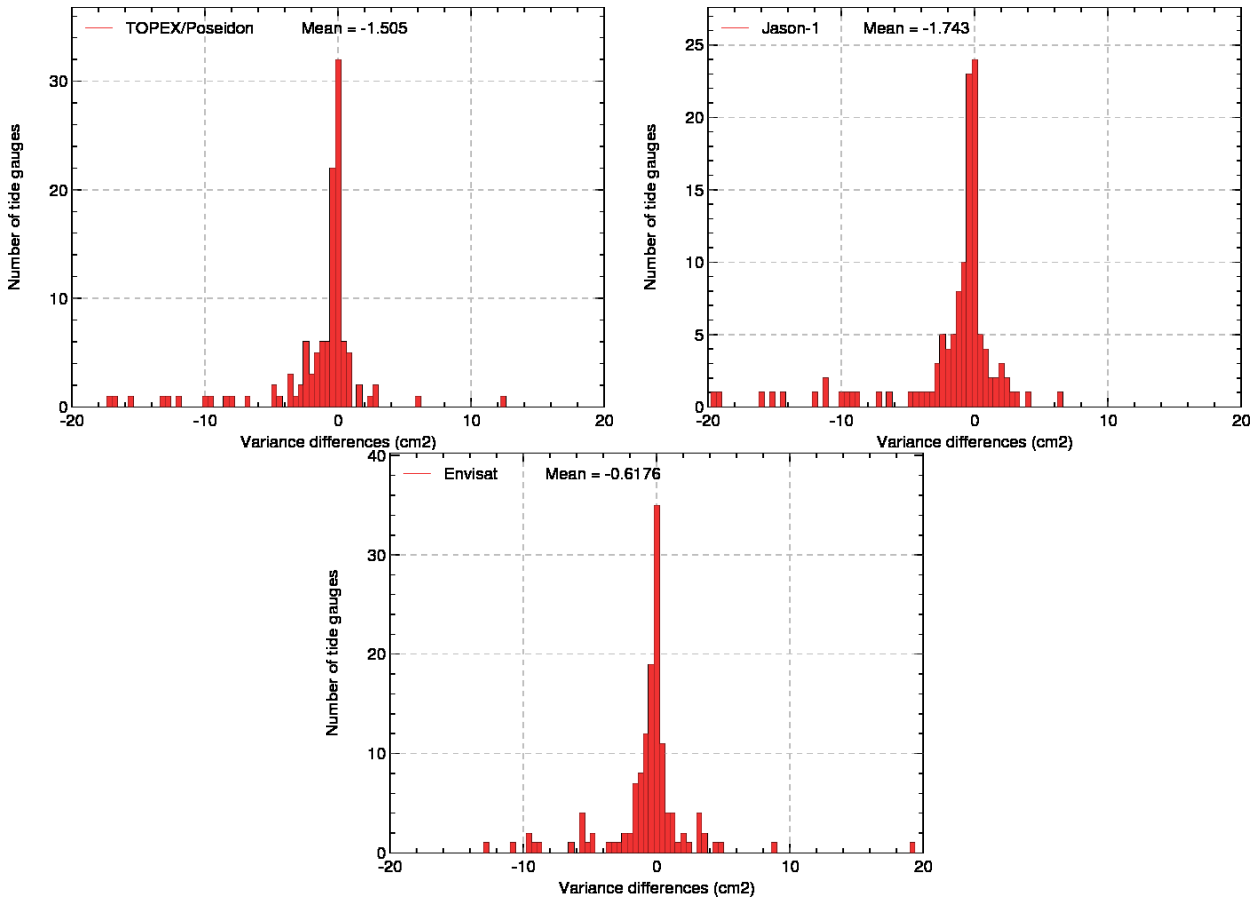

FIG. 13 – *Histograms of SLA variance differences between altimeter and in-situ data using successively GOT4.7 and GOT00V2 tide models. Top left : TOPEX/Poseidon, top right : Jason-1, bottom : Envisat*

5.3. Impact of the coastal editing flag on altimeter/in-situ SLA consistency

With the same method as previously, we also studied the performances of the new coastal editing flag. In figure 14 is plotted the histogram of the variance SLA differences as function of the tide gauge number in order to estimate the impact of new editing criteria allowing to compute the SSH closer from the coasts. Negative values indicate that the coastal editing flag is better. Results provided explain how can be improved the consistency between altimeter data and in-situ measurements at the different tide gauge locations. Here the impact of the coastal editing flag is relevant, with a mean variance of -2.9 cm^2 for Jason-1 and -2 cm^2 for Envisat, which demonstrates the improvement of altimeter/in-situ SLAs consistency using this criterion.

Proprietary information : no part of this document may be reproduced divulged or used in any form without prior permission from CLS and CNES.

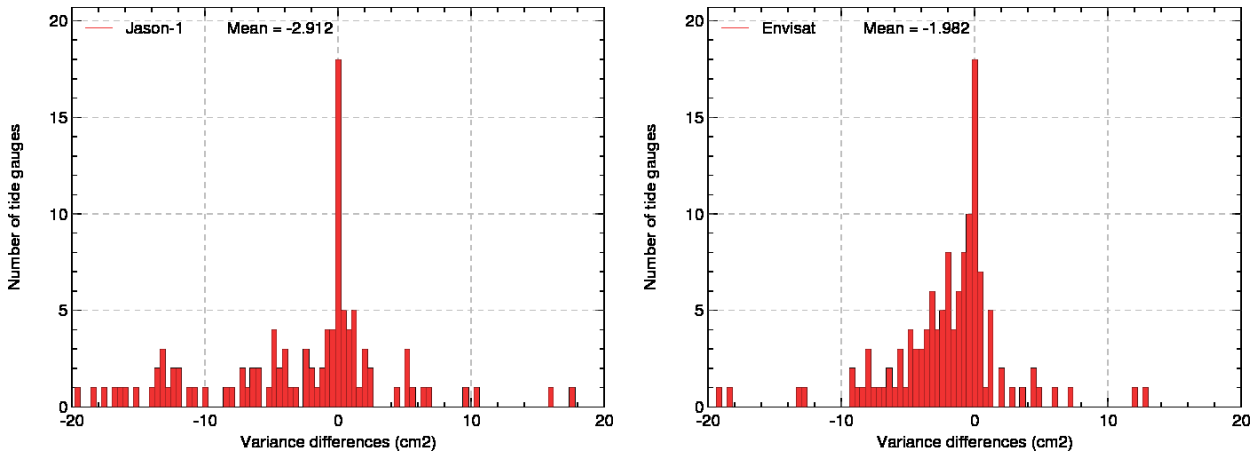

FIG. 14 – *Differences of SLA variance differences between altimeter and in-situ data using successively basic and coastal editing flag. Left : Jason-1, right : Envisat*

5.4. Impact of the GDR-C reprocessing on altimeter/in-situ SLA consistency

As for the two previous kind of corrections and described in the overview section, the impact of the new GDR-C reprocessing on Jason-1 can be estimated from the SSH provided by correction without using altimetric measurements. Here are the main improvements released in this reprocessing (see [5] and [6]) :

- the main change of the new version is the POE orbit solution, which includes a new gravity model (EIGENGL04C instead of EIGEN-CG03C), and a time-varying part (without drifts).
- the JMR (radiometer) has been recalibrated with parameters derived from cycles 1 to 227 (GDR-B) so as to provide more accurate brightness temperature and therefore wet tropospheric correction.
- altimeter instrument corrections were updated. This has an impact on several altimeter parameters : backscattering coefficient (sigma0), sea wave height, range. Through the range, the bifrequency ionospheric correction is also slightly modified.
- a new sea state bias (SSB) solution, computed on a 3-year basis of GDR version B (cycles 1 to 111), improves significantly the sea surface height (SSH) calculation.
- the dry troposphere correction still uses the ECMWF model, which has evolved to correct for spurious oscillation effects.
- the dynamical atmospheric correction (DAC), which includes inverse barometer and MOG2D model, now uses high resolution MOG2D grids.
- for FES2004 ocean tide model, S1, K2 and loading tides have been updated.
- an empirically-computed pseudo time-tag bias correction has been added in the product and taken into account in SSH calculation, and a mean dynamic topography (MDT Rio, 2005) has been added too.
- a new algorithm, based on AGC instead of sigma0, is used for rain flag estimation.
- the computation of the ice flag is also slightly changed. It no longer shows a discontinuity in the Hudson bay.

While the main benefit is to estimate the performance of the GDR-C reprocessing through in-situ independent datasets comparison, the drawback of this method is that each correction can't be

Proprietary information : no part of this document may be reproduced divulged or used in any form without prior permission from CLS and CNES.

individually assessed in the global reprocessing. Results displayed on figure 15 show the better temporal consistency between altimeter data and tide gauge measurements with a mean value of -0.73 cm^2. However, like previously, a residual annual signal is remaining, which periodically inverts the consistency to either GDR-C or GDR-B orbit. In agreement with Calval studies, this annual signal may be due to the new gravity model and the time-varying part used in the POE orbit solution.
Moreover, at tide gauge locations, the SSH consistency is also slightly improved, maybe influenced by the sign inversion of variance differences. Thus the mean is -0.13 cm^2 and confirm the enhancement of the consistency between altimeter and in-situ data thanks to GDR-C reprocessing.

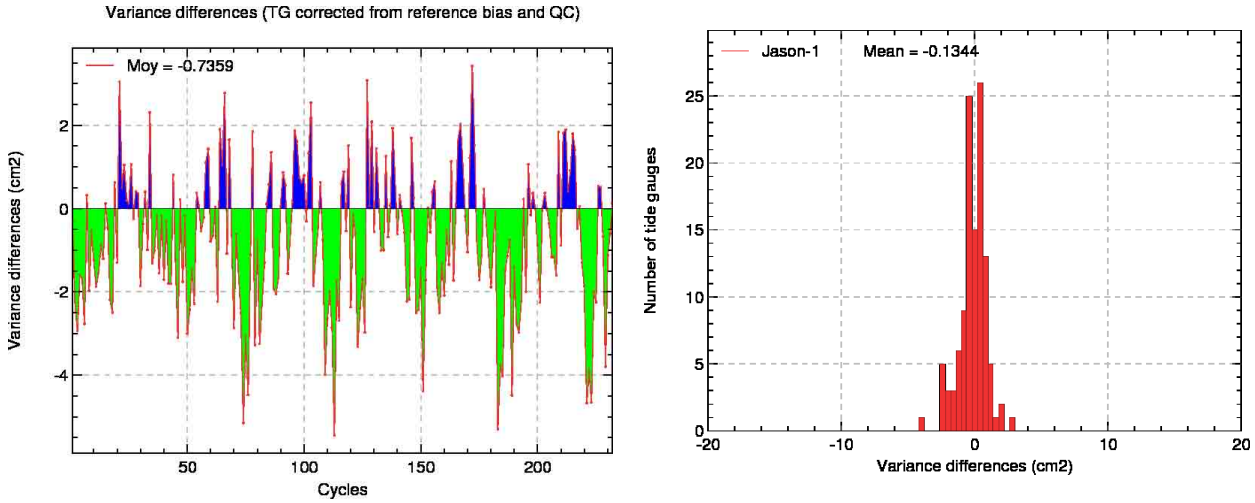

FIG. 15 – *Monitoring of SSH variance differences computed with GDR-C and GDR-B for Jason-1 (cm^2)*

5.5. Impact of new Sea State Bias (SSB) correction on TOPEX/Poseidon

Reprocessings of SSALTO/DUACS multimission products aim at computing the latest and most accurate altimetric corrections in the SSH calculation (GSFC orbit, GOT4.7 tide correction ...). The use of the Gourrion wind, more relevant than Chelton's one, have led to a new computation of the TOPEX/Poseidon SSH (see technical note [9]). Next to the study between the old and the new SSB corrections, the altimeter and in-situ long term differences provide results as seen on figure 16. On the left, a drift is observed on the TOPEX-A time period, corresponding to instrumental problems (OSTST, Seattle 2009). When comparing new results to in-situ tide gauge measurements, this drift is strongly decreased, which indicates the new TOPEX MSL is more reliable. The new trend on TOPEX-A is 0.8 mm/year with the new 2-parameters SSB computed with Gourrion's wind whereas it was 1.5 mm/year with Chelton's wind.

Moreover, as presented on figure 17, the histogram of variance differences between both solutions of Sea State Bias show that altimeter and in-situ measurements are more consistent using the 2-parameters Sea State Bias calculated with Gourrion's wind. Thus, the mean of variance differences is -0.6 cm^2, which is a good improvement in the altimeter SSH computation.

Proprietary information : no part of this document may be reproduced divulged or used in any form without prior permission from CLS and CNES.

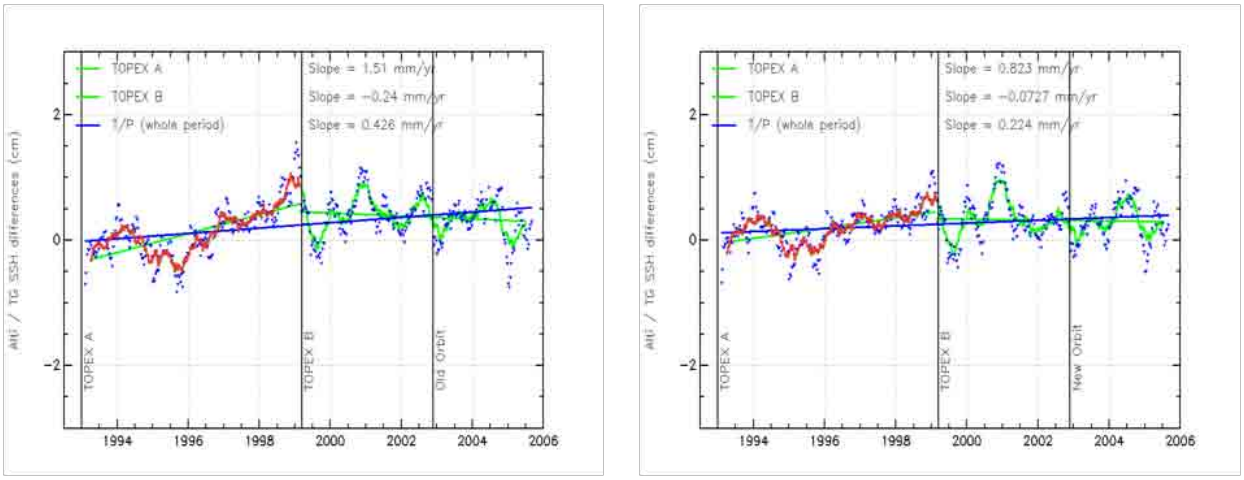

FIG. 16 – *Impact of the new 2-parameters Sea State Bias computed with Gourrion's wind on the monitoring of the mean altimeter/in-situ tide gauge differences. Left : Old SSB (Chelton's wind). Right : New SSB (Gourrion's wind)*

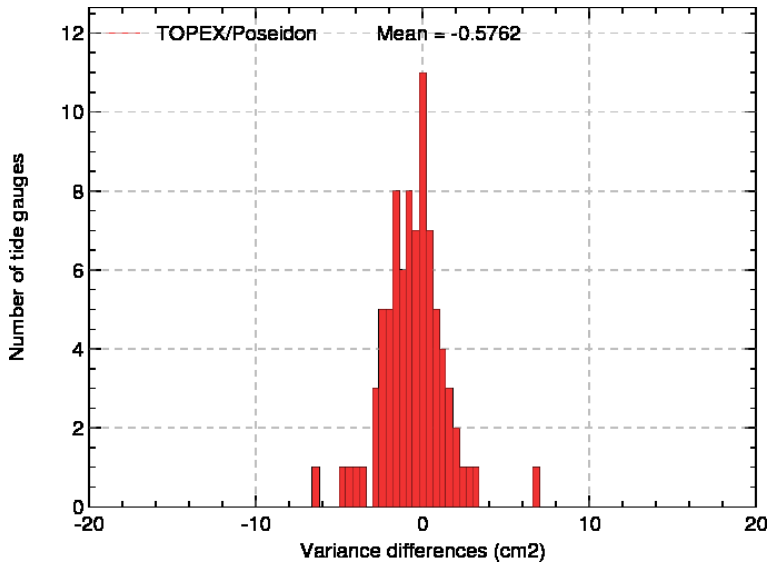

FIG. 17 – *Monitoring of SSH variance differences computed with GDR-C and GDR-B for TOPEX/Poseidon (cm^2)*

Proprietary information : no part of this document may be reproduced divulged or used in any form without prior permission from CLS and CNES.

6. Quality assessment of in-situ tide gauge time series

In order to complete the global assessment of altimeter data where in-situ measurements are used as independent sources of comparison, tide gauge networks have been compared to altimeter SLA time series. The main objective of this part is the detection of anomalies on in-situ time series thanks to the cross-comparison with all available altimeter measurements. This is mainly possible comparing SLA differences. This diagnostic allows us to detect jumps on in-situ time series which are not detected on altimeter ones. Moreover, maps of temporal correlation between altimeter and in-situ SLA time data series are systematically produced for each tide gauge and altimeter.

6.1. Presentation of the tide gauge information cards

The basic principle of tide gauge information cards is based on a summary of in-situ informations compared to altimeter data. These informations are then used to perform a quality control on each tide gauge.
Here are the main purposes of such information cards (figure 18) :

- Tide Gauge identification : this part contains general informations about the tide gauge (network, coordinates, time period coverage and potential colocated GPS close to the tide gauge). The latter is important to correct the tide gauge from vertical movements. But to date, only a few tide gauge are colocated to a GPS beacon, that's why tide gauges are corrected from a global bias of -0.2 mm/year (Peltier, 2004).

- Temporal SLA comparisons with TOPEX/Poseidon, Envisat, Jason-1 : in this part results from the tide gauge processing data are used to compare the in-situ and altimeter SLAs and their differences on the tide gauge time period. Thanks to the multi-cross-calibration, drifts or jumps on tide gauge time series can be detected and then be used to perform the quality control.

- Maps of SLA correlation with Jason-1, TOPEX/Poseidon and Envisat : to make the multi-cross-calibration reliable, another useful diagnostic concerns the correlation between altimeter and in-situ SLAs. Such maps have a double interest, first to estimate the distance between altimeter tracks and the tide gauge and second to see if both SLA are well correlated. The proximity of altimeter tracks depends on the mission itself, thus the distance between Envisat tracks and tide gauges is logically smaller than for Jason-1 (which does not mean correlations are even better). Concerning TOPEX/Poseidon, the tandem mission has a positive effect on this proximity with regard to Jason-1. Generally the correlation is good close to the coasts up to 0.9. But for some tide gauges, the value is low, maybe due to geophysical processes but also to jump or drift in in-situ data. The comparison of altimeter and in-situ SLA allows us to assess the tide gauge SLA as well as the altimeter SLA.

- Tide Gauge reliability : finally the information card gives a summary of different relevant diagnostics such as the slope of the potential tide gauge crustal drift, the SLA maximal correlation, the filtered and non-filtered SLA differences RMS, the SLA differences slope and finally the quality control applied on each tide gauge deduced from all these informations.

Proprietary information : no part of this document may be reproduced divulged or used in any form without prior permission from CLS and CNES.

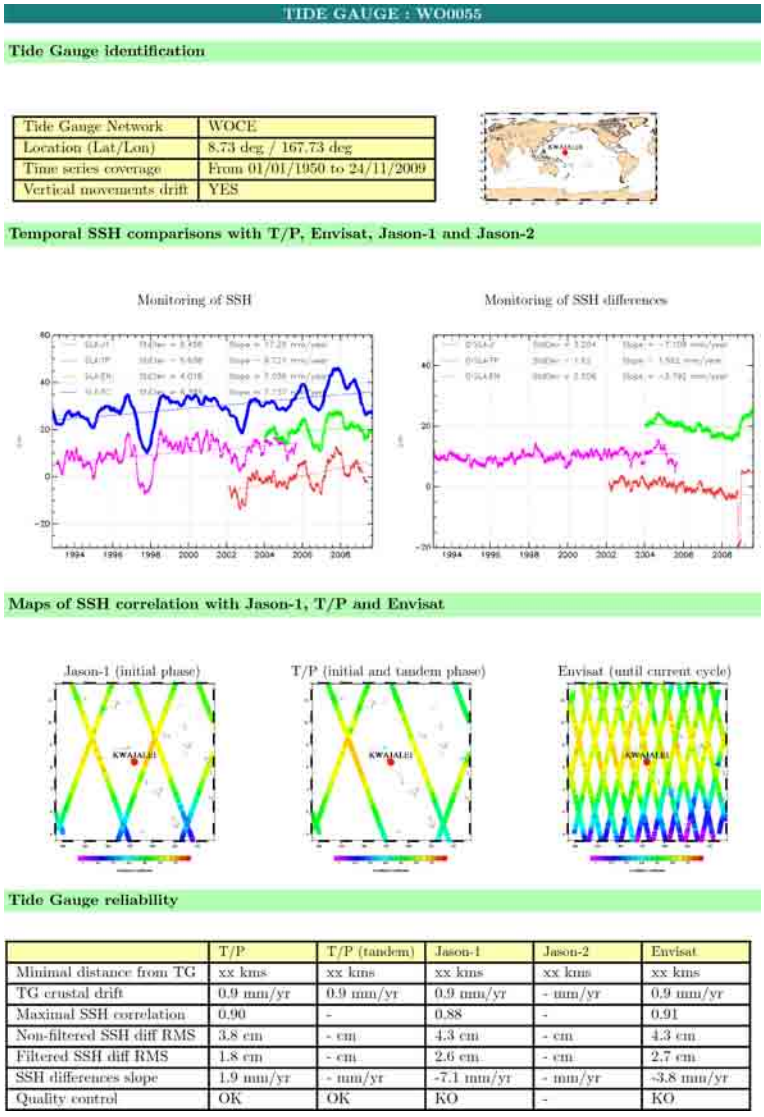

TIDE GAUGE : WO0055

Tide Gauge identification

Tide Gauge Network	WOCE
Location (Lat/Lon)	8.73 deg / 167.73 deg
Time series coverage	From 01/01/1950 to 24/11/2009
Vertical movements drift	YES

Temporal SSH comparisons with T/P, Envisat, Jason-1 and Jason-2

Monitoring of SSH

Monitoring of SSH differences

Maps of SSH correlation with Jason-1, T/P and Envisat

Jason-1 (initial phase)

T/P (initial and tandem phase)

Envisat (until current cycle)

Tide Gauge reliability

	T/P	T/P (tandem)	Jason-1	Jason-2	Envisat
Minimal distance from TG	xx kms	xx kms	xx kms	xx kms	xx kms
TG crustal drift	0.9 mm/yr	0.9 mm/yr	0.9 mm/yr	- mm/yr	0.9 mm/yr
Maximal SSH correlation	0.90	-	0.88	-	0.91
Non-filtered SSH diff RMS	3.8 cm	- cm	4.3 cm	- cm	4.3 cm
Filtered SSH diff RMS	1.8 cm	- cm	2.6 cm	- cm	2.7 cm
SSH differences slope	1.9 mm/yr	- mm/yr	-7.1 mm/yr	- mm/yr	-3.8 mm/yr
Quality control	OK	OK	KO	-	KO

FIG. 18 – *Example of an information card for the Kwajalei tide gauge*

From these information cards, 4 quality control flags can be applied :

- 1 : in-situ and altimeter SLA time series are consistent
- 2 : a problem is detected on one of the in-situ or altimeter time series
- 3 : a problem is detected on the in-situ time series
- 4 : a problem is detected on the method or on the altimeter SLA time series

To date, only tide gauges which quality control is 1 are considered reliable and used to detect potential drifts or jumps on altimeter time series, or in the estimate of the quality of new altimeter standards. Moreover, this quality control has only be performed on the GLOSS/CLIVAR and the SONEL networks for now, which means that about 100 tide gauges are not used in the altimeter/in-situ SLA comparisons. The quality control for the whole networks will be performed

Proprietary information : no part of this document may be reproduced divulged or used in any form without prior permission from CLS and CNES.

in 2010.

6.2. Availability of tide gauge information cards

Since September 2009, information cards for both GLOSS/CLIVAR and SONEL networks are routinely performed each week and distributed on the AVISO website (*www.aviso.oceanobs.com/fr/calval/in-situ-global-statistics*).
A googlemap mapplet has been developed and information cards can be visualized online (figure 19). As the tide gauge coordinates accuracy is on the order of the minute, the geodetic reference system of our database may slightly differ from the googlemap one, which can induce some slight differences in tide gauge locations. Future actions in 2010 will improve this googlemap on the AVISO website, especially with arrows concerning the Mean Sea Level trend at the tide gauge location.

FIG. 19 – *Availability on tide gauge information cards on the AVISO website*

Proprietary information : no part of this document may be reproduced divulged or used in any form without prior permission from CLS and CNES.

7. Conclusion

This report demonstrates the interest of this comparison method in order to assess potential drifts or jumps in the altimetric measurements. Reliable results are obtained thanks to a data processing procedure performed in a operational frame (development and operational account, automatic processing, ...). This operational aspect of the data processing procedure is fundamental to quickly reprocess the whole altimetric period and take into account new altimetric standards as it has been planned this year for the new Jason-1 and will be in 2010 for Envisat GDR-C releases.

Thanks to the comparison of altimeter data with in-situ measurements, the MSL drift can be more precisely estimate. Drifts for Jason-1 and TOPEX/Poseidon have been respectively estimated to 0.1 $\pm$ 0.2 mm/year and -0.3 $\pm$ 0.1 mm/year. In the meantime an Envisat MSL drift close to -2.8 $\pm$ 0.2 mm/year is detected. The comparison between altimetry and tide gauges suggests that there are spatial inhomogeneities of the Envisat MSL trend. These results are in agreement with global Cal/Val studies. Finally, the use of independent in-situ tide gauge measurements is a way of getting an assessment of the error on the global MSL trend.

We also demonstrate the interest of the method to estimate the impact of new altimeter standards in the SSH calculation. Though the tide gauge coverage is poor (only close to the coast), the SSH consistency analysis between altimeter and tide gauge gives independent information to measure the quality of new altimetric standards. Thus, new diagnostics have been developed this year, like the spatial distribution of variance differences at tide gauge locations, which explain how can be improved the consistency between altimeter data and in-situ measurements at the tide gauge locations. The performance of Jason-1 GDR-C reprocessing has thus been assessed thanks to in-situ data and this method will be able to be used for instance in 2010 to quantify the consistency of Envisat SSH after the GDR-C reprocessing or update SSHs'space missions with the latest and almost accurate altimetric, radiometric and geophysical corrections.

Moreover, the method presented here can provide a quality assessment on both altimeter and in-situ datasets through SSH comparisons. Thus, information cards for both GLOSS/CLIVAR and SONEL networks are now routinely performed each week and distributed on the AVISO website (*www.aviso.oceanobs.com/fr/calval/in-situ-global-statistics*). Thanks to such comparisons, a relevant selection of reliable tide gauges is performed so as to detect potential drifts or jumps on altimeter time series, or to estimate the quality of new altimeter standards. To date, about 300 tide gauges are used in the altimeter/in-situ SLA comparisons.

Although the main objectives of this activity have been reached, several improvements are planned for the next years in order to better benefit from tide gauge measurements and thus enhance the relevance of analyses. To date, at least 3 points have to be investigated to give better results :

- the way of computing vertical movements, by using more GPS at tide gauge locations
- the correction of jumps in tide gauge time data series
- the errors on the method itself (especially the colocation with the nearest points on altimeter tracks)

To reach such goals, future actions will be performed in 2010, and some new ideas to get better results will be investigated :

- How to explain Jason-1 residual annual signals (atmospheric loading, land waters, rainfall...) ?

Proprietary information : no part of this document may be reproduced divulged or used in any form without prior permission from CLS and CNES.

- A new method based on the maximum of correlation between altimeter and in-situ tide gauge SSHs will be developed.

- The tide gauge quality control has to be performed on the whole tide gauge networks.
- Concerning vertical movements, several tests on regional areas or specific basins are expected to be done in order to quantify the impact of this correction with a better GPS space sampling at tide gauge locations. Moreover, the use of GIA model to get a better estimate of vertical movements at tide gauge locations is to be planned.
- The tide gauge googlemap will be improved, especially with arrows concerning the Mean Sea Level trend at tide gauge locations.

Finally, this work has been presented this year at the OSTST in Seattle [2] and at the OceanObs'09 conference in Venice [1] (see annex).

Proprietary information : no part of this document may be reproduced divulged or used in any form without prior permission from CLS and CNES.

8. References

Références

[1] Ablain M., G. Valladeau, A. Lombard, E. Bronner, P. Femenias : Quality assessment of in-situ and altimeter measurementsthrough SSH comparison. OceanObs'09, Venise, 2009.

[2] Ablain M., G. Valladeau, A. Lombard, E. Bronner, P. Femenias : Quality assessment of in-situ and altimeter measurements through SSH comparison. OSTST, Seattle, 2009.

[3] Ablain M., A. Cazenave, G. Valladeau, and S. Guinehut : A new assessment of global mean sea level from altimeters highlights a reduction of global trend from 2005 to 2008. Ocean Sci. Disc., 6, 31-56, 2009

[4] Beckley B. D., F. G. Lemoine, S. B. Luthcke, R. D. Ray, and N. P. Zelensky, 2007 : A reassessment of global and regional mean sea level trends from TOPEX and Jason-1 altimetry based on revised reference frame and orbits. Geophysical Research Letters, Vol. 34, L14608, doi :10.1029/2007GL030002, 2007

[5] Commien L., S.Philipps, 2009 : Reprocessing of Jason-1 GDR-C. Technical Note CLS.DOS/NT/09-198, Contract N° SALP-RP-MA-EA-21731-CLS

[6] Commien L., S.Philipps, M.Ablain, N.Picot : Calval performance assessment Jason-1 GDR C/ GDR B. OSTST, Nice, 2008.

[7] Dorandeu J., M. Ablain, Y. Faugere, F. Mertz and B. Soussi, 2004 : Jason-1 global statistical evaluation and performance assessment. Calibration and cross-calibration results. Marine GEODESY, 27, 345-372

[8] Ollivier A., Y. Faugere, 2009 : Envisat data validation and cross-calibration activities. Yearly report. Technical Note CLS.DOS/NT/10-18, Contract N° SALP-RP-MA-EA-21800-CLS.

[9] Valladeau G., 2009 : Influence de l'algorithme de calcul de vitesse de vent Gourrion à 2 paramètres pour l'altimètre de TOPEX/Poseidon. Technical Note CLS-DOS-NT-09-206

[10] Valladeau G., M. Ablain, F. Lefèvre, S. Guinehut, A. Cazenave, A. Lombard, 2008 : Using in-situ measurements to assess the error on the global mean sea level trend. EGU, Vienne, 2008

[11] Valladeau G., M. Ablain, F. Lefèvre, S. Guinehut, A. Cazenave, A. Lombard, 2008 : Assessment of global mean sea level from altimeters cross-calibration with in-situ measurements (TOPEX/Poseidon, Jason-1 and Envisat). OSTST, Nice, 2008

[12] Vincent, P., S. D. Desai, J. Dorandeu, M. Ablain, B. Soussi, P. S. Callahan, and B. J. Haines 2003a. Jason-1 Geophysical Performance Evaluation. *Mar. Geod.***26(3-4) : 167-186.**

[13] Legeais J.F., M. Ablain, G. Valladeau, 2008 : Bilan annuel CalVal In-Situ. Validation des données altimétriques par comparaison aux mesures in-situ T/S. Note technique CLS.DOS/NT/10-017, Contrat SALP-NT-MA-P2-21799-CLS.

Proprietary information : no part of this document may be reproduced divulged or used in any form without prior permission from CLS and CNES.

9. Annexes

9.1. Annex : General operating diagram

The following diagram sums up the main steps of the altimeter/tide gauges comparison procedure :

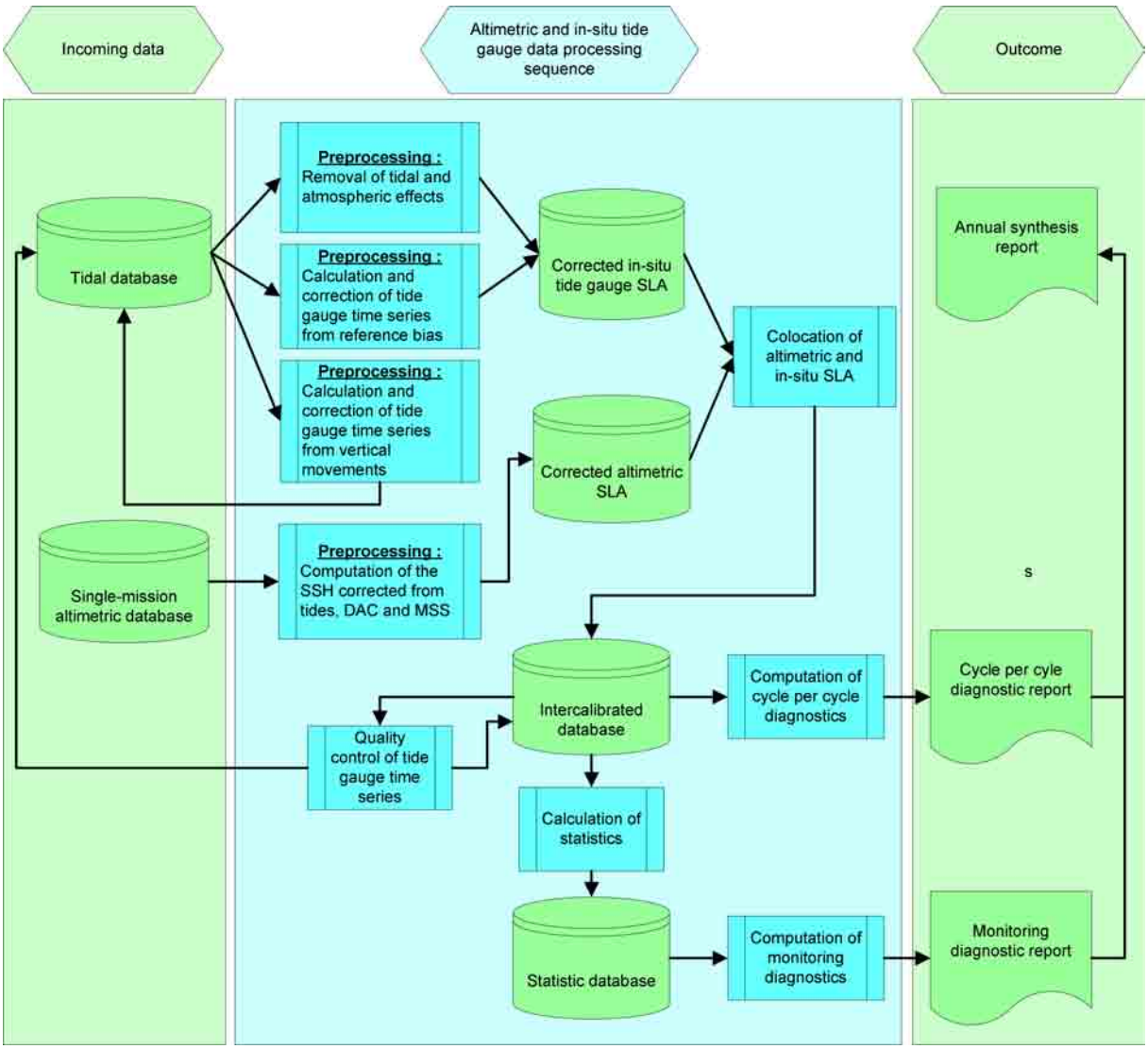

FIG. 20 – *General operating diagram of the tide gauge data processing sequence*

The main point is to underline the matter of the whole components of the Calval activity and their flexibility in performing this data processing sequence. In addition, the method presented here is scalable and thus reliable, which makes the altimeter/tide gauges comparison procedure a perennial validation activity for space missions in the Space Oceanography Division at CLS.

Proprietary information : no part of this document may be reproduced divulged or used in any form without prior permission from CLS and CNES.

9.2. Annex : OceanObs'09 poster

Proprietary information : no part of this document may be reproduced divulged or used in any form without prior permission from CLS and CNES.

Quality assessment of in-situ and altimeter measurements through SSH comparison

Michaël Ablain (1), Guillaume Valladeau (1), Alix Lombard (2), Emilie Bronner (2), Pierre Femenias (3)
(1) Collecte Localisation Satellite (CLS), Toulouse, France.
(2) Centre National d'Etudes Spatiales (CNES), Toulouse, France.
(3) ESA-ESRIN, Via Galileo Galilei CP64 I-00044, Frascati, Italy
E-mail: guillaume.valladeau@cls.fr

Overview

Altimetry missions provide accurate measurements of sea surface height (SSH) from 1992 onwards with TOPEX/Poseidon (T/P), and until now thanks to Jason-1, Envisat and more recently Jason-2. A global assessment of these data is systematically performed in order to detect potential anomalies and estimate system performances. In addition, cross-calibration between each altimeter mission is carried out to thoroughly analyze SSH bias, and potential drifts or jumps in the global Mean Sea Level (MSL), see MSL AVISO website **(1)**. In order to complete this assessment, in-situ measurements are also used as independent sources of comparison. In this way, tide gauge networks have been compared to altimeter data **(2)**.

In this study, we present the main results obtained from these comparisons (for T/P, Jason-1, Jason-2 and Envisat) through the 3 following objectives linked together. The first one consists in detecting drifts or jumps in altimeter SSH by comparison with in-situ measurements. The second goal is the analysis of the SSH consistency improvement between altimeter and in-situ data using new altimeter standards (orbit, geophysical corrections, ground processing...). The last objective is the detection of anomalies on in-situ time series thanks to the cross-comparison with all available altimeter data. In-situ measurements can thus be corrected or even removed in order to further improve the SSH comparison with altimeters.

References :
-(1) **MSL Aviso website:** www.aviso.oceanobs.com/msl/
-- (2)Ablain et al., 2009: "A new assessment of global mean sea level from altimeters highlights a reduction of global trend from 2005 to 2008" (in press)

Estimation of altimeter MSL drift

Data & Method

Altimeter drift is estimated using the GLOSS/CLIVAR "fast" sea level database: about 255 tide gauges uniformly widespread (see fig.1).
After colocating the nearest altimeter measurements with each tide gauge, time series which are not well correlated are edited. Finally, a dataset of about 120 tide gauge is selected.

Fig1

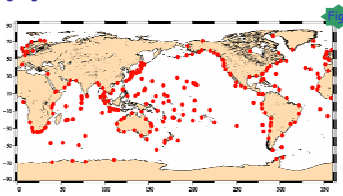

In addition, a drift correction is applied (**+0.2 mm/yr**) in order to take into account vertical movements observed only by tide gauges. This correction has been estimated using GPS data, but at the moment its accuracy is on the order of the correction value.

Accuracy of the method

The accuracy of the drift estimation is impacted by the formal error adjustment (on the order of 0.2 mm/yr), the uncertainty to take into account the vertical movements (using GPS station network), and also the sensitivity to the tide gauges number impacting the drift around ± 0.2 mm/yr.
Finally the accuracy of the method to estimate the MSL drift is close to **±0.5 mm/yr** over Jason-1, Envisat or T/P time periods. This uncertainty increases considering shorter periods.

Main results

Considering Jason-1 (from GDR-C and GDR-B products linked correctly together), the altimeter drift estimate is almost null : **-0.1 mm/yr.**
The first 24 cycles of Jason-2 have been overlayed (green dots) but for instance its very short time period doesn't allow an altimeter drift assessment.
This result highlights the Jason-1 reliability to calculate the global MSL trend.

Fig2

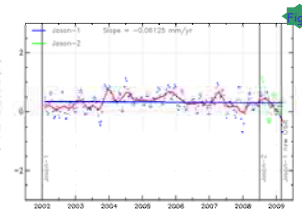

For Envisat, a negative drift close to **-2.2 mm/yr** is detected from 2002 to 2009 after homogenizing as well as possible the Envisat GDR products.
However, focusing only on the end of the period (GDR-A products are excluded), this drift is now weaker close to **-0.2 mm/yr.**
These results are in well agreement with global Cal/Val studies, showing the reliability of the method.

Fig3

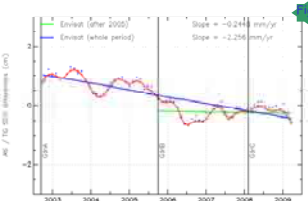

The T/P MSL drift have been calculated from updated M-GDR products (GSFC orbit , corrected TMR, ...) : it is slightly positive close to **+0.5 mm/yr** .
The slope estimate is almost null on the TOPEX-B time period (**-0.2 mm/yr**) whereas a drift is detected on TOPEX-A around **+1.3 mm/yr**. This drift seems correlated with TOPEX-A anomaly: SWH and SIGMA-0 drifts are observed on this period.

Fig4

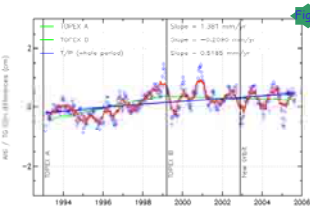

Quality assessment of in-situ tide gauge time series

The cross-comparison of altimeter and tide gauges SSH comparisons obtained from all the missions allows us to detect anomalies on tide gauge time series. This is mainly possible comparing SLA differences (fig.6-7). This diagnostic allows us to detect jumps as displayed in fig. 7 (a jump is observed simultaneously at the end of the Jason-1 and Envisat time periods). Unlike fig.7, fig. 6 doesn't highlight any anomaly on tide gauge.

On the other hand, maps of temporal correlation between altimeter and in-situ SSH time series (fig.8-9) are systematically produced for each tide gauge and altimeter. Generally the correlation is good close to the coasts close to 0.9 (fig. 8). But for some tide gauges, it is bad (> 0.5 in fig. 9). This might be due to geophysical processes but also to jump or drift in in-situ data.

Finally the comparison of altimeter and in-situ SSH allows us to assess the tide gauge SSH as well as the altimeter SSH.

Fig6

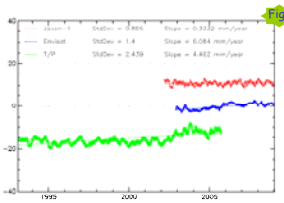

Fig7

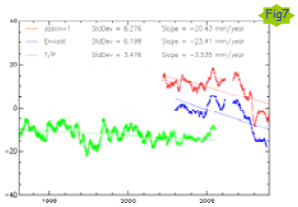

SLA differences for J1, Envisat and T/P missions for Pohnpei (fig.6) and Valparaiso (fig.7) tide gauges

Fig8

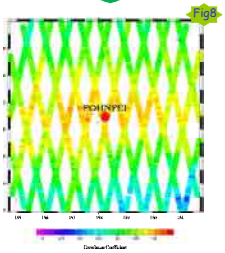

Fig9

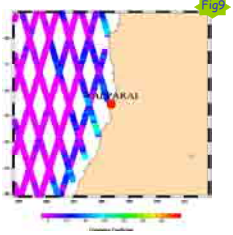

SSH correlation with Envisat for Pohnpei (fig.8) and Valparaiso (fig.9) tide gauges

Impact of new standards in the SSH consistency

This part aims at presenting the capability of the altimeter/tide gauges comparison procedure to measure the impact of new altimeter standards on the SSH consistency. The basic principle of the method is to compare the SLA consistency between altimeter and tide gauge data using successively the old and new standards in the altimeter SSH calculation. The main criteria used is the analyze of SLA variance differences.

In figure 5 is plotted the histogram of the variance SLA differences as function of the tide gauge number in order to estimate the impact of new editing criteria allowing to compute the SSH closer from the coasts.

Results provided explain how can be improved the consistency between altimeter data and in-situ measurements at the different tide gauge locations. Here the impact of the coastal editing flag is relevant, with a mean variance of 2 cm² for Envisat, which demonstrates the improvement of altimeter/in-situ SLAs consistency using this criterion.

Fig5

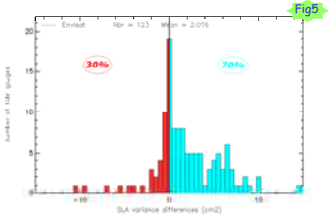

Histogram of SLA variance differences as function of the tide gauge number for Envisat, using successively the basic and the coastal editing flags

Conclusion

Thanks to the comparison of altimeter data with in-situ measurements, the MSL drift can be more precisely estimate. Moreover, the method presented here can provide a quality assessment on both altimeter and in-situ datasets through SSH comparisons.
To date, 3 limited points have to be investigated to give even better results:

- the way of computing vertical movements , by using more GPS at tide gauge location
- the correction of jumps in tide gauge time data series
- the errors on the method itself (especially the colocation with the nearest points on altimeter tracks)

Collecte Localisation Satellites
8-10 rue Hermes
31520 Ramonville Saint-Agne - France

OceanObs09
Venice, September 2009

9.3. Annex : Corrections applied for altimetric SSH calculation

All the corrections applied on SSH for TOPEX/Poseidon, Jason-1, Envisat, Geosat Follow-On and ERS-2 space altimetric missions are summarize in the following table. The geophysical corrections used are similar for all the missions and corresponds on the Jason-1 and Envisat products. However they are some exceptions. For instance the ECMWF model is used for the wet tropospheric correction to remove the relative drift due between each mission due to the radiometer correction. But for T/P the model is not stable until from the beginning of the mission in 1992 until 1999. The the the radiometer corrections with radiometer's drift correction (Scharroo et al, 2004) is applied for this mission. Moreover, there are specific correction due the particularities of each mission often linked to instrument anomalies.

Orbits and corrections	T/P[1]	J1[2]	EN[3]	G2[4]	E2[5]
POE Orbit	Nasa (M-GDR)	Cnes (GDR)	Cnes (GDR)	Nasa	DGME 04
Mono-mission orbital error	×	×	×	×	×
GOT 2000 v2 ocean tide with S1 and S2 waves atmospheric tide corrections	×	×	×	×	×
Terrestrial tide	×	×	×	×	×
Polar tide	×	×	×	×	×
Non-parametrical bias in main band	×	×	×	×	×
ECMWF dry tropospheric with S1 and S2 waves atmospheric tide corrections	×	×	×	×	×
Dynamical Atmospheric Correction (DAC)	×	×	×	×	×
CLS 2001 (v1) mean sea surface		×	×	×	×
TP radiometer's wet tropospheric correction with radiometer's drift correction	×				
ECMWF wet tropospheric correction on a gaussian grid			×		
ECMWF wet tropospheric correction on a cartesian grid				×	
TRO_HUM_RAD neuronal algorithm		×			×
DORIS main band ionospheric correction	×				
Main band filtered ionospheric correction for open ocean valid data	×	×	×		
GIM ionospheric correction			×	×	×
Main band BENT ionospheric correction					×
BM4 bias in main band	×				

.../...

Proprietary information : no part of this document may be reproduced divulged or used in any form without prior permission from CLS and CNES.

Orbits and corrections	T/P[1]	J1[2]	EN[3]	G2[4]	E2[5]
Bias between bifrequency and DORIS ionospheric correction	×				
Bias between TOPEX and Poseidon and between TOPEX A and TOPEX B	×				
USO drift correction			×		
Correction deducted from time-tag bias				×	×
E1/E2 SPTR 2000 bias (device power off)/USO drift					×

TAB. 1: *Corrections applied for altimetric SSH calculation*

[1]T/P : TOPEX/Poseidon
[2]J1 : Jason-1
[3]EN : Envisat
[4]G2 : Geosat Follow-On
[5]E2 : ERS-2

Proprietary information : no part of this document may be reproduced divulged or used in any form without prior permission from CLS and CNES.

9.4. Annex : Information cards for the Rodrigue and Cocos Island tide gauges

Proprietary information : no part of this document may be reproduced divulged or used in any form without prior permission from CLS and CNES.

TIDE GAUGE : WO0001

Tide Gauge identification

Tide Gauge Network	WOCE
Location (Lat/Lon)	6.99 deg / 158.24 deg
Time series coverage	From 01/01/1975 to 28/02/2010
Vertical movements drift	YES

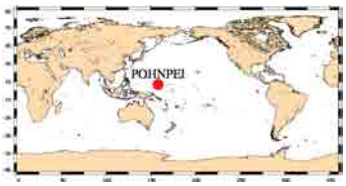

Temporal SSH comparisons with T/P, Envisat, Jason-1 and Jason-2

Monitoring of SSH

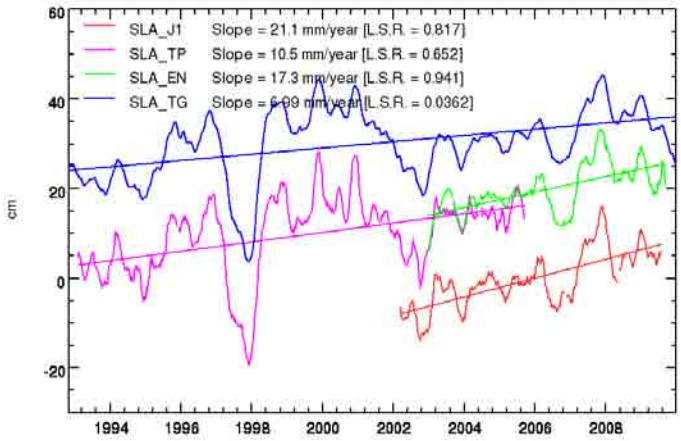

Monitoring of SSH differences

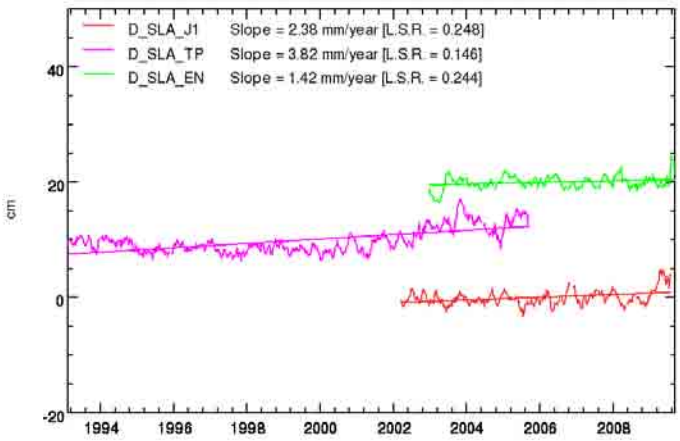

Maps of SSH correlation with Jason-1, T/P and Envisat

Jason-1 (initial phase)

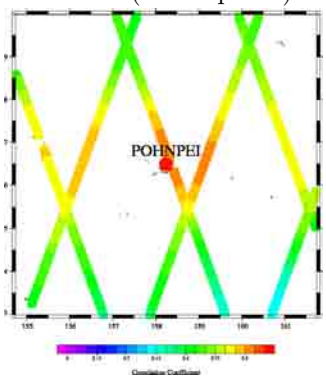

T/P (initial and tandem phase)

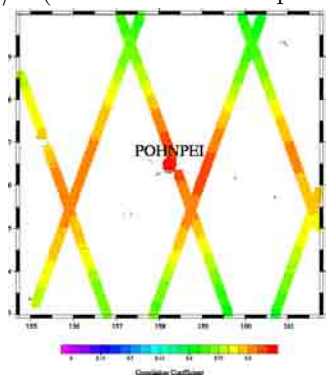

Envisat (until current cycle)

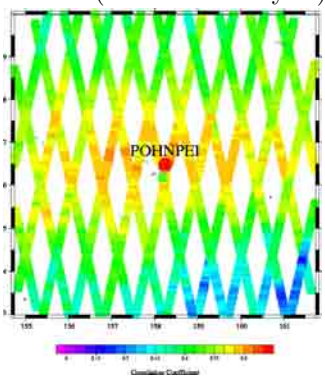

Tide Gauge reliability

	T/P	T/P (tandem)	Jason-1	Jason-2	Envisat
Minimal distance from TG	xx kms	xx kms	xx kms	xx kms	xx kms
TG crustal drift	-1.3 mm/yr	-1.3 mm/yr	-1.3 mm/yr	- mm/yr	-1.3 mm/yr
Maximal SSH correlation	0.96	0.88	0.93	-	0.92
Non-filtered SSH diff RMS	4.5 cm	5.4 cm	4.5 cm	- cm	3.9 cm
Filtered SSH diff RMS	1.1 cm	1.7 cm	1.5 cm	- cm	1 cm
SSH differences slope	-0.1 mm/yr	3.2 mm/yr	2.4 mm/yr	- mm/yr	1.4 mm/yr
Quality control	OK	OK	OK	-	OK

TIDE GAUGE : WO0081

Tide Gauge identification

Tide Gauge Network	WOCE
Location (Lat/Lon)	-33.03 deg / 288.37 deg
Time series coverage	From 01/01/1950 to 31/08/2009
Vertical movements drift	YES

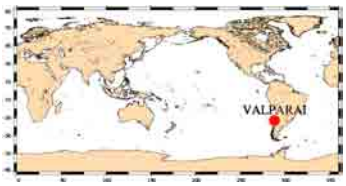

Temporal SSH comparisons with T/P, Envisat, Jason-1 and Jason-2

Monitoring of SSH

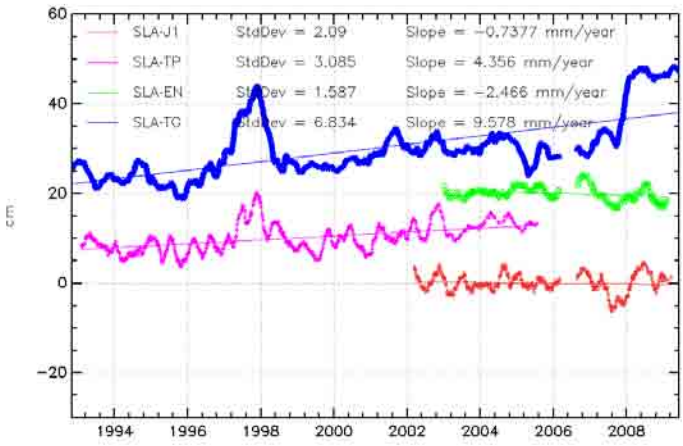

Monitoring of SSH differences

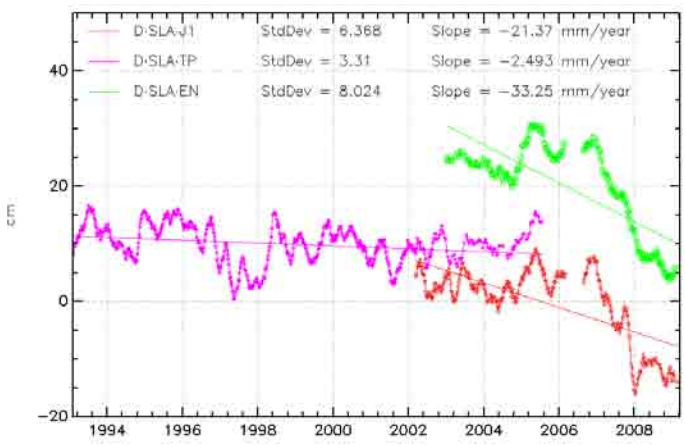

Maps of SSH correlation with Jason-1, T/P and Envisat

Jason-1 (initial phase)

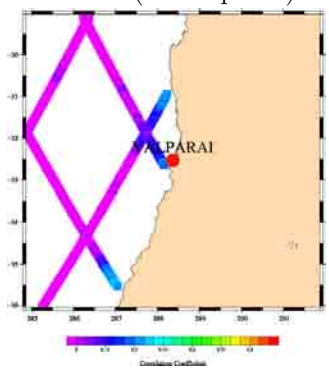

T/P (initial and tandem phase)

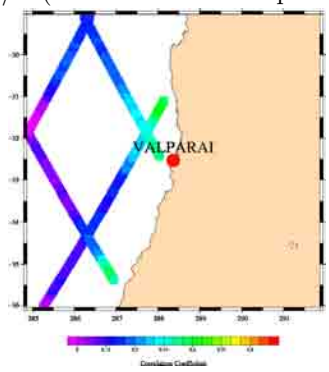

Envisat (until current cycle)

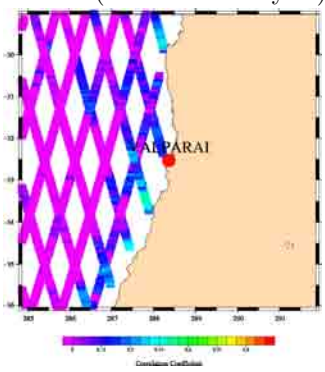

Tide Gauge reliability

	T/P	T/P (tandem)	Jason-1	Jason-2	Envisat
Minimal distance from TG	xx kms	xx kms	xx kms	xx kms	xx kms
TG crustal drift	-9.1 mm/yr	-9.1 mm/yr	-9.1 mm/yr	- mm/yr	-9.1 mm/yr
Maximal SSH correlation	0.64	0.73	0.39	-	0.51
Non-filtered SSH diff RMS	6.2 cm	7.1 cm	8.8 cm	- cm	11 cm
Filtered SSH diff RMS	3.5 cm	2.1 cm	6.4 cm	- cm	8.1 cm
SSH differences slope	-4.6 mm/yr	13.3 mm/yr	-21.4 mm/yr	- mm/yr	-33.3 mm/yr
Quality control	OK	OK	KO	-	KO

9.5. Annex : Jason-1 global monitoring report

Proprietary information : no part of this document may be reproduced divulged or used in any form without prior permission from CLS and CNES.

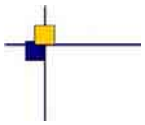

Rapport des Suivis de la chaîne CalVal

Mission j1 Dif / Cycle -1

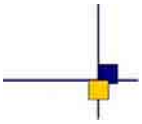

Référence : -
Nomenclature : -
Version : -
Date : 2010-06-04

Table des matières

1. Comparaison de la SLA de référence avec les mesures marégraphiques **5**

1.1. **Dérive de la SLA (non ajustée des signaux annuels et semi-annuels, sans pondération et avec calcul par boîtes pondéré par la latitude)** . . . 5

1.1.1. Suivi par cycle du champ SMOY_D_SLA_BIAIS_MSL_F . . . 5

1.1.2. Suivi par cycle du champ SMOY_D_SLA_BIAIS_MSL_F par hémisphère . . . 6

1.1.3. Suivi par cycle du champ SMOY_D_SLA_BIAIS_MSL_F par type de trace . . . 7

1.1.4. Suivi par cycle du champ SMOY_D_SLA_BIAIS_MSL_F Est/Ouest . . . 8

1.1.5. Suivi par cycle du champ SMOY_D_SLA_BIAIS_DERIVE_MSL_F . . . 9

1.2. **Dérive de la SLA (ajustée des signaux annuels et semi-annuels)** . . . 10

1.2.1. Suivi par cycle du champ SMOY_D_SLA_BIAIS_MSL_F . . . 10

1.2.2. Suivi par cycle du champ SMOY_D_SLA_BIAIS_DERIVE_MSL_F . . . 11

1.2.3. Histogrammes des écart-types des différences de SLA Alti/TG (avec prise en compte du biais marégraphique et avec/sans contrôle qualité) . . . 12

1.2.4. Suivis des écart-types des différences de SLA Alti/TG (avec prise en compte du biais marégraphique et avec contrôle qualité) . . . 13

2. Impact des SLA altimétriques secondaires **14**

2.1. **FLG_VAL** . . . 14

2.1.1. Dérive de la SLA (filtrée à 2 et 6 mois et non ajustée des signaux annuels et semi-annuels) . . . 14

2.1.2. Dérive de la SLA (filtrée à 2 et 6 mois et ajustée des signaux annuels et semi-annuels) 15

2.1.3. Histogrammes des différences de variance . . . 16

2.1.4. Suivis des différences de variance . . . 17

2.2. **TRO_HUM_ECMWF_G** . . . 18

2.2.1. Dérive de la SLA (filtrée à 2 et 6 mois et non ajustée des signaux annuels et semi-annuels) . . . 18

2.2.2. Dérive de la SLA (filtrée à 2 et 6 mois et ajustée des signaux annuels et semi-annuels) 19

2.2.3. Histogrammes des différences de variance . . . 20

2.2.4. Suivis des différences de variance . . . 21

2.3. **TRO_HUM_RAD** . . . 22

2.3.1. Dérive de la SLA (filtrée à 2 et 6 mois et non ajustée des signaux annuels et semi-annuels) . . . 22

2.3.2. Dérive de la SLA (filtrée à 2 et 6 mois et ajustée des signaux annuels et semi-annuels) 23

2.3.3. Histogrammes des différences de variance . . . 24

2.3.4. Suivis des différences de variance . . . 25

2.4. **EO_POE_C** . . . 26

2.4.1. Dérive de la SLA (filtrée à 2 et 6 mois et non ajustée des signaux annuels et semi-annuels) . . . 26

2.4.2. Dérive de la SLA (filtrée à 2 et 6 mois et ajustée des signaux annuels et semi-annuels) 27

2.4.3. Histogrammes des différences de variance . . . 28

2.4.4. Suivis des différences de variance . . . 29

3. Annexes **30**

3.1. **CLIPs utilisés** . . . 30

3.1.1. CLIP altimétrique . . . 30

3.1.2. SLA_REF . . . 30

3.2. **Description des champs** . . . 30

3.2.1. CLIP marégraphique . . . 31

3.2.2. SLA_TG . . . 31

3.3. **Description des champs** . . . 31

3.4. **Suivi de la SLA satellite colocalisée aux marégraphes** . . . 32

3.4.1. Suivi par cycle du champ SLA_SAT_QUAL_BRUTE . . . 32
3.4.2. Suivi par cycle du champ SLA_SAT_QUAL_VAL . . . 33
3.4.3. Suivi par cycle du champ SLA_SAT_QUAL_VAL_HN . . . 34
3.4.4. Suivi par cycle du champ SLA_SAT_QUAL_VAL_HS . . . 35
3.4.5. Suivi par cycle du champ SLA_SAT_QUAL_VAL_TrP . . . 36
3.4.6. Suivi par cycle du champ SLA_SAT_QUAL_VAL_TrI . . . 37
3.5. **Suivi de la SLA marégraphique non corrigée du biais entre les marégraphes et de la dérive crustale** . . . 38
3.5.1. Suivi par cycle du champ SLA_TG_QUAL_NOCORR_BRUTE . . . 38
3.5.2. Suivi par cycle du champ SLA_TG_QUAL_NOCORR_VAL . . . 39
3.5.3. Suivi par cycle du champ SLA_TG_QUAL_NOCORR_VAL_HN . . . 40
3.5.4. Suivi par cycle du champ SLA_TG_QUAL_NOCORR_VAL_HS . . . 41
3.5.5. Suivi par cycle du champ SLA_TG_QUAL_NOCORR_VAL_TrP . . . 42
3.5.6. Suivi par cycle du champ SLA_TG_QUAL_NOCORR_VAL_TrI . . . 43
3.5.7. Suivi par cycle du champ SLA_TG_QUAL_BIAIS_BRUTE . . . 44
3.5.8. Suivi par cycle du champ SLA_TG_QUAL_BIAIS_VAL . . . 45
3.5.9. Suivi par cycle du champ SLA_TG_QUAL_BIAIS_VAL_HN . . . 46
3.5.10. Suivi par cycle du champ SLA_TG_QUAL_BIAIS_VAL_HS . . . 47
3.5.11. Suivi par cycle du champ SLA_TG_QUAL_BIAIS_VAL_TrP . . . 48
3.5.12. Suivi par cycle du champ SLA_TG_QUAL_BIAIS_VAL_TrI . . . 49
3.5.13. Suivi par cycle du champ SLA_TG_QUAL_BIAIS_DERIVE_BRUTE . . . 50
3.5.14. Suivi par cycle du champ SLA_TG_QUAL_BIAIS_DERIVE_VAL . . . 51
3.5.15. Suivi par cycle du champ SLA_TG_QUAL_BIAIS_DERIVE_VAL_HN . . . 52
3.5.16. Suivi par cycle du champ SLA_TG_QUAL_BIAIS_DERIVE_VAL_HS . . . 53
3.5.17. Suivi par cycle du champ SLA_TG_QUAL_BIAIS_DERIVE_VAL_TrP . . . 54
3.5.18. Suivi par cycle du champ SLA_TG_QUAL_BIAIS_DERIVE_VAL_TrI . . . 55
3.6. **Suivi de la différence de SLA satellite et marégraphique sans correction du biais entre les marégraphes et sans la dérive crustale** . . . 56
3.6.1. Suivi par cycle du champ D_SLA_QUAL_NOCORR_BRUTE . . . 56
3.6.2. Suivi par cycle du champ D_SLA_QUAL_NOCORR_VAL . . . 57
3.6.3. Suivi par cycle du champ D_SLA_QUAL_NOCORR_VAL_HN . . . 58
3.6.4. Suivi par cycle du champ D_SLA_QUAL_NOCORR_VAL_HS . . . 59
3.6.5. Suivi par cycle du champ D_SLA_QUAL_NOCORR_VAL_TrP . . . 60
3.6.6. Suivi par cycle du champ D_SLA_QUAL_NOCORR_VAL_TrI . . . 61
3.6.7. Suivi par cycle du champ D_SLA_QUAL_BIAIS_BRUTE . . . 62
3.6.8. Suivi par cycle du champ D_SLA_QUAL_BIAIS_VAL . . . 63
3.6.9. Suivi par cycle du champ D_SLA_QUAL_BIAIS_VAL_HN . . . 64
3.6.10. Suivi par cycle du champ D_SLA_QUAL_BIAIS_VAL_HS . . . 65
3.6.11. Suivi par cycle du champ D_SLA_QUAL_BIAIS_VAL_TrP . . . 66
3.6.12. Suivi par cycle du champ D_SLA_QUAL_BIAIS_VAL_TrI . . . 67
3.6.13. Suivi par cycle du champ D_SLA_QUAL_BIAIS_DERIVE_BRUTE . . . 68
3.6.14. Suivi par cycle du champ D_SLA_QUAL_BIAIS_DERIVE_VAL . . . 69
3.6.15. Suivi par cycle du champ D_SLA_QUAL_BIAIS_DERIVE_V_HN . . . 70
3.6.16. Suivi par cycle du champ D_SLA_QUAL_BIAIS_DERIVE_V_HS . . . 71
3.6.17. Suivi par cycle du champ D_SLA_QUAL_BIAIS_DERIVE_V_TrP . . . 72
3.6.18. Suivi par cycle du champ D_SLA_QUAL_BIAIS_DERIVE_V_TrI . . . 73
3.7. **Suivi de la dérive liée aux mouvements verticaux** . . . 74
3.7.1. Suivi par cycle du champ DERIVE_TG . . . 74
3.8. **Suivi de la différence de SLA satellite et marégraphique avec application du contrôle qualité marégraphique et correction du biais entre les marégraphes et sans la dérive crustale (après filtrage et ajustement)** . . . 75
3.8.1. Suivi par cycle du champ SMOY_D_SLA_QUAL_BIAIS_VAL_F . . . 75

3.9. **Suivi de la différence de SLA satellite et marégraphique avec application du contrôle qualité marégraphique et correction du biais entre les marégraphes et de la dérive crustale (après filtrage et ajustement)** 76
3.9.1. Suivi par cycle du champ SMOY_D_SLA_QUAL_BIAIS_DERIVE_VAL_F 76

1. Comparaison de la SLA de référence avec les mesures marégraphiques

1.1. Dérive de la SLA (non ajustée des signaux annuels et semi-annuels, sans pondération et avec calcul par boîtes pondéré par la latitude)

1.1.1. Suivi par cycle du champ SMOY_D_SLA_BIAIS_MSL_F

11338 SMOY_D_SLA_BIAIS_MSL_F : Moyenne : Différence des hauteurs de mer validées et filtrées, altimétrique et marégraphique, avec application du contrôle qualité marégraphique et correction du biais (calcul des tendances du MSL)

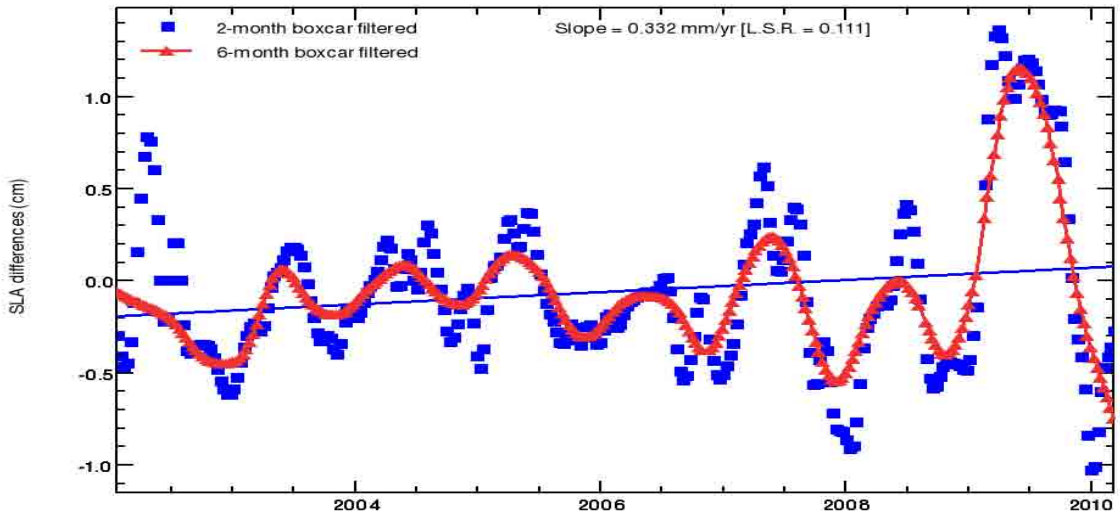

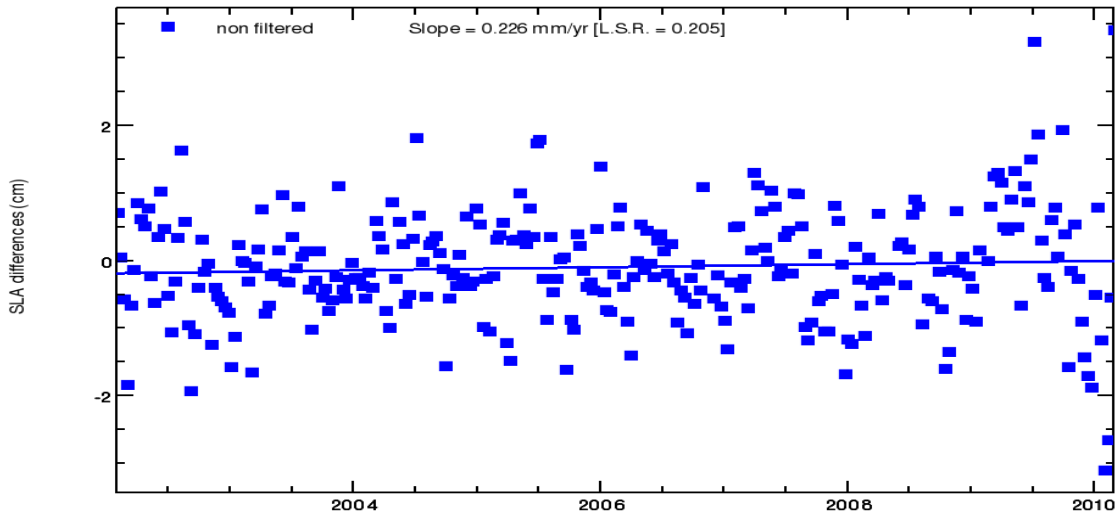

1.1.2. Suivi par cycle du champ SMOY_D_SLA_BIAIS_MSL_F par hémisphère

11565 SMOY_D_SLA_BIAIS_MSL_HN_F : Moyenne : Différence des hauteurs de mer alti/TG validées et filtrées, avec application du contrôle qualité marégraphique et correction du biais (calcul des tendances du MSL pour l'hémisphère Nord)

11566 SMOY_D_SLA_BIAIS_MSL_HS_F : Moyenne : Différence des hauteurs de mer alti/TG validées et filtrées, avec application du contrôle qualité marégraphique et correction du biais (calcul des tendances du MSL pour l'hémisphère Sud)

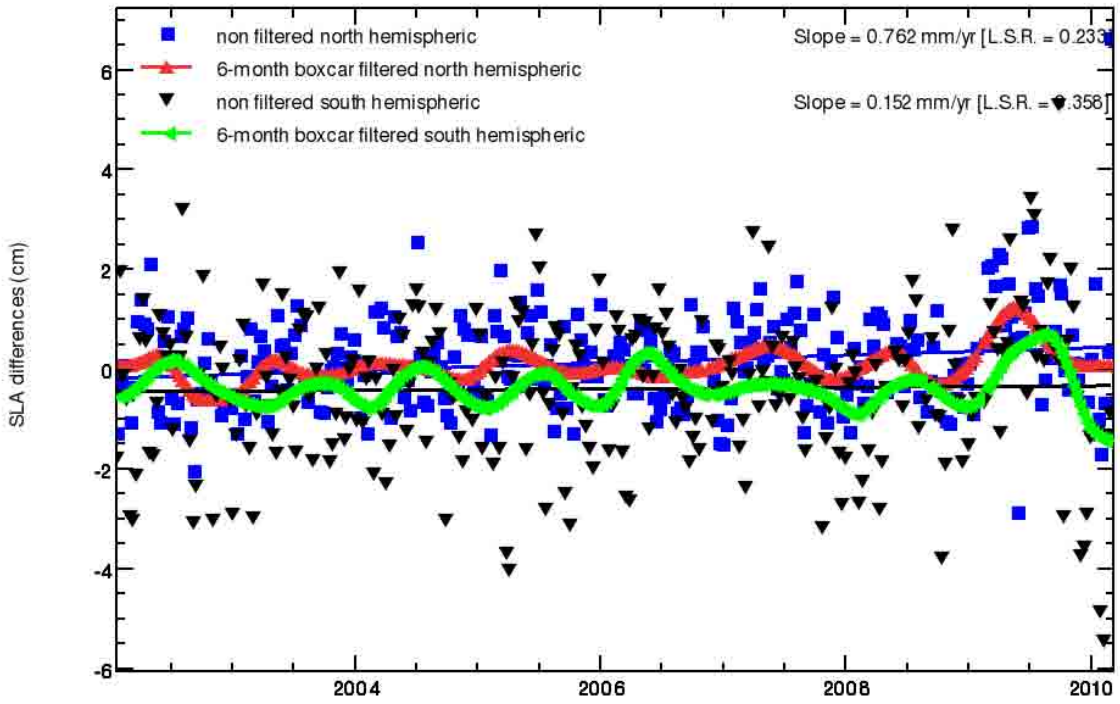

1.1.3. Suivi par cycle du champ SMOY_D_SLA_BIAIS_MSL_F par type de trace

11567 SMOY_D_SLA_BIAIS_MSL_TRP_F : Moyenne : Différence des hauteurs de mer alti/TG validées et filtrées, avec application du contrôle qualité marégraphique et correction du biais (calcul des tendances du MSL pour les traces paires)

11568 SMOY_D_SLA_BIAIS_MSL_TRI_F : Moyenne : Différence des hauteurs de mer alti/TG validées et filtrées, avec application du contrôle qualité marégraphique et correction du biais (calcul des tendances du MSL pour les traces impaires)

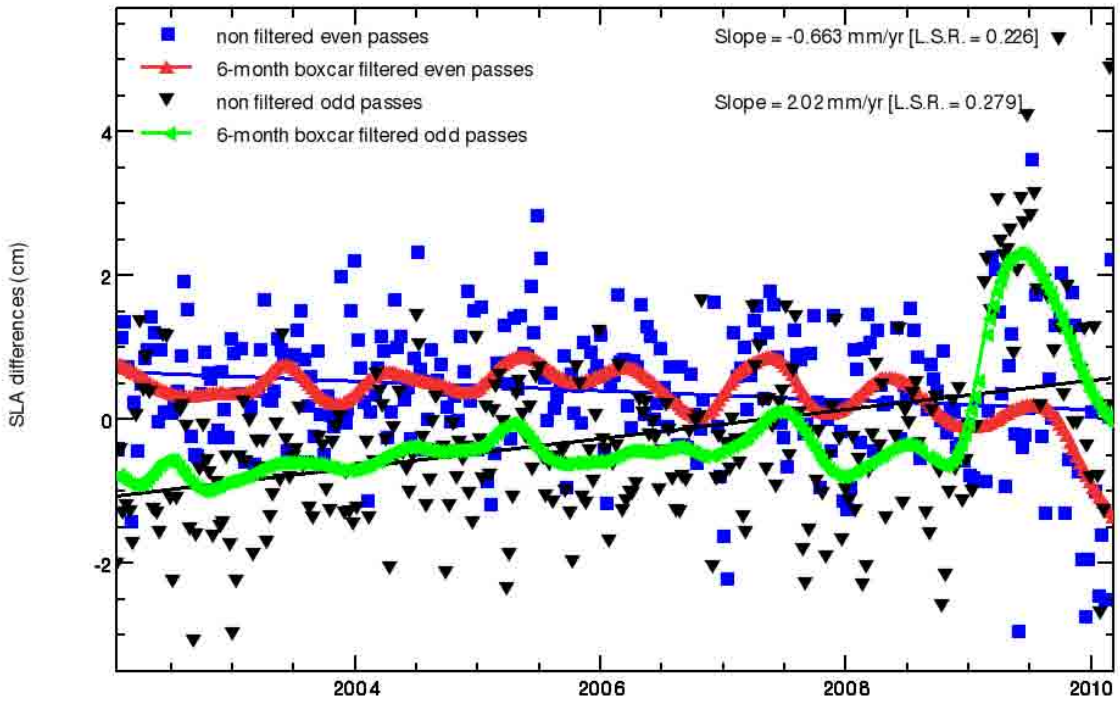

1.1.4. Suivi par cycle du champ SMOY_D_SLA_BIAIS_MSL_F Est/Ouest

11629 SMOY_D_SLA_BIAIS_MSL_HE_F : Moyenne : Différence des hauteurs de mer alti/TG validées et filtrées, avec application du contrôle qualité marégraphique et correction du biais (calcul des tendances du MSL - Est)

11630 SMOY_D_SLA_BIAIS_MSL_HW_F : Moyenne : Différence des hauteurs de mer alti/TG validées et filtrées, avec application du contrôle qualité marégraphique et correction du biais (calcul des tendances du MSL - Ouest)

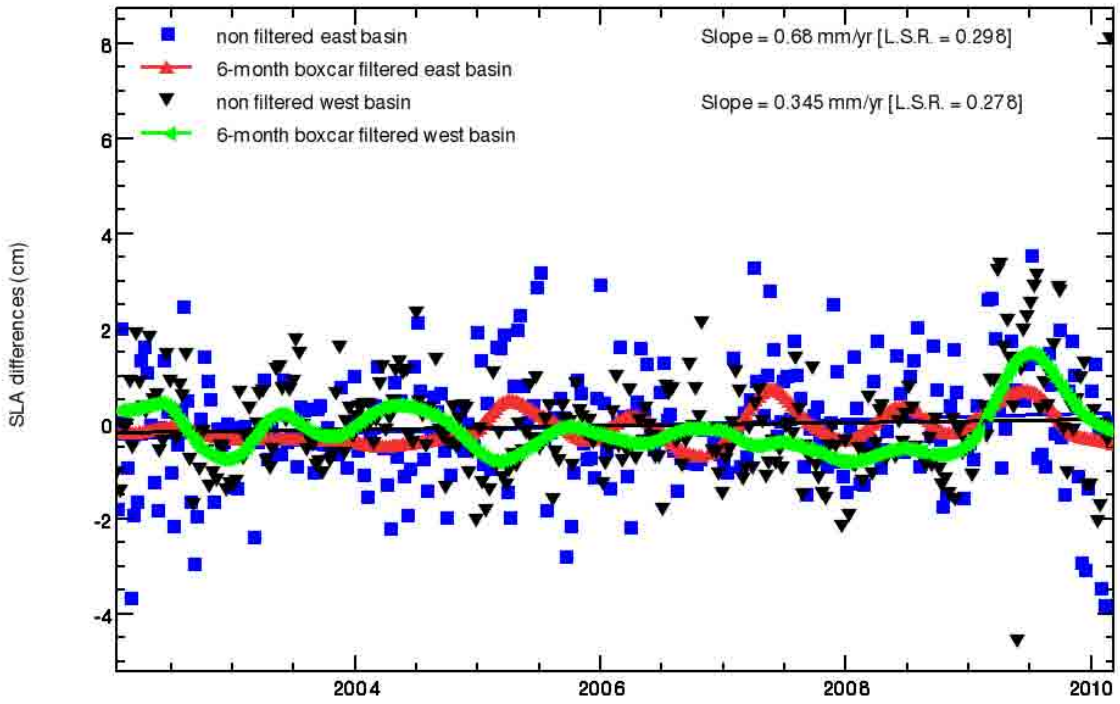

1.1.5. Suivi par cycle du champ SMOY_D_SLA_BIAIS_DERIVE_MSL_F

11339 SMOY_D_SLA_BIAIS_DERIVE_MSL_F : Moyenne : Différence des hauteurs de mer validées et filtrées, altimétrique et marégraphique, avec application du contrôle qualité marégraphique et correction du biais et de la dérive (calcul de la dérive des tendances du MSL)

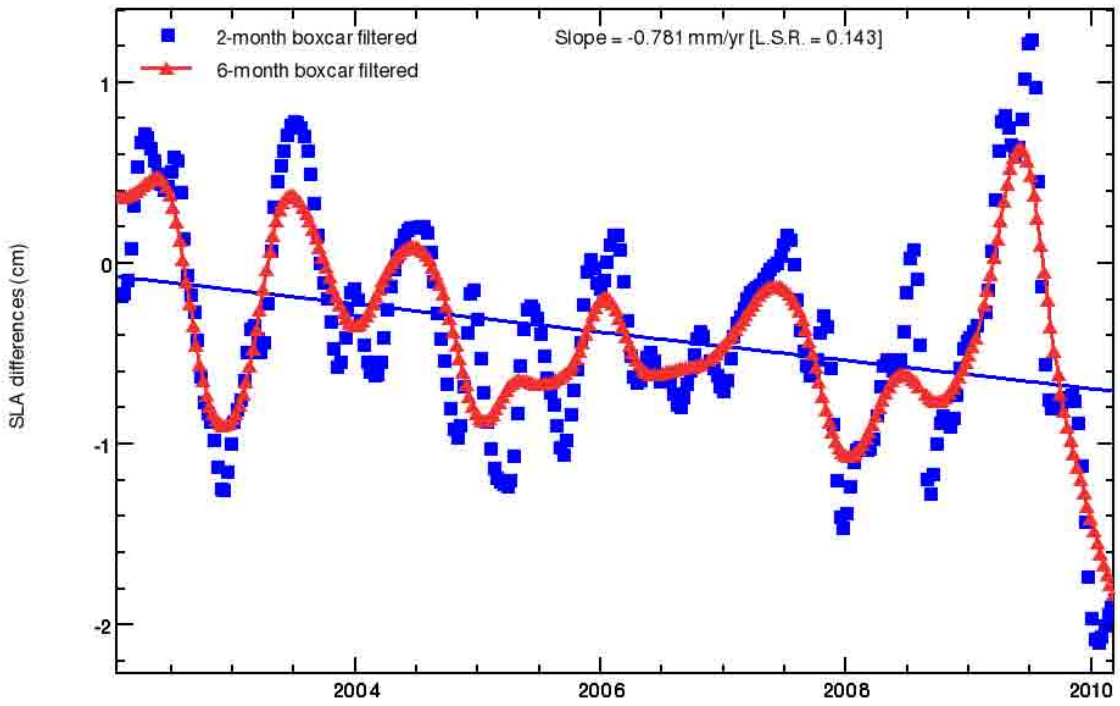

1.2. Dérive de la SLA (ajustée des signaux annuels et semi-annuels)

1.2.1. Suivi par cycle du champ SMOY_D_SLA_BIAIS_MSL_F

11338 SMOY_D_SLA_BIAIS_MSL_F : Moyenne : Différence des hauteurs de mer validées et filtrées, altimétrique et marégraphique, avec application du contrôle qualité marégraphique et correction du biais (calcul des tendances du MSL)

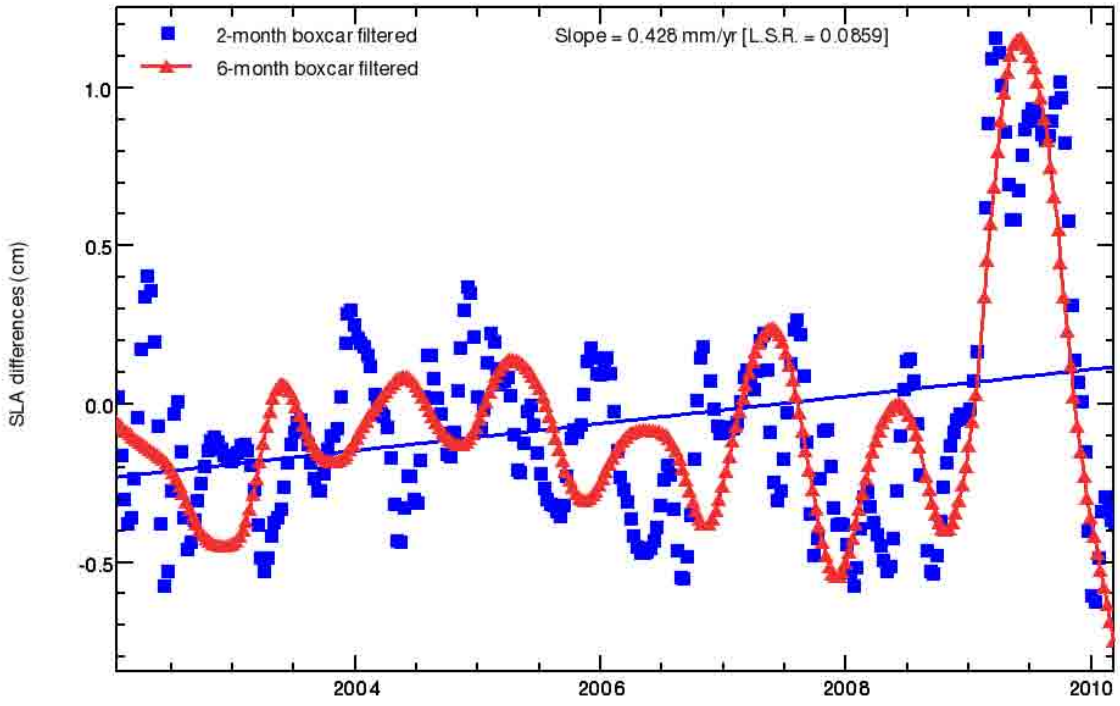

1.2.2. Suivi par cycle du champ SMOY_D_SLA_BIAIS_DERIVE_MSL_F

11339 SMOY_D_SLA_BIAIS_DERIVE_MSL_F : Moyenne : Différence des hauteurs de mer validées et filtrées, altimétrique et marégraphique, avec application du contrôle qualité marégraphique et correction du biais et de la dérive (calcul de la dérive des tendances du MSL)

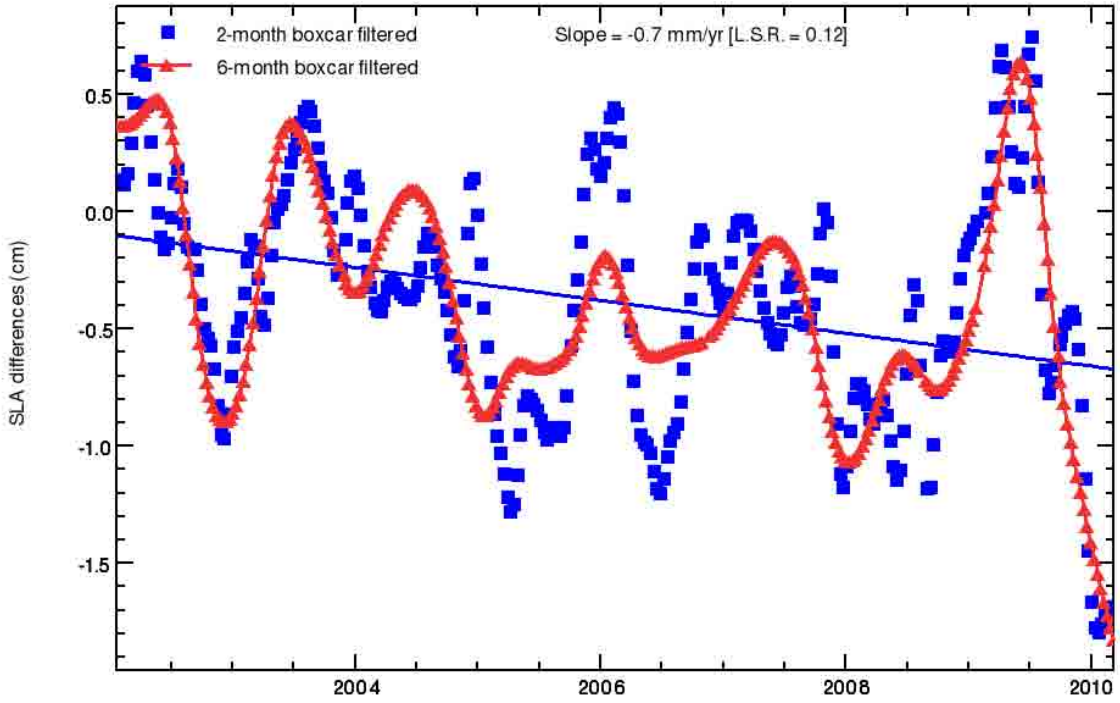

1.2.3. Histogrammes des écart-types des différences de SLA Alti/TG (avec prise en compte du biais marégraphique et avec/sans contrôle qualité)

16177 SECT_D_SLA_BIAIS_VALIDE : Ecart type : Différence des hauteurs de mer validées, altimétrique et marégraphique, avec correction du biais

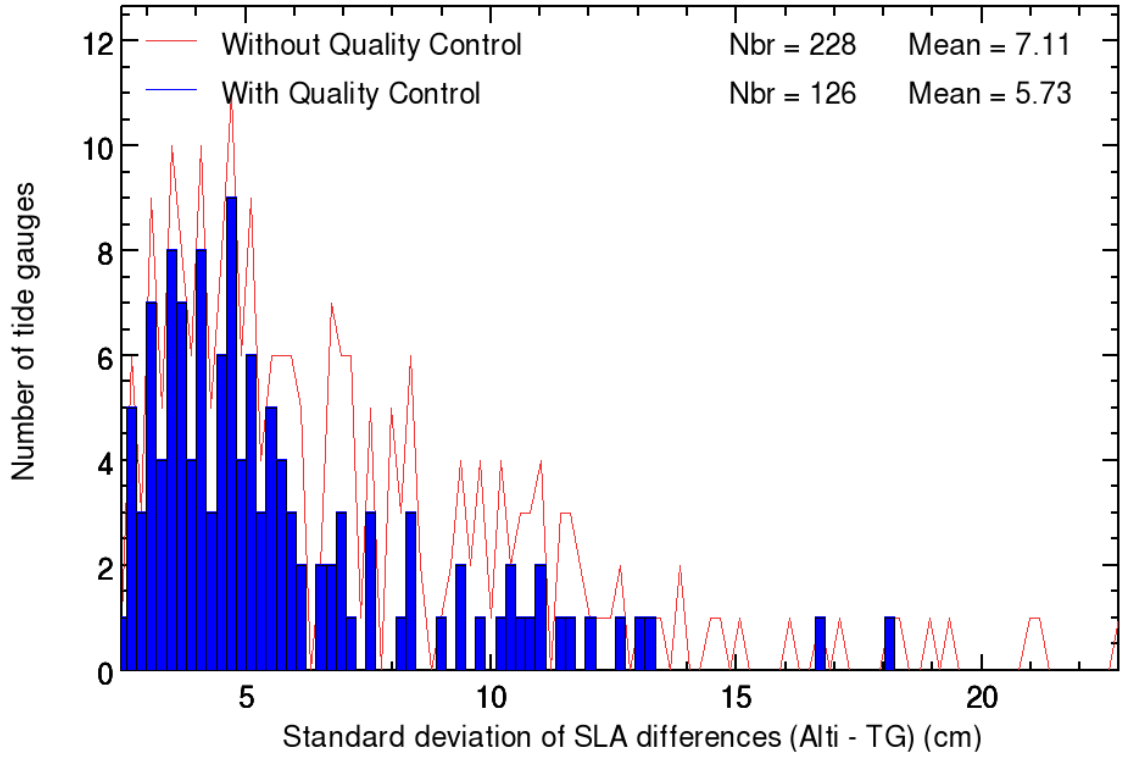

1.2.4. Suivis des écart-types des différences de SLA Alti/TG (avec prise en compte du biais marégraphique et avec contrôle qualité)

16338 SECT_D_SLA_BIAIS_MSL_F : Ecart type : Différence des hauteurs de mer validées et filtrées, altimétrique et marégraphique, avec application du contrôle qualité marégraphique et correction du biais (calcul des tendances du MSL)

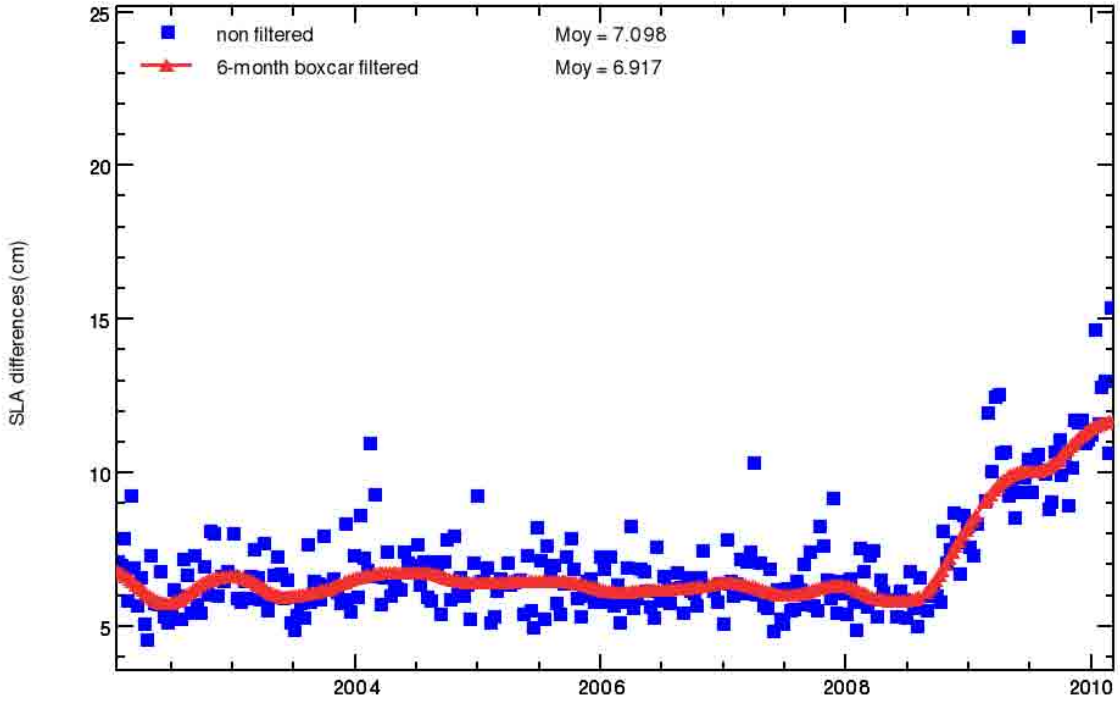

2. Impact des SLA altimétriques secondaires

2.1. FLG_VAL

2.1.1. Dérive de la SLA (filtrée à 2 et 6 mois et non ajustée des signaux annuels et semi-annuels)

1553 D_SLA1_QUAL_BIAIS_VAL : Différence des hauteurs de mer alti/TG validées (avec FLG_VAL) avec application du contrôle qualité marégraphique et correction du biais

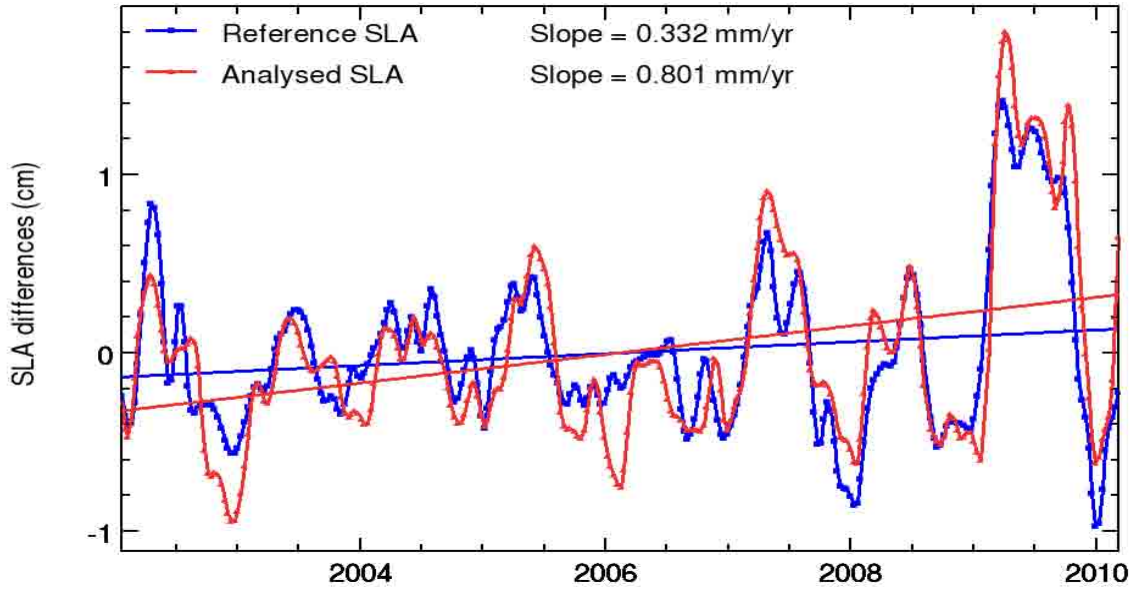

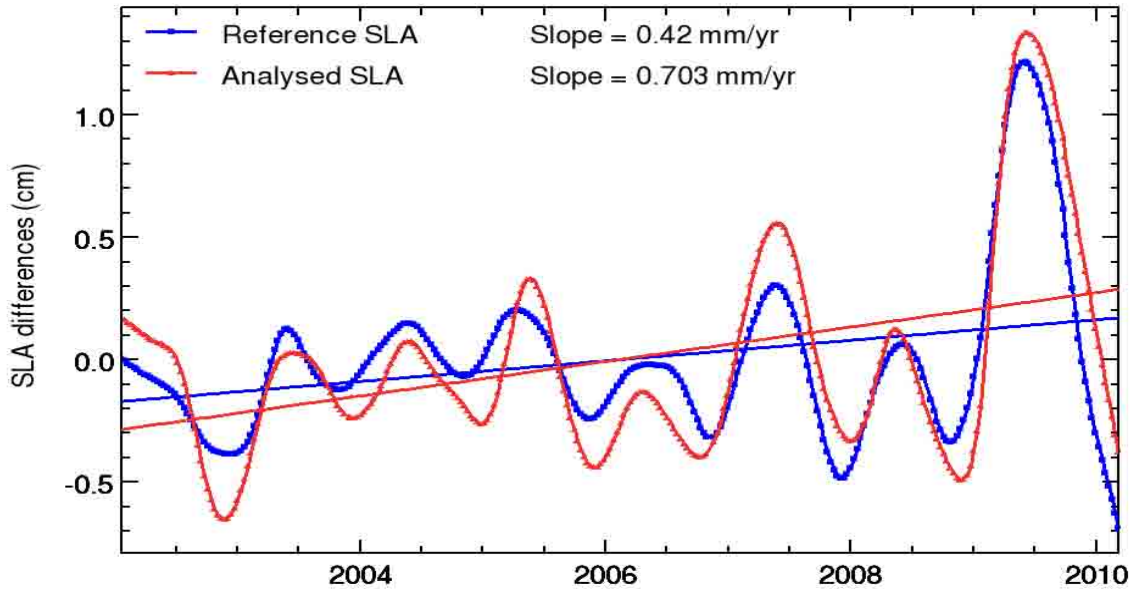

2.1.2. Dérive de la SLA (filtrée à 2 et 6 mois et ajustée des signaux annuels et semi-annuels)

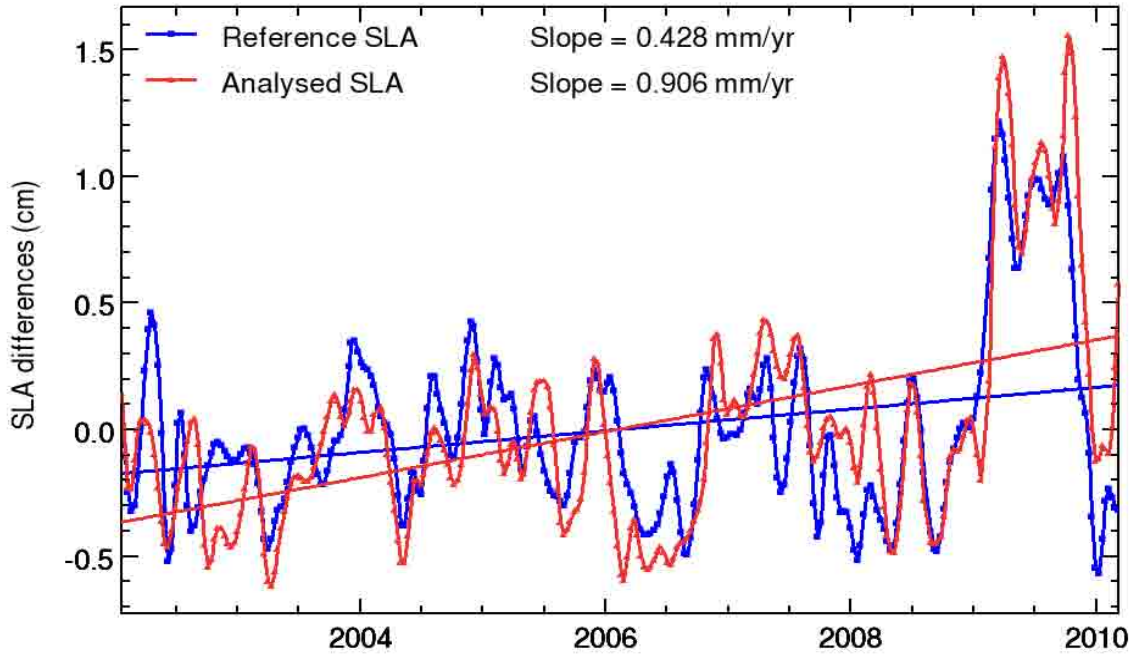

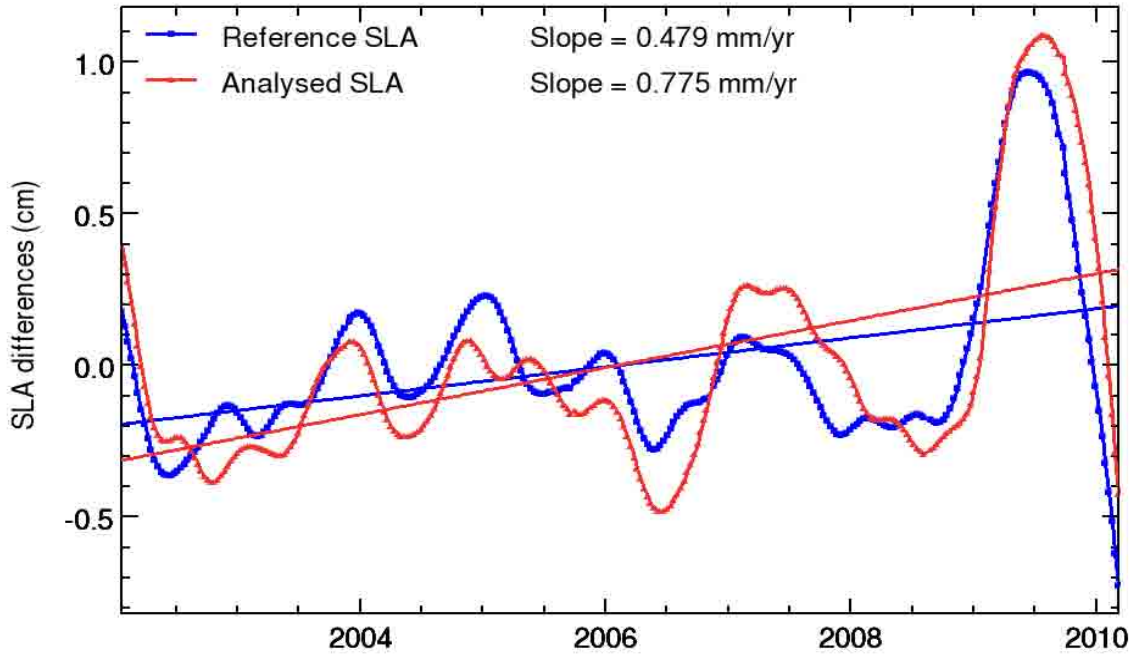

2.1.3. Histogrammes des différences de variance

La figure suivante présente les différences de variance SLA Alti/TG en utilisant successivement FLG_VAL et FLG_VAL_COTIER dans le calcul de la SLA altimétrique.
Le gain en variance est alors la différence entre :
- la variance de la différence entre la SLA altimétrique calculée avec FLG_VAL et la SLA des marégraphes
- la variance de la différence entre la SLA altimétrique calculée avec FLG_VAL_COTIER et la SLA des marégraphes

Des valeurs positives signifient que la SLA altimétrique utilisant FLG_VAL_COTIER est plus cohérente avec la SLA marégraphique que la SLA altimétrique utilisant FLG_VAL et inversement. Des valeurs négatives signifient alors que l'utilisation de FLG_VAL pour le calcul de la SLA altimétrique reduit la variance (de la différence entre les SLA altimétrique et marégraphique).

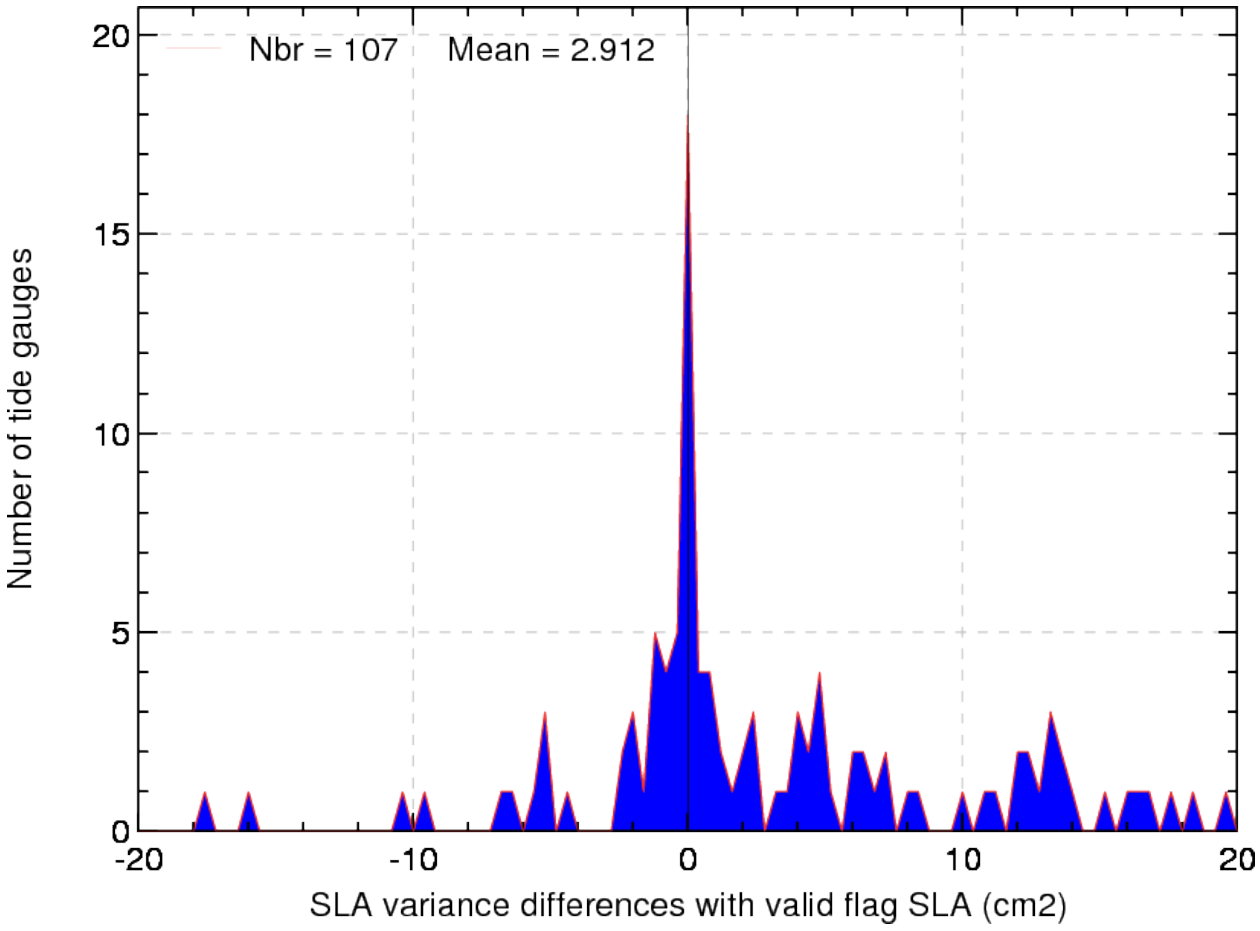

2.1.4. Suivis des différences de variance

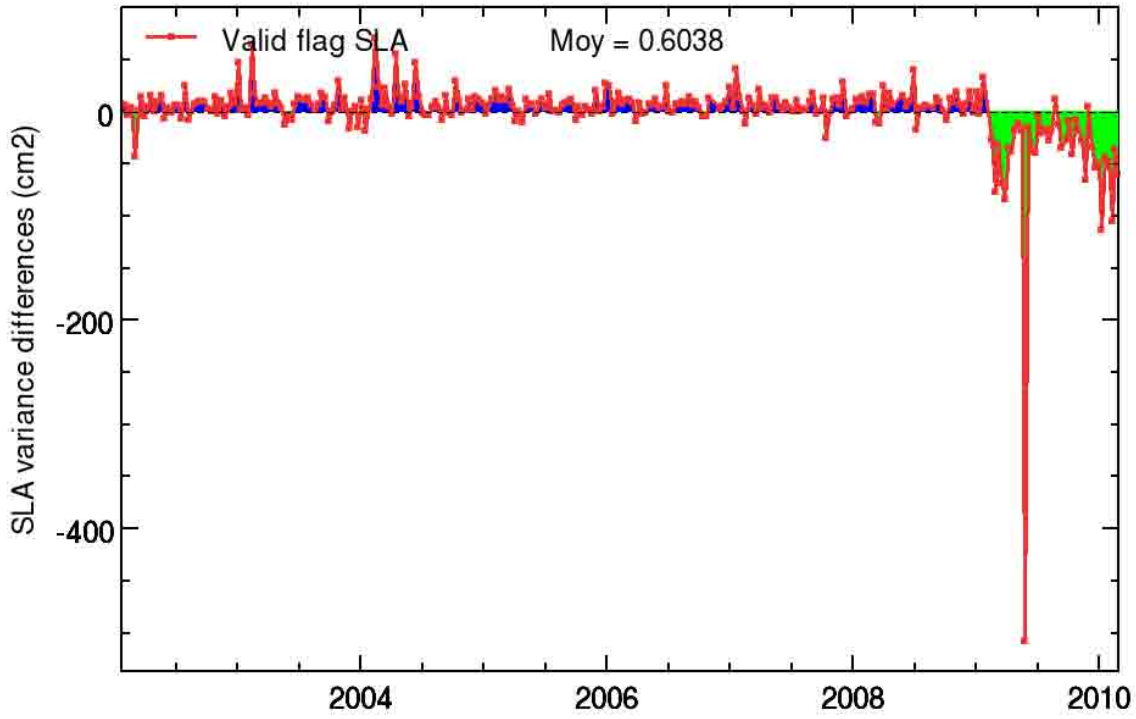

2.2. TRO_HUM_ECMWF_G

2.2.1. Dérive de la SLA (filtrée à 2 et 6 mois et non ajustée des signaux annuels et semi-annuels)

1554 D_SLA1_SL_QUAL_BIAIS_VAL : Différence des hauteurs de mer alti/TG validées (avec FLG_VAL_COTIER et TRO_HUM_ECMWF_G) avec application du contrôle qualité marégraphique et correction du biais

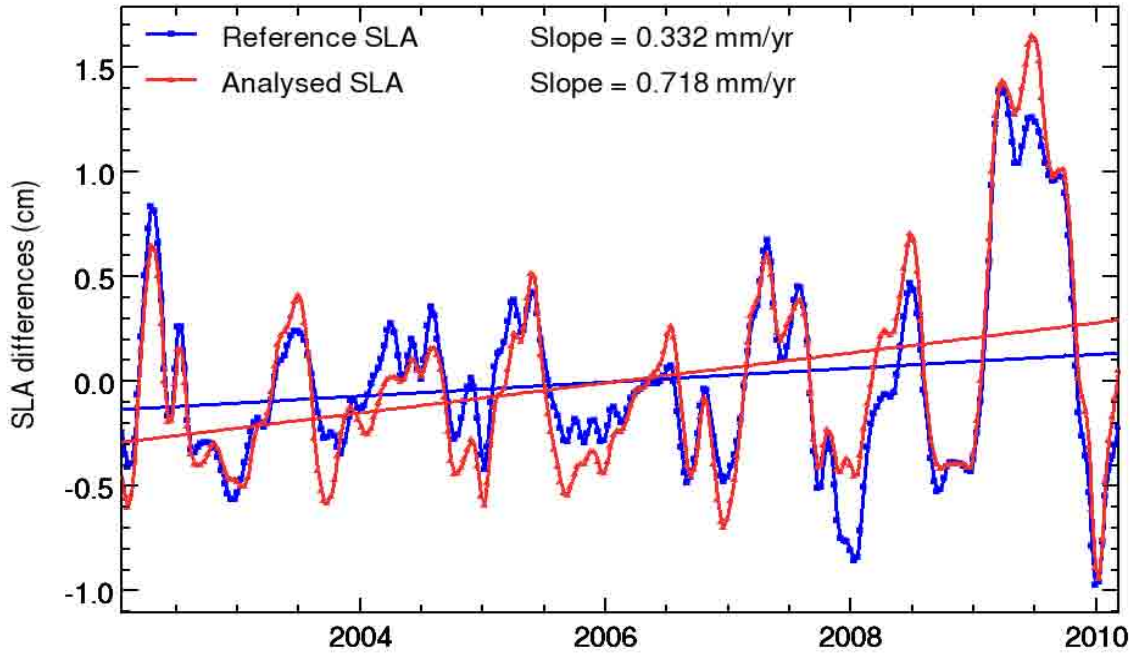

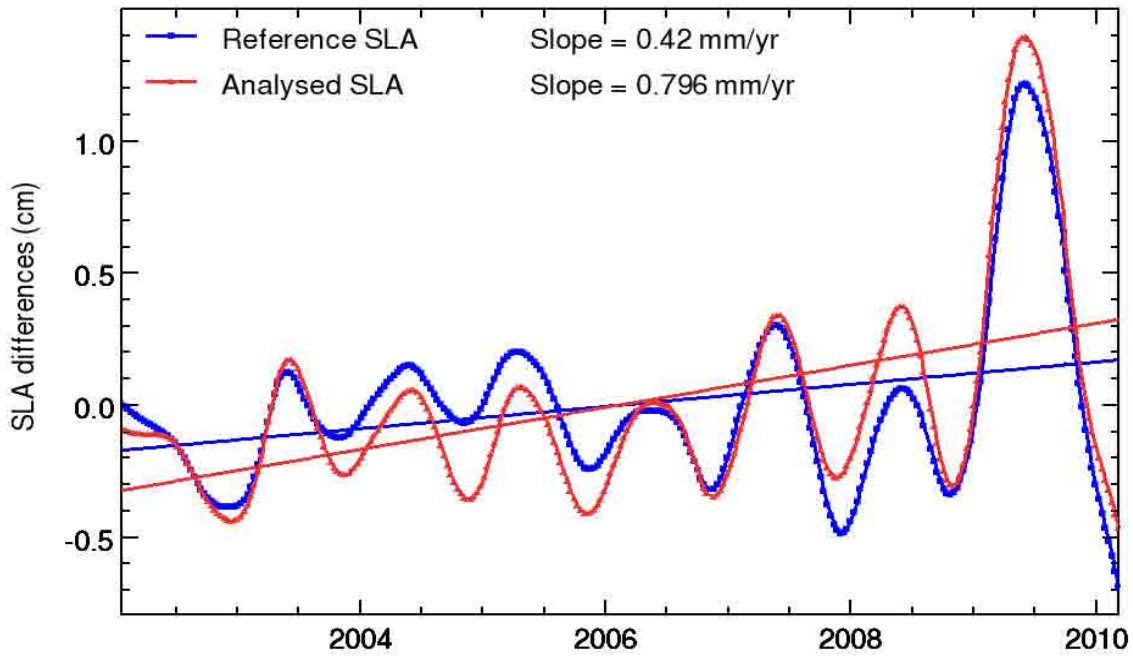

2.2.2. Dérive de la SLA (filtrée à 2 et 6 mois et ajustée des signaux annuels et semi-annuels)

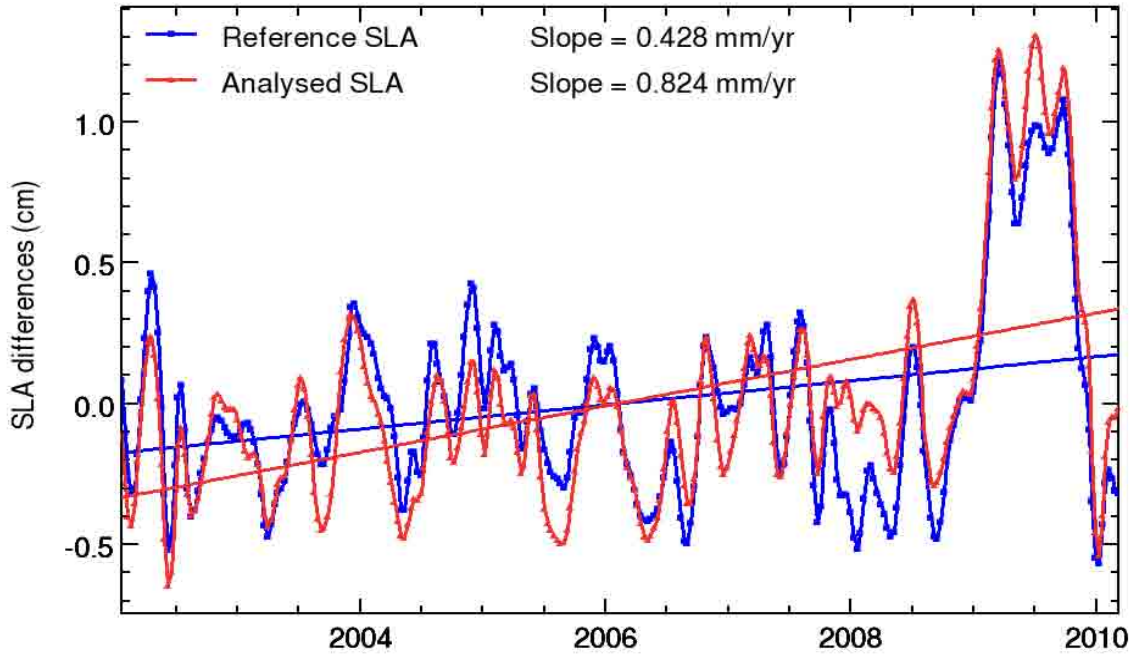

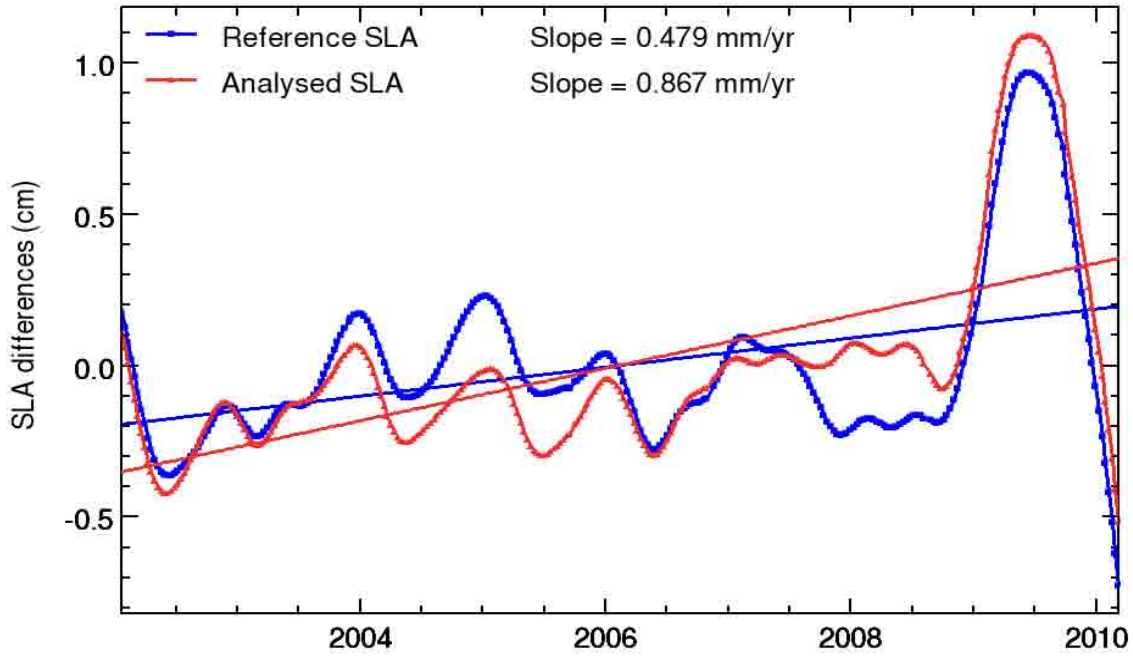

2.2.3. Histogrammes des différences de variance

La figure suivante présente les différences de variance SLA Alti/TG en utilisant successivement TRO_HUM_ECMWF et
TRO_HUM_COMPOSITE dans le calcul de la SLA altimétrique.
Le gain en variance est alors la différence entre :
- la variance de la différence entre la SLA altimétrique calculée avec TRO_HUM_ECMWF_G et la SLA des marégraphes
- la variance de la différence entre la SLA altimétrique calculée avec TRO_HUM_COMPOSITE et la SLA des marégraphes

Des valeurs positives signifient que la SLA altimétrique utilisant TRO_HUM_COMPOSITE est plus cohérente avec la SLA marégraphique que la SLA altimétrique utilisant TRO_HUM_ECMWF_G et inversement. Des valeurs négatives signifient alors que l'utilisation de TRO_HUM_ECMWF_G pour le calcul de la SLA altimétrique reduit la variance (de la différence entre les SLA altimétrique et marégraphique).

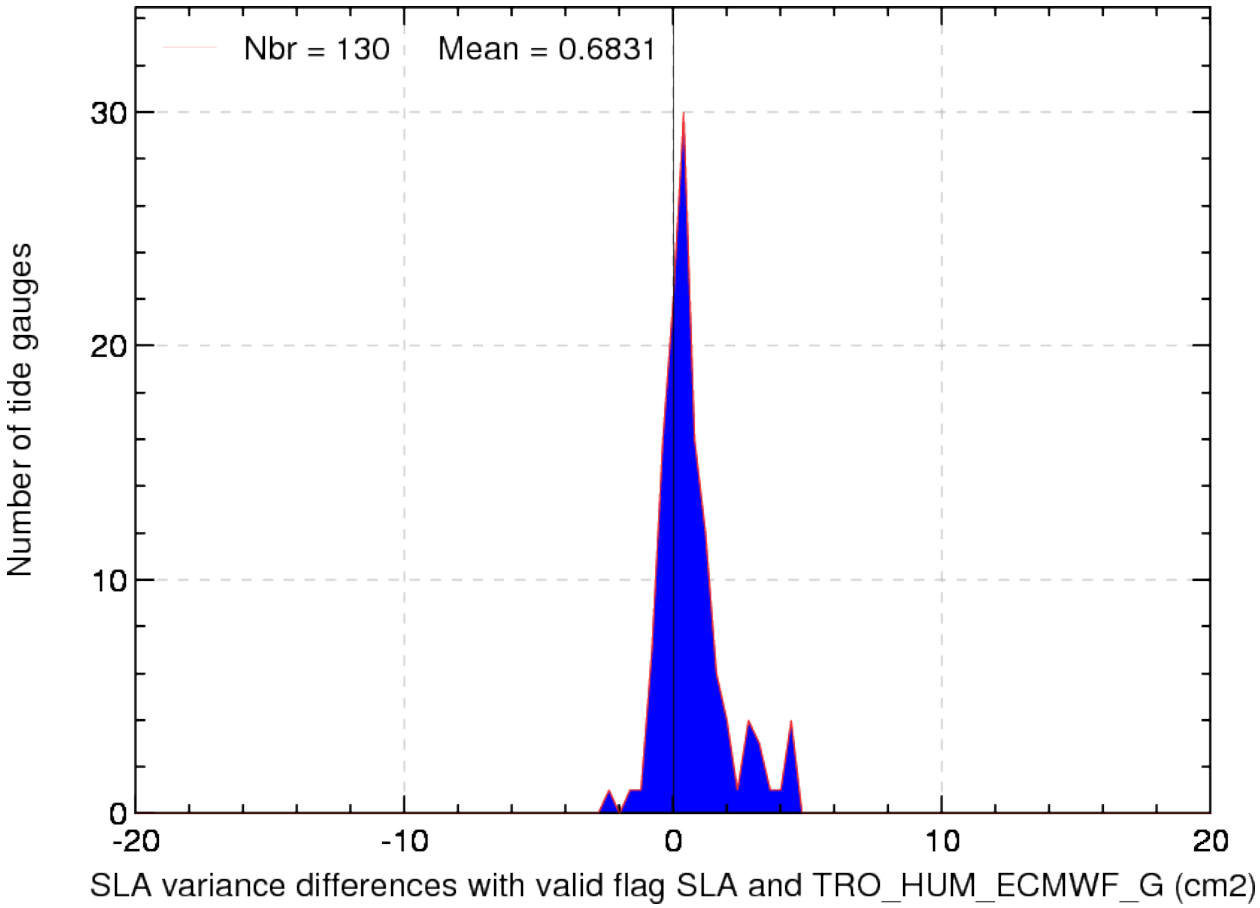

2.2.4. Suivis des différences de variance

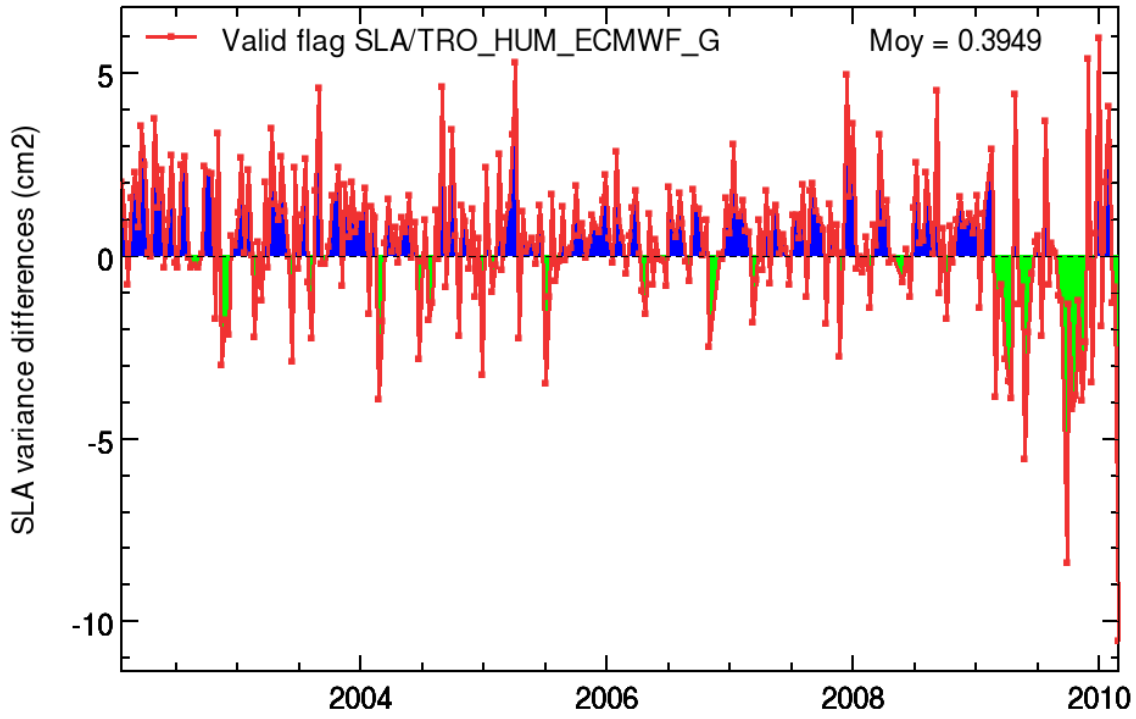

2.3. TRO_HUM_RAD

2.3.1. Dérive de la SLA (filtrée à 2 et 6 mois et non ajustée des signaux annuels et semi-annuels)

1555 D_SLA1_SL2_QUAL_BIAIS_VAL : Différence des hauteurs de mer alti/TG validées (avec FLG_VAL et TRO_HUM_RAD) avec application du contrôle qualité marégraphique et correction du biais

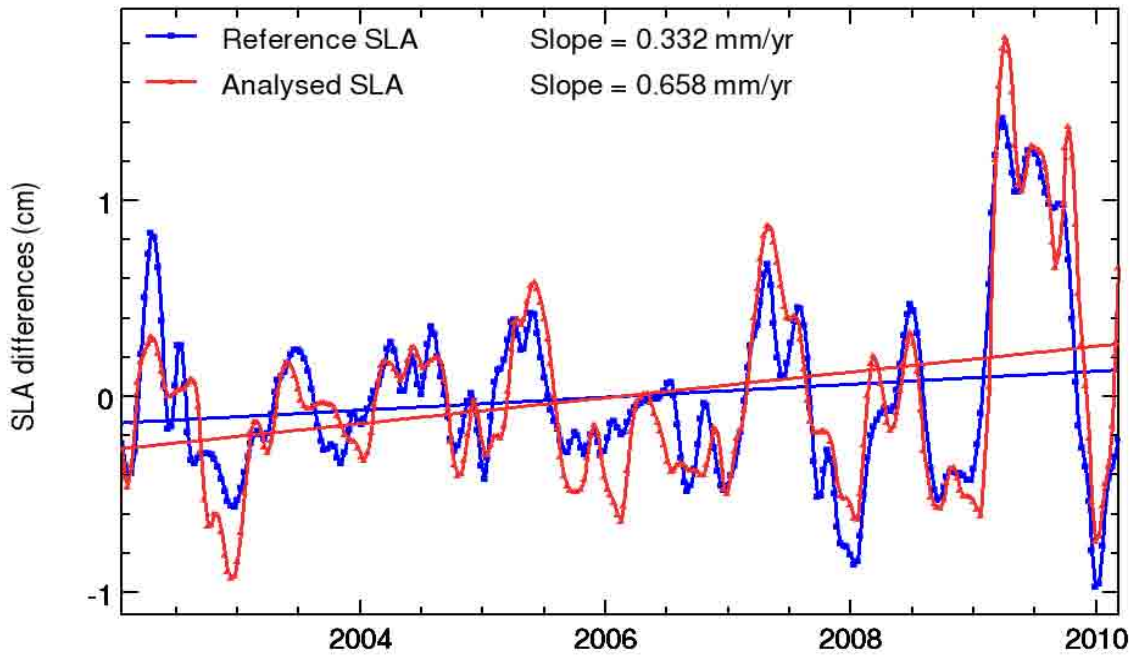

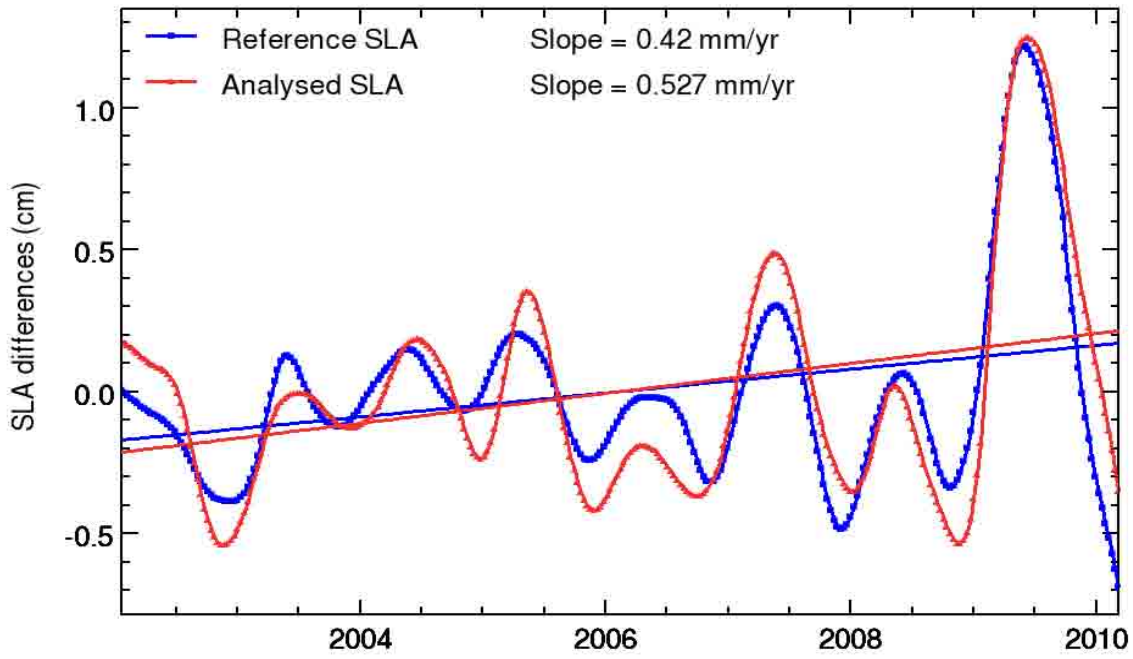

2.3.2. Dérive de la SLA (filtrée à 2 et 6 mois et ajustée des signaux annuels et semi-annuels)

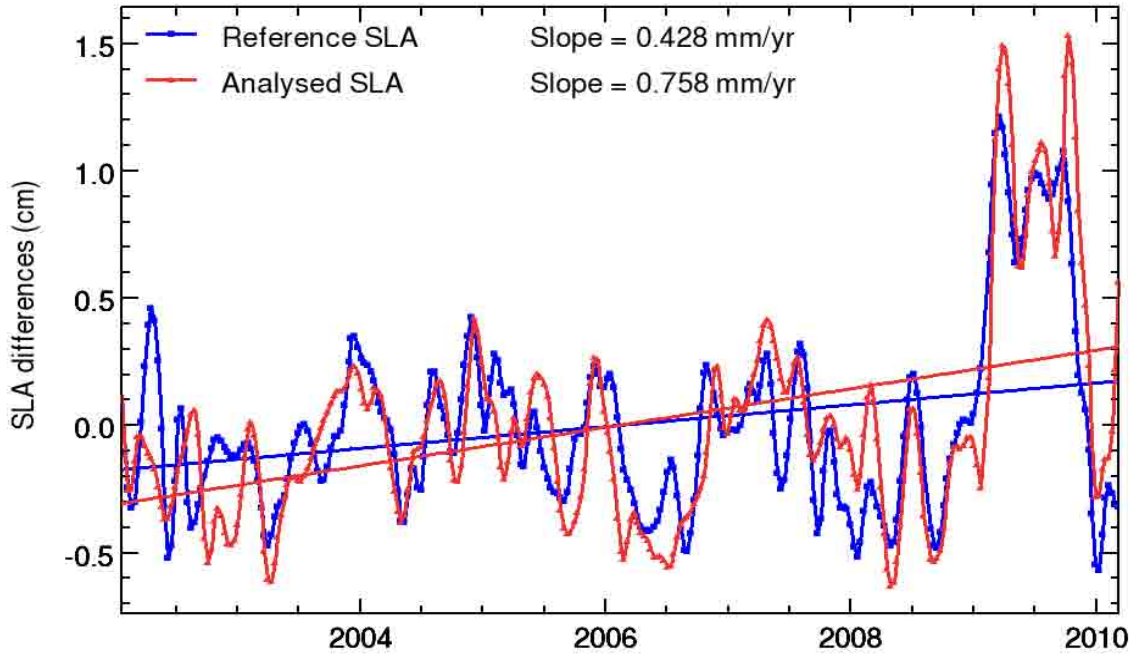

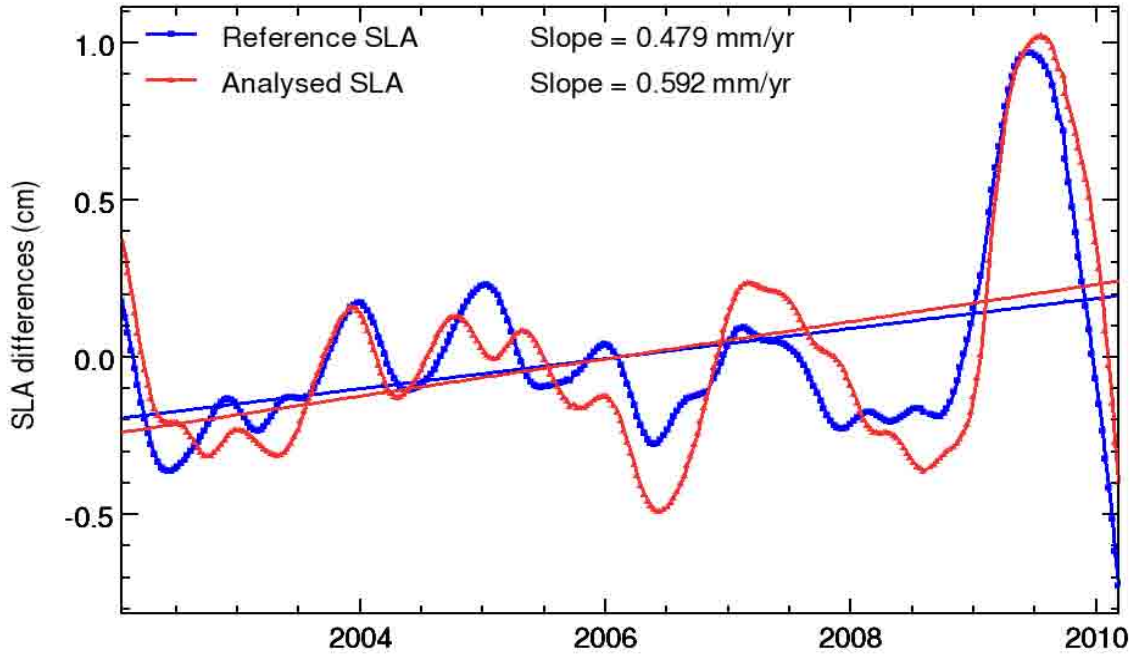

2.3.3. Histogrammes des différences de variance

La figure suivante présente les différences de variance SLA Alti/TG en utilisant successivement TRO_HUM_RAD et
TRO_HUM_COMPOSITE dans le calcul de la SLA altimétrique.
Le gain en variance est alors la différence entre :
- la variance de la différence entre la SLA altimétrique calculée avec TRO_HUM_RAD et la SLA des marégraphes
- la variance de la différence entre la SLA altimétrique calculée avec TRO_HUM_COMPOSITE et la SLA des marégraphes
Des valeurs positives signifient que la SLA altimétrique utilisant TRO_HUM_COMPOSITE est plus cohérente avec la SLA marégraphique que la SLA altimétrique utilisant TRO_HUM_RAD et inversement. Des valeurs négatives signifient alors que l'utilisation de TRO_HUM_RAD pour le calcul de la SLA altimétrique reduit la variance (de la différence entre les SLA altimétrique et marégraphique).

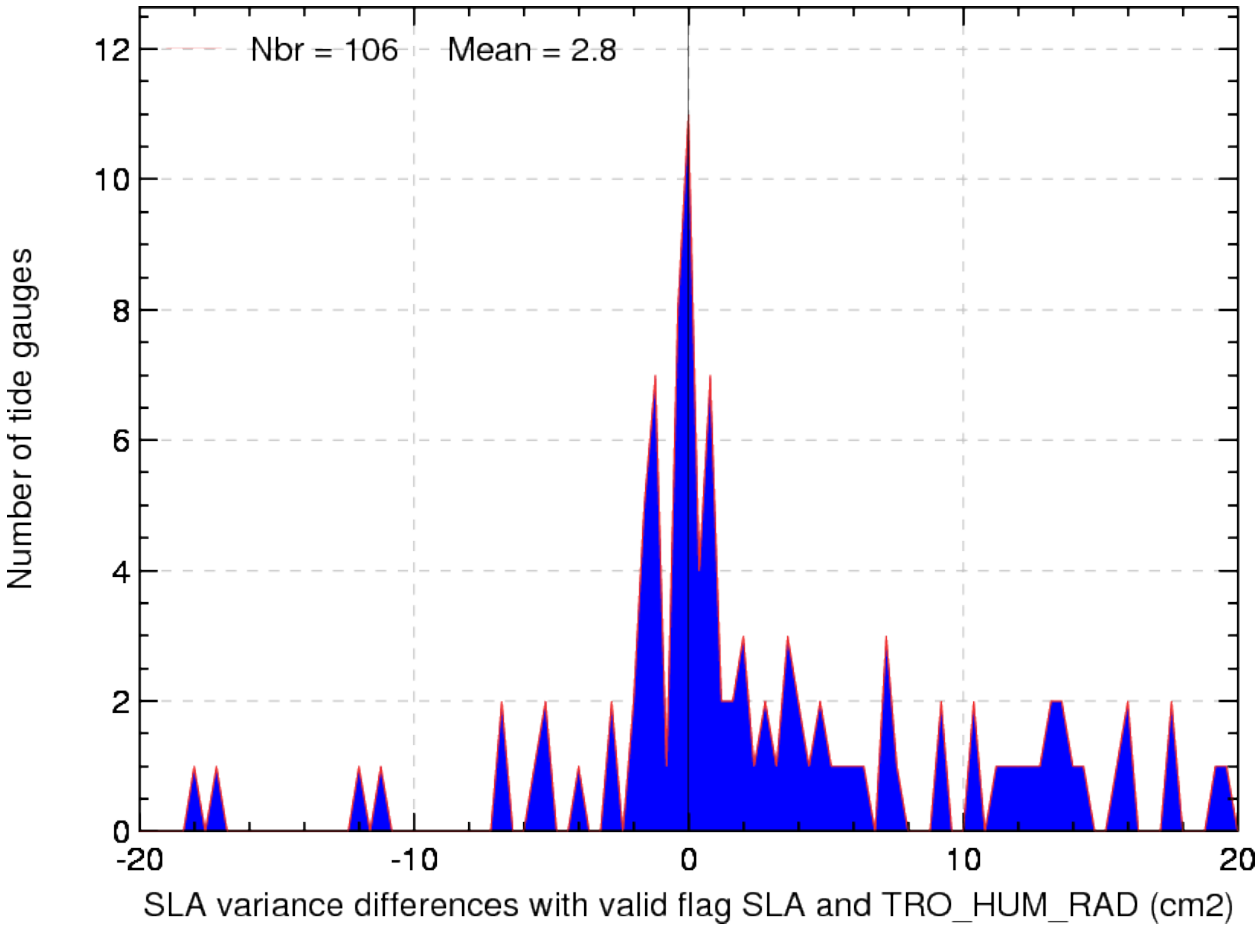

2.3.4. Suivis des différences de variance

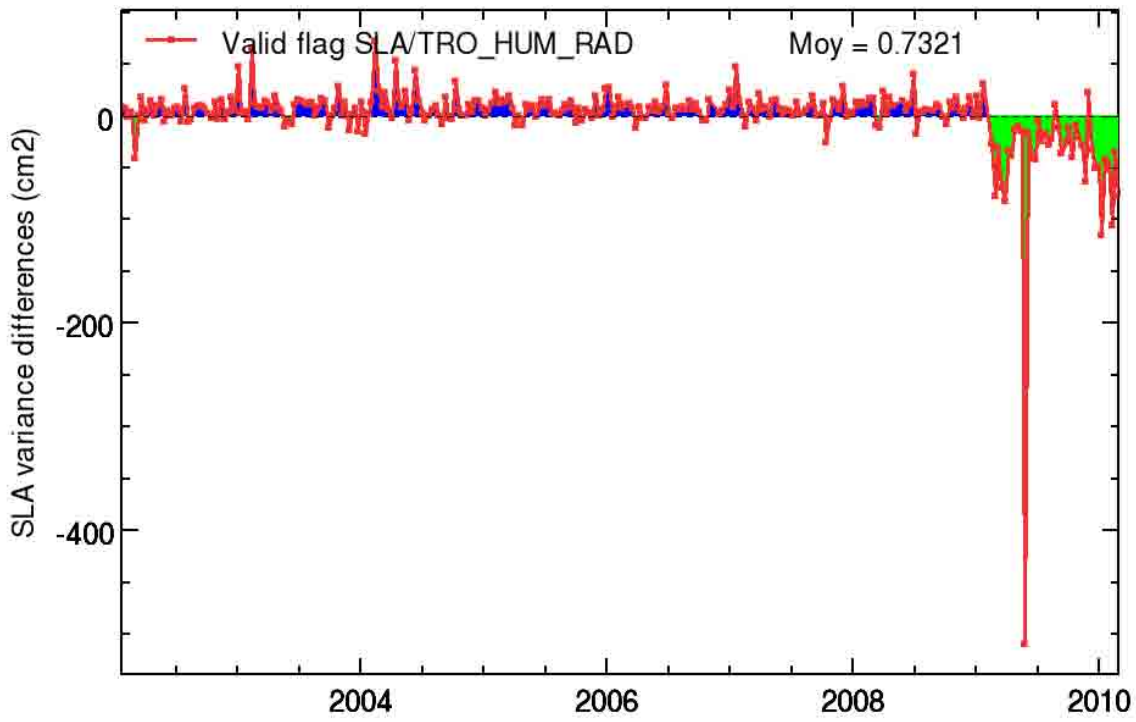

2.4. EO_POE_C

2.4.1. Dérive de la SLA (filtrée à 2 et 6 mois et non ajustée des signaux annuels et semi-annuels)

1556 D_SLA1_EO_QUAL_BIAIS_VAL : Différence des hauteurs de mer alti/TG validées (avec FLG_VAL_COTIER et EO_POE_C) avec application du contrôle qualité marégraphique et correction du biais

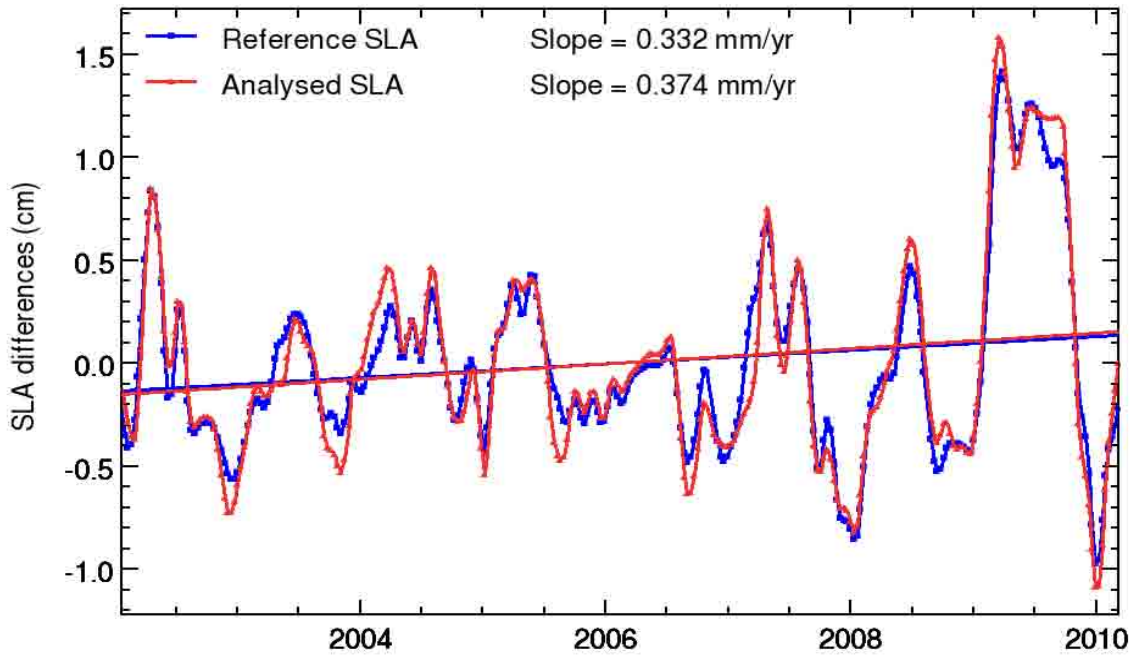

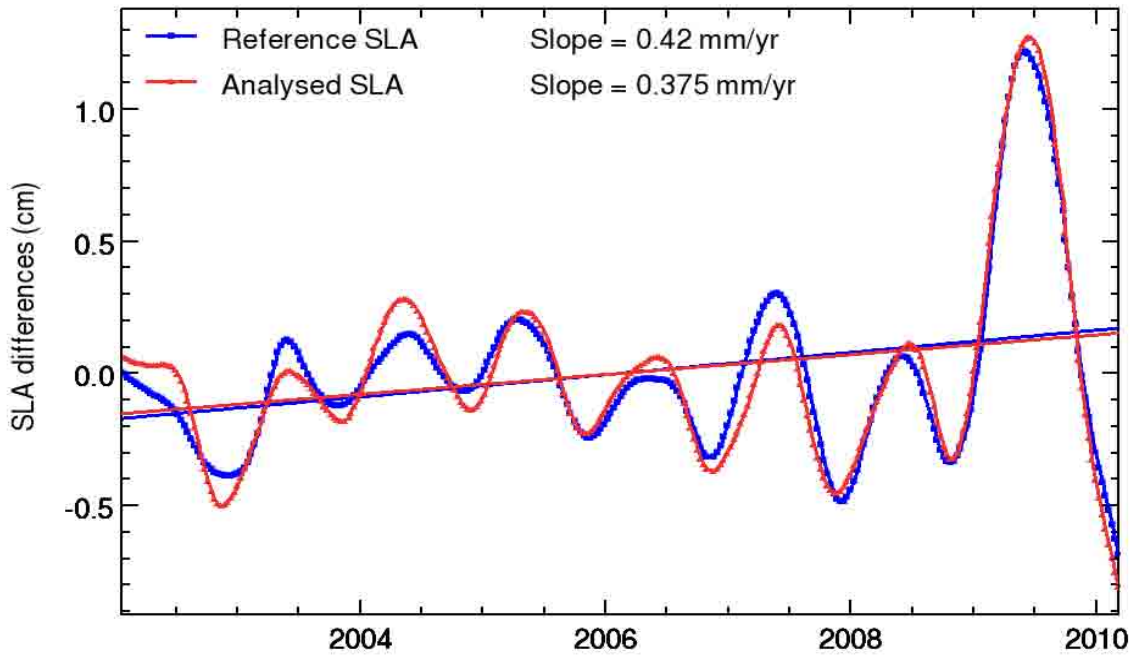

2.4.2. Dérive de la SLA (filtrée à 2 et 6 mois et ajustée des signaux annuels et semi-annuels)

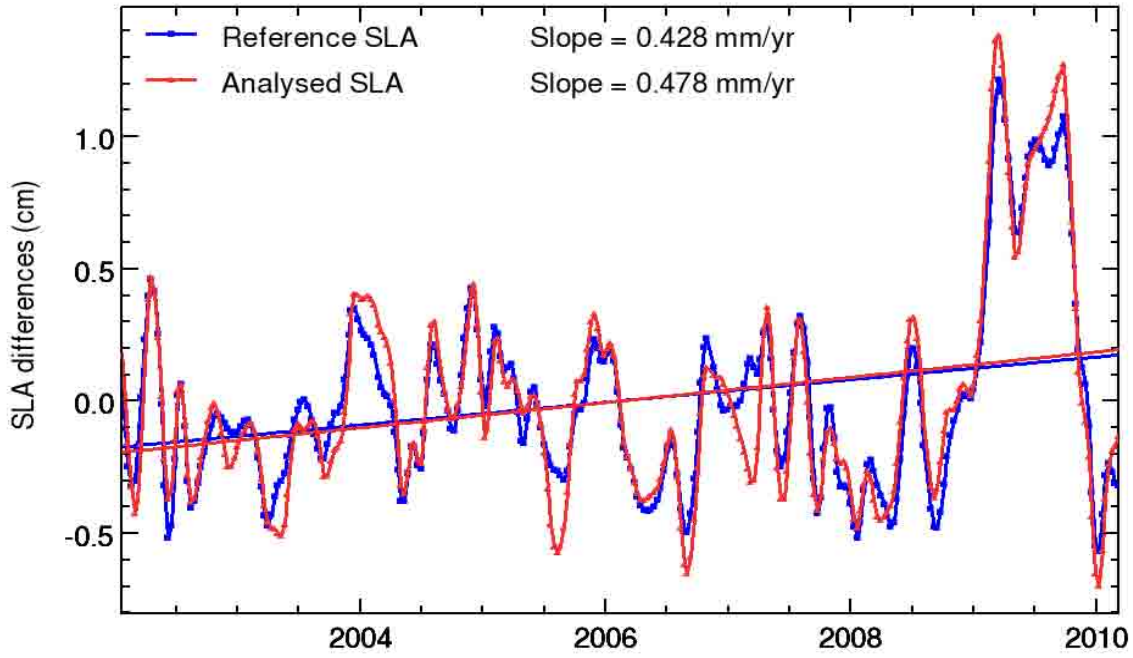

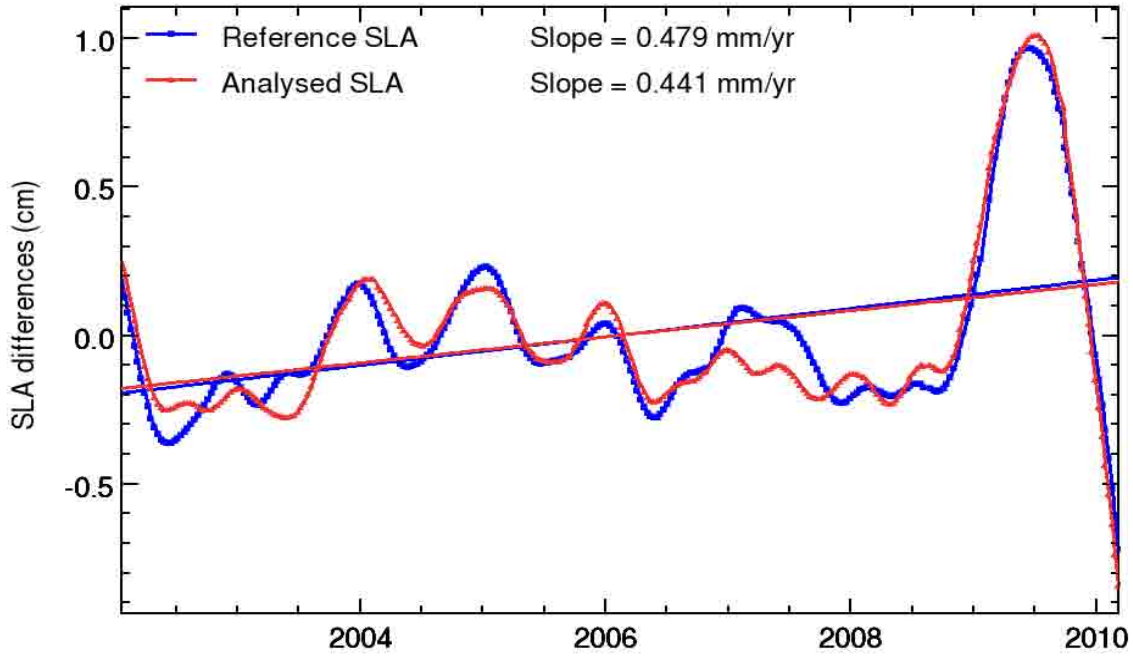

2.4.3. Histogrammes des différences de variance

La figure suivante présente les différences de variance SLA Alti/TG en utilisant successivement EO_POE_C ou pas
dans le calcul de la SLA altimétrique.
Le gain en variance est alors la différence entre :
- la variance de la différence entre la SLA altimétrique calculée avec EO_POE_C et la SLA des marégraphes
- la variance de la différence entre la SLA altimétrique calculée sans EO_POE_C et la SLA des marégraphes
Des valeurs positives signifient que la SLA altimétrique sans correction de l'erreur d'orbite EO_POE_C est plus cohérente avec la SLA marégraphique que la SLA altimétrique utilisant EO_POE_C et inversement. Des valeurs négatives signifient alors que l'utilisation de EO_POE_C pour le calcul de la SLA altimétrique reduit la variance (de la différence entre les SLA altimétrique et marégraphique).

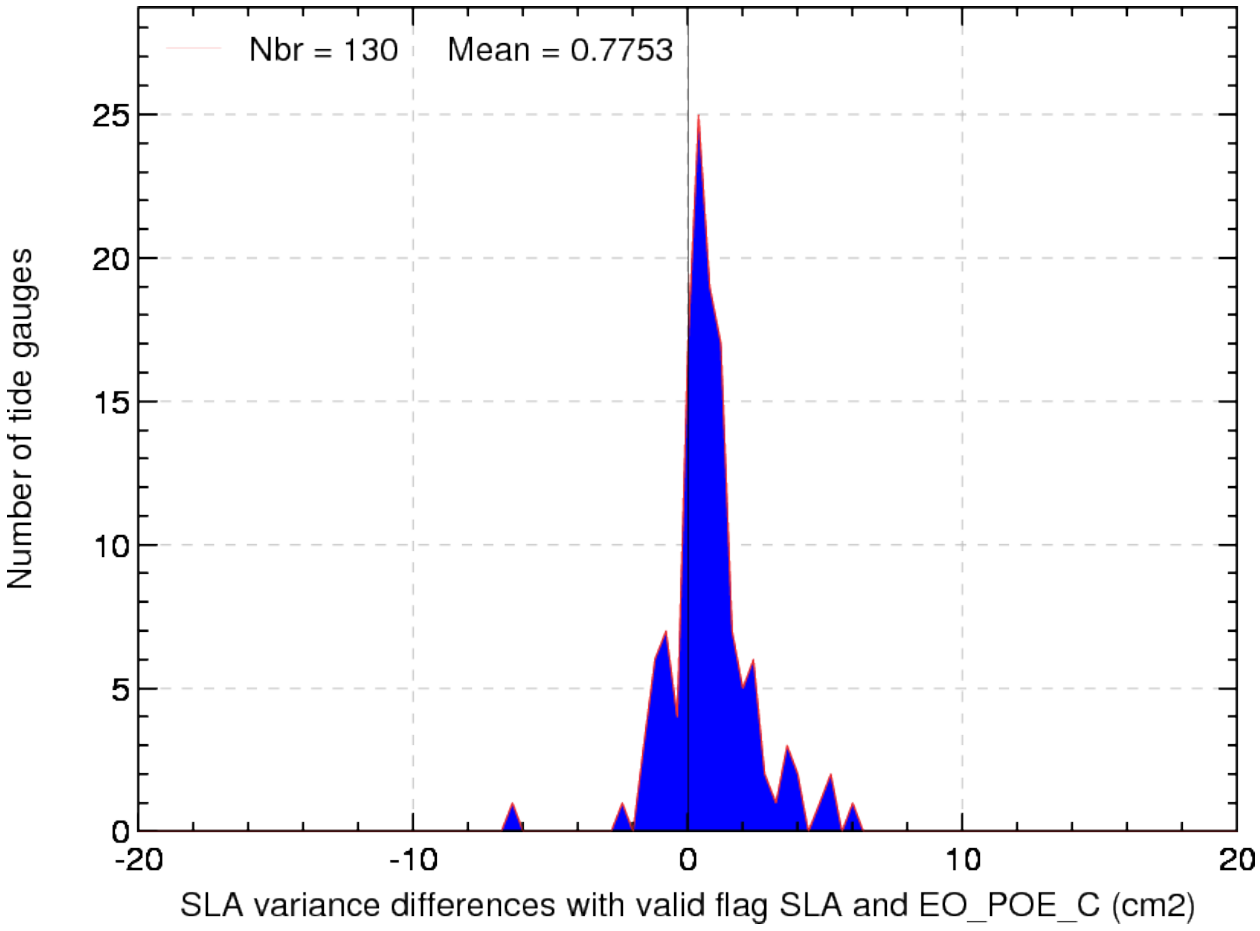

2.4.4. Suivis des différences de variance

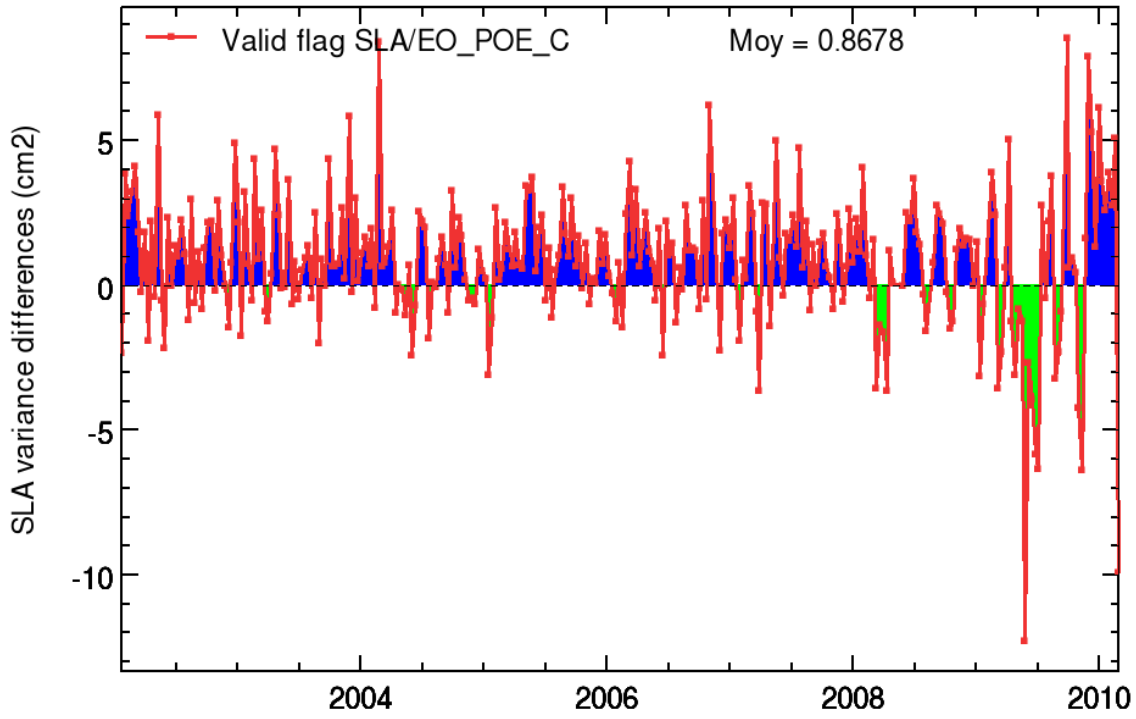

3. Annexes

3.1. CLIPs utilisés

3.1.1. CLIP altimétrique

3.1.2. SLA_REF

La SLA de référence s'exprime de la manière suivante :

SLA_REF = IIF(FLG_VAL_PRODUIT_REF==0,SSH_INTERP - TRO_SEC_ECMWF_C_S1_S2 - MAR_TER - BEM_NPARAM - MAR_POL - BIAIS_DAT - MAR_GOT4V7 - MOG2D_HR - TRO_HUM_COMPOSITE - IONO_FILTR_PRODUIT_REF - MSS_CLS01V1, DV)

3.2. Description des champs

Les champs utilisés dans le calcul de la SLA de référence sont les suivants :

783 FLG_VAL_PRODUIT_REF : Flag de validation des produits de références contenant le no de l'algo ayant rejeté le point invalide.

72 SSH_INTERP : Hauteur de la surface de la mer interpolée (ORB-DALT)

844 TRO_SEC_ECMWF_C_S1_S2 : Correction de troposphère sèche (ECMWF) sur grille Cartésienne avec corrections des marées atmosphériques des ondes S1 et S2

88 MAR_TER : Marée terrestre

69 BEM_NPARAM : Biais non paramétrique en bande principale

89 MAR_POL : Marée polaire

149 BIAIS_DAT : Correction déduite du biais de datation

1399 MAR_GOT4V7 : Marée océanique GOT version 4.7

1163 MOG2D_HR : Correction combinée issue du modèle MOG2D haute résolution

926 TRO_HUM_COMPOSITE : Correction de troposphère humide composite issue de la correction tropo humide radiomètre et modèle

789 IONO_FILTR_PRODUIT_REF : Correction ionosphérique filtrée pour les produits de référence

145 MSS_CLS01V1 : Surface Moyenne océanique CLS 2001 (v1)

3.2.1. CLIP marégraphique

3.2.2. SLA_TG

La SLA marégraphique s'exprime de la manière suivante :

SLA_TG = HDM_BRUTE - MOG2D_HR - MAR_DEMERLIAC_MOG2D_HR

3.3. Description des champs

Les champs utilisés dans le calcul de la SLA marégraphique sont les suivants :

919 HDM_BRUTE : Hauteur de mer directement mesurée

1163 MOG2D_HR : Correction combinée issue du modèle MOG2D haute résolution

1501 MAR_DEMERLIAC_MOG2D_HR : Hauteur de marée corrigée MOG2D_HR et filtrée Demerliac

3.4. Suivi de la SLA satellite colocalisée aux marégraphes

3.4.1. Suivi par cycle du champ SLA_SAT_QUAL_BRUTE

1096 SLA_SAT_QUAL_BRUTE : Anomalie de hauteur de mer brute avec application du contrôle qualité marégraphique, mesurée par l'altimètre au marégraphe

Les figures sont rangées dans l'ordre suivant (de gauche à droite et de haut en bas) :
Nombre, Moyenne, Ecart-type, Minimum, Maximum.

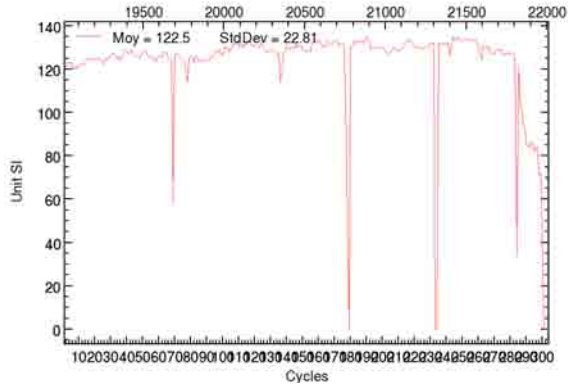

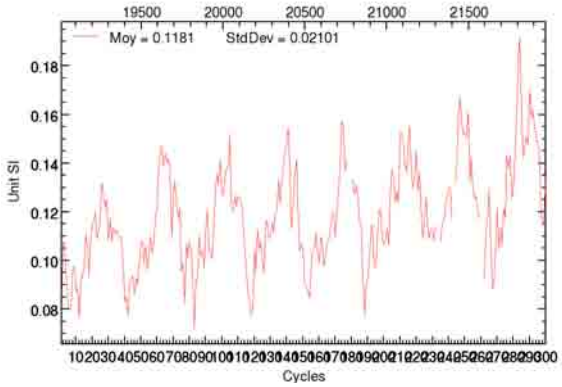

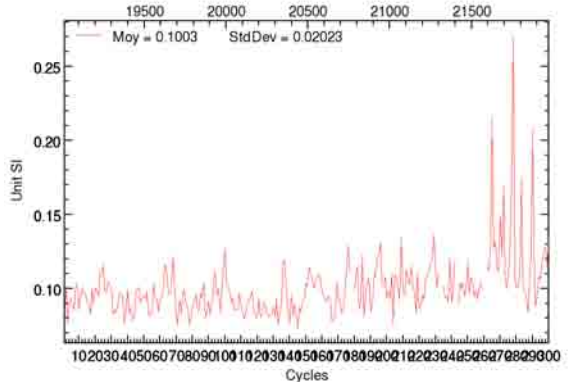

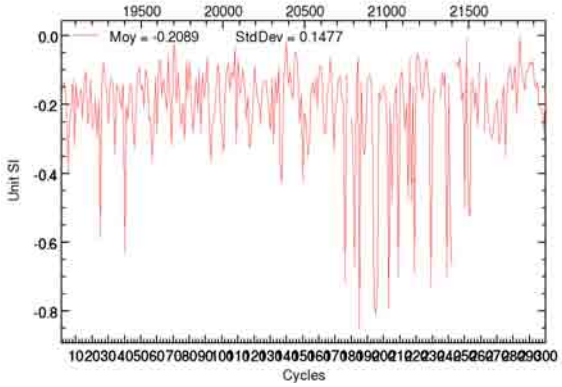

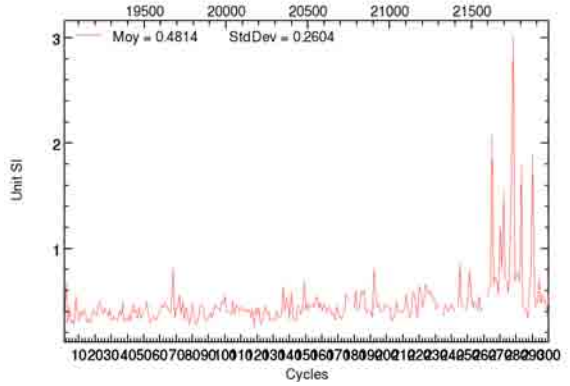

3.4.2. Suivi par cycle du champ SLA_SAT_QUAL_VAL

1103 SLA_SAT_QUAL_VAL : Anomalie de hauteur de mer validée avec application du contrôle qualité marégraphique, mesurée par l'altimètre au marégraphe

Les figures sont rangées dans l'ordre suivant (de gauche à droite et de haut en bas) :
Nombre, Moyenne, Ecart-type, Minimum, Maximum.

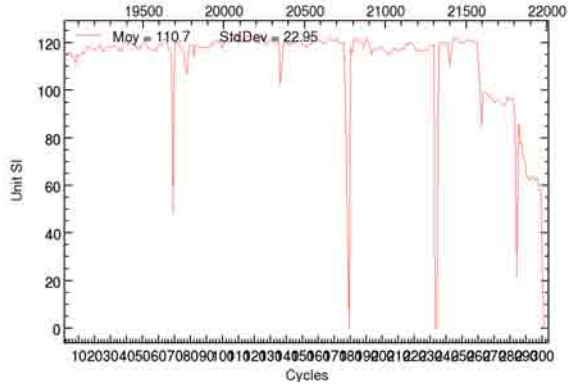

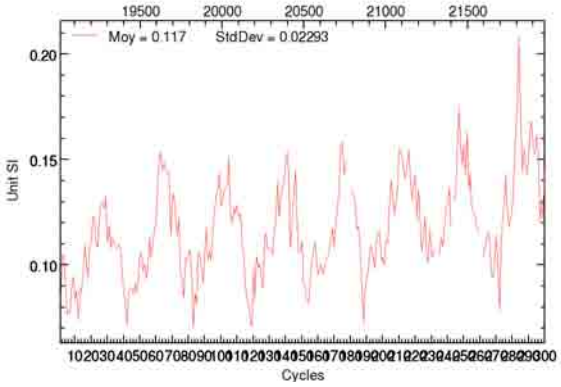

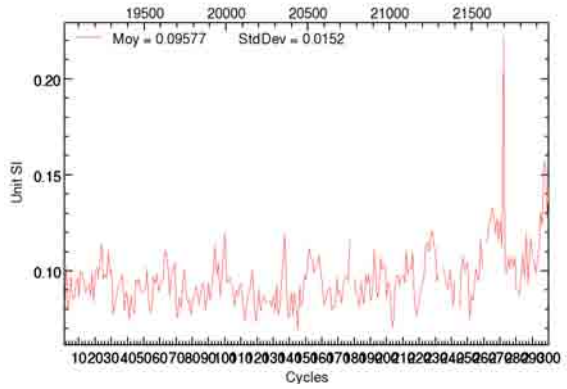

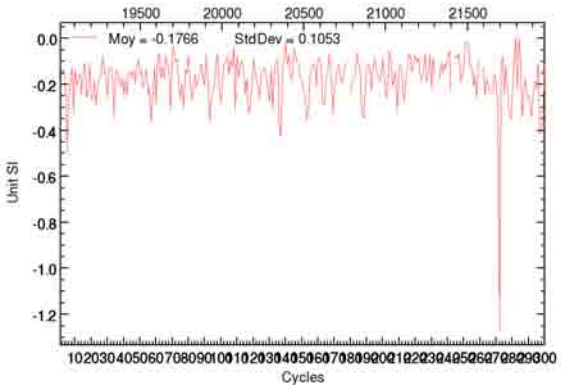

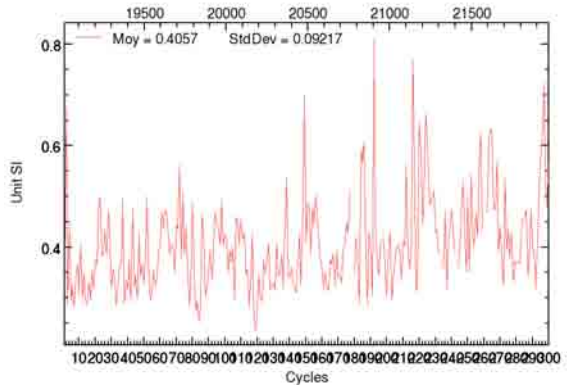

3.4.3. Suivi par cycle du champ SLA_SAT_QUAL_VAL_HN

1525 SLA_SAT_QUAL_VAL_HN : Anomalie de hauteur de mer validée avec application du contrôle qualité marégraphique, mesurée par l'altimètre au marégraphe (Hémisphère Nord)

Les figures sont rangées dans l'ordre suivant (de gauche à droite et de haut en bas) :
Nombre, Moyenne, Ecart-type, Minimum, Maximum.

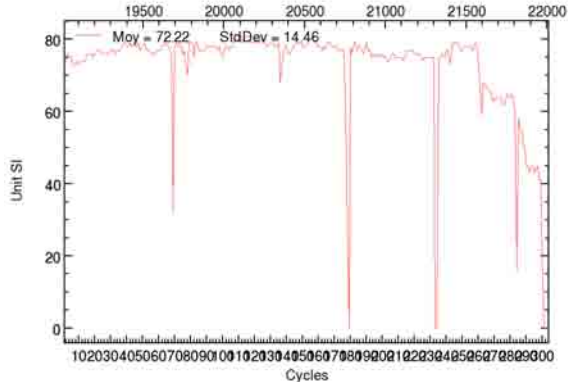

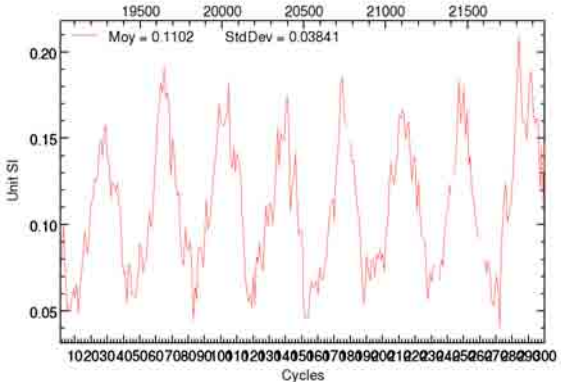

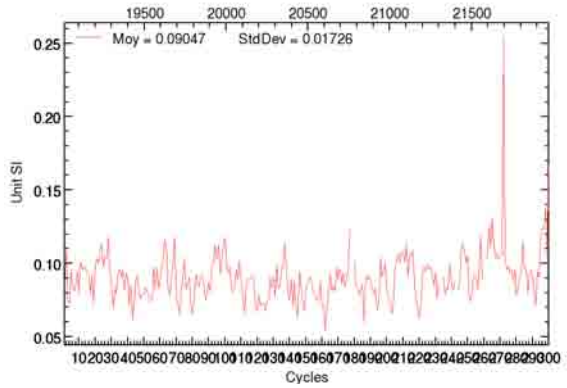

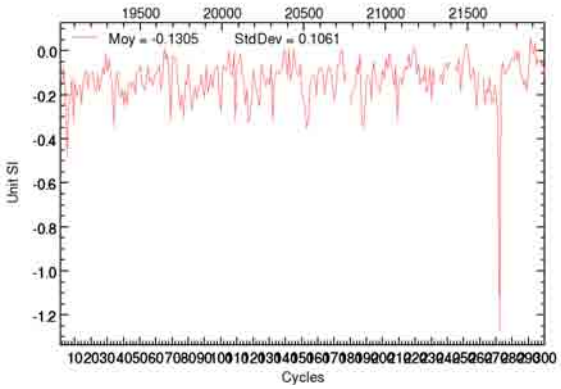

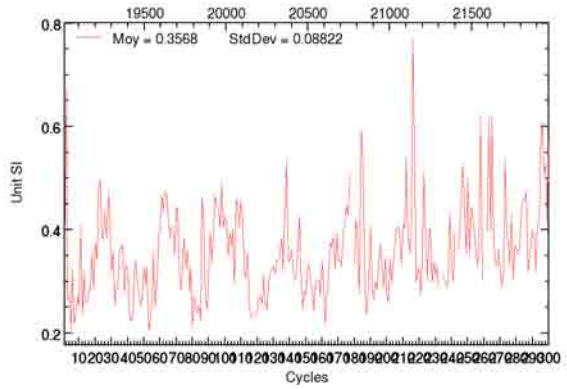

3.4.4. Suivi par cycle du champ SLA_SAT_QUAL_VAL_HS

1532 SLA_SAT_QUAL_VAL_HS : Anomalie de hauteur de mer validée avec application du contrôle qualité marégraphique, mesurée par l'altimètre au marégraphe (Hémisphère Sud)

Les figures sont rangées dans l'ordre suivant (de gauche à droite et de haut en bas) :
Nombre, Moyenne, Ecart-type, Minimum, Maximum.

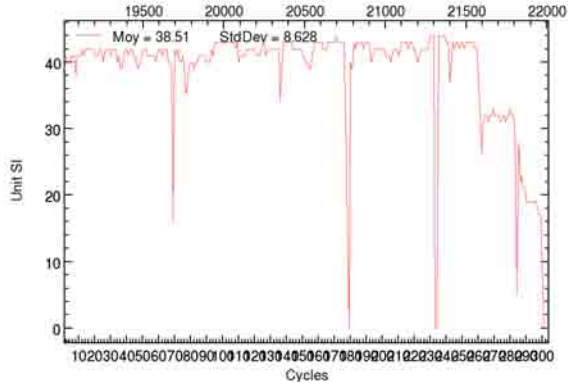

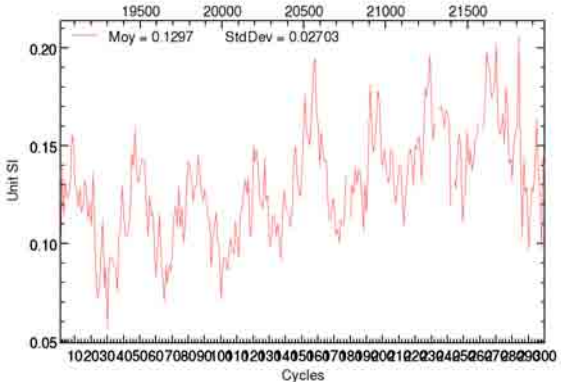

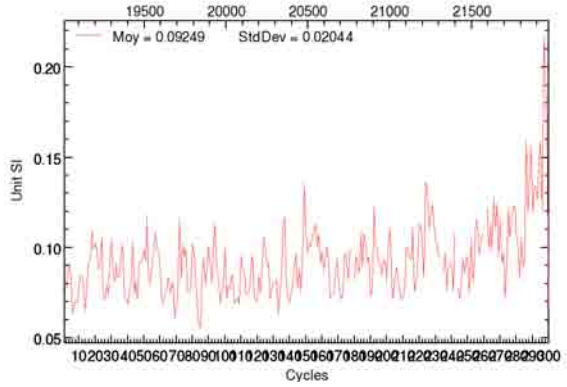

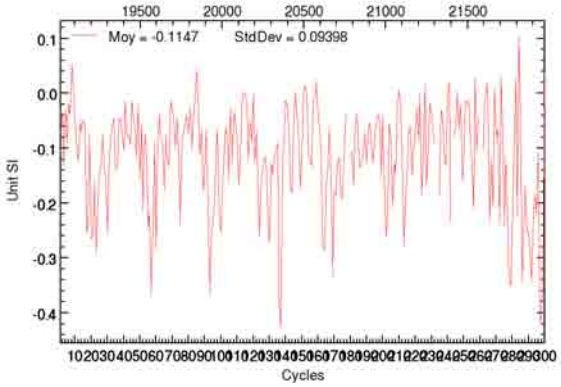

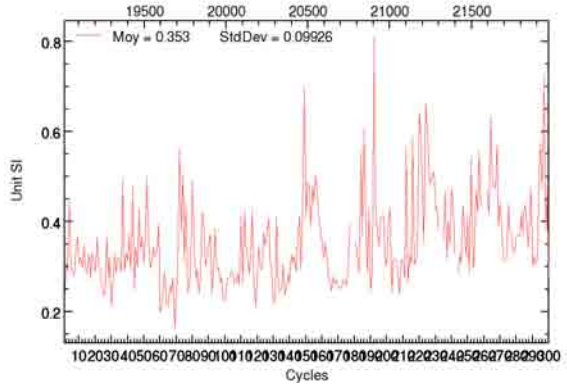

3.4.5. Suivi par cycle du champ SLA_SAT_QUAL_VAL_TrP

1539 SLA_SAT_QUAL_VAL_TRP : Anomalie de hauteur de mer validée avec application du contrôle qualité marégraphique, mesurée par l'altimètre au marégraphe (Hémisphère Nord)

Les figures sont rangées dans l'ordre suivant (de gauche à droite et de haut en bas) :
Nombre, Moyenne, Ecart-type, Minimum, Maximum.

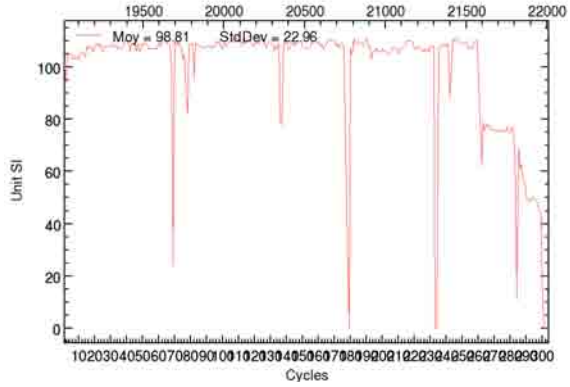

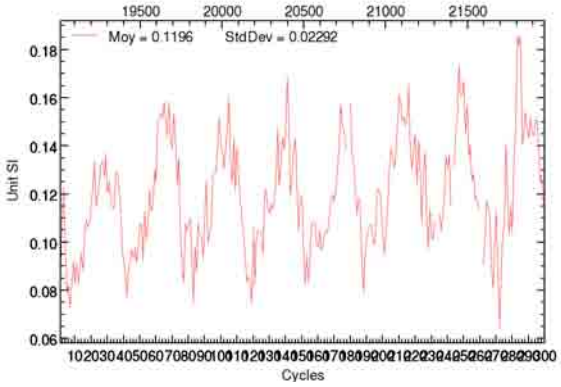

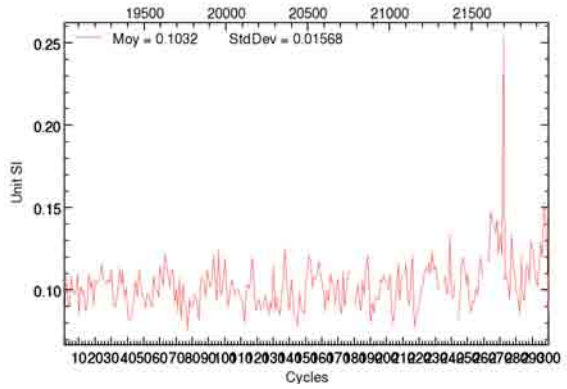

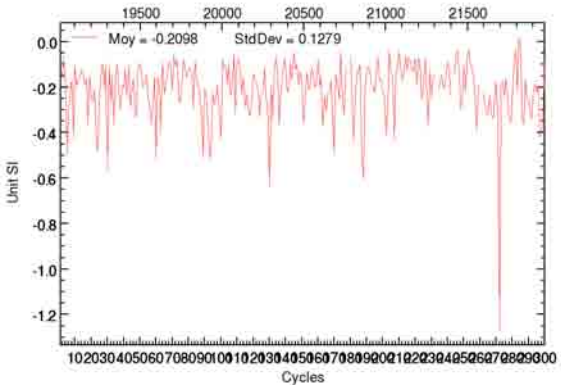

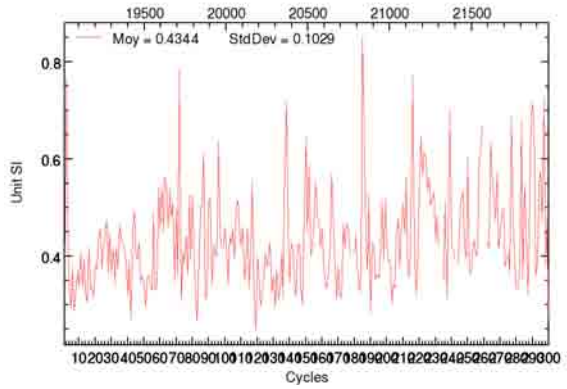

3.4.6. Suivi par cycle du champ SLA_SAT_QUAL_VAL_TrI

1546 SLA_SAT_QUAL_VAL_TRI : Anomalie de hauteur de mer validée avec application du contrôle qualité marégraphique, mesurée par l'altimètre au marégraphe (Hémisphère Sud)

Les figures sont rangées dans l'ordre suivant (de gauche à droite et de haut en bas) :
Nombre, Moyenne, Ecart-type, Minimum, Maximum.

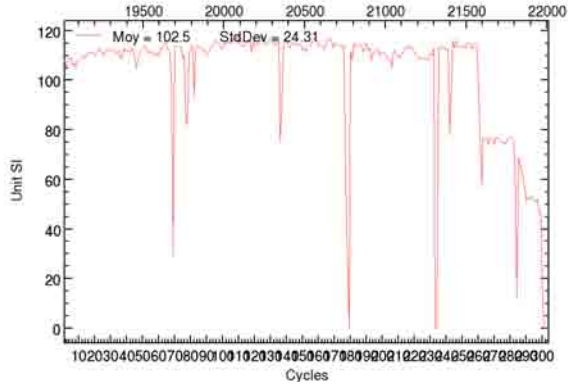

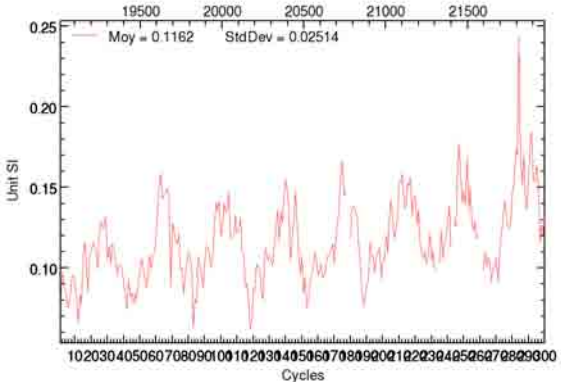

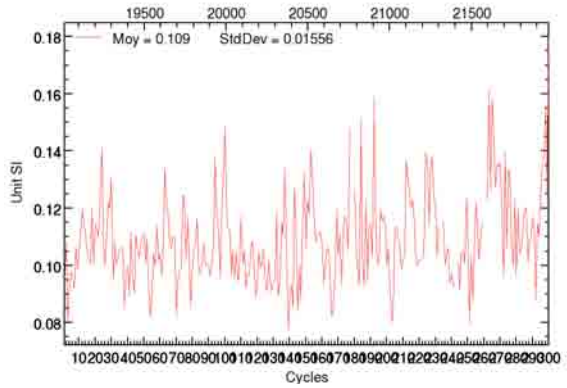

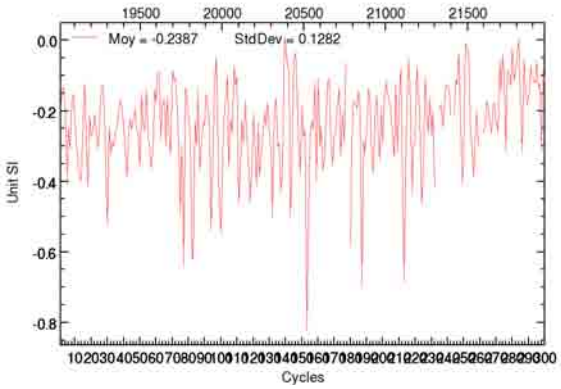

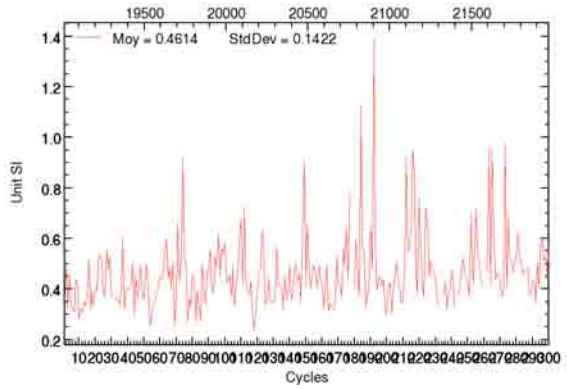

3.5. Suivi de la SLA marégraphique non corrigée du biais entre les marégraphes et de la dérive crustale

3.5.1. Suivi par cycle du champ SLA_TG_QUAL_NOCORR_BRUTE

1097 SLA_TG_QUAL_NOCORR_BRUTE : Anomalie de hauteur de mer brute avec application du contrôle qualité marégraphique, mesurée par le marégraphe

Les figures sont rangées dans l'ordre suivant (de gauche à droite et de haut en bas) :
Nombre, Moyenne, Ecart-type, Minimum, Maximum.

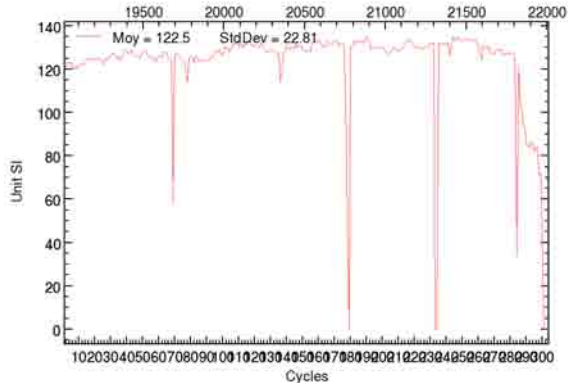

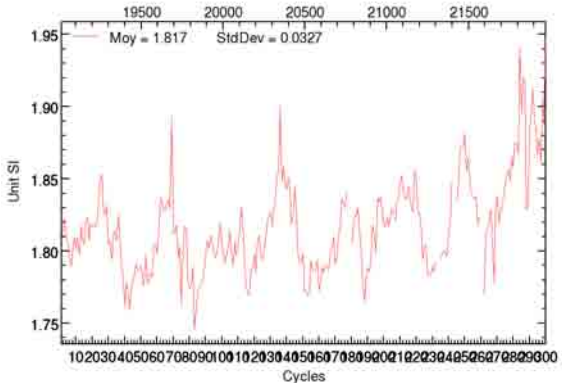

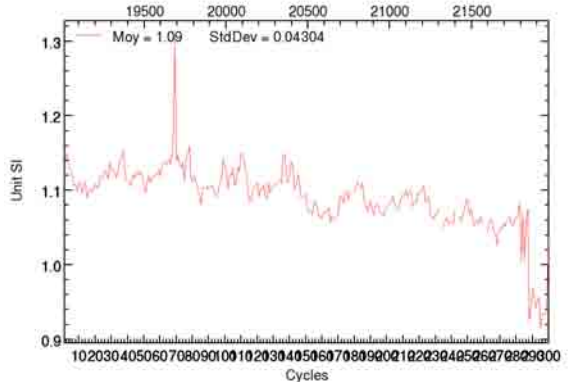

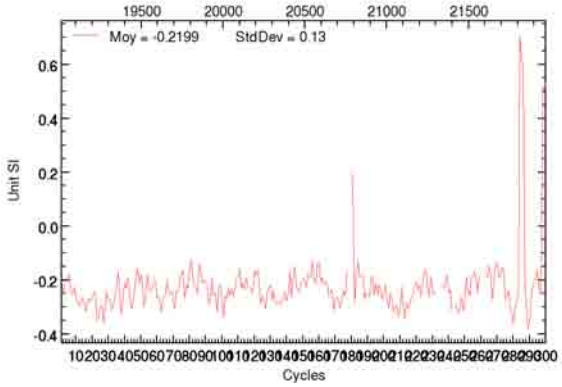

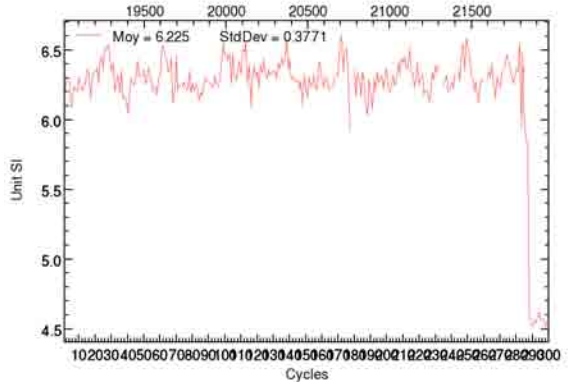

3.5.2. Suivi par cycle du champ SLA_TG_QUAL_NOCORR_VAL

1104 SLA_TG_QUAL_NOCORR_VAL : Anomalie de hauteur de mer validée avec application du contrôle qualité marégraphique, mesurée par le marégraphe

Les figures sont rangées dans l'ordre suivant (de gauche à droite et de haut en bas) :
Nombre, Moyenne, Ecart-type, Minimum, Maximum.

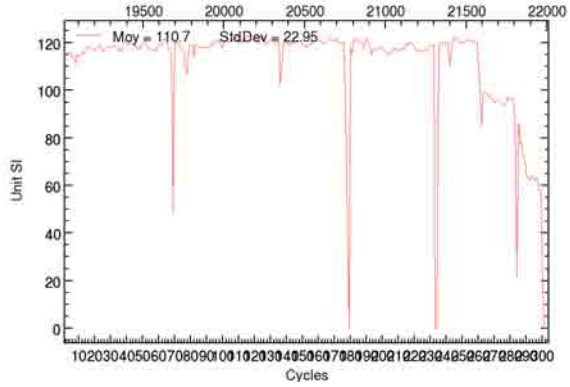

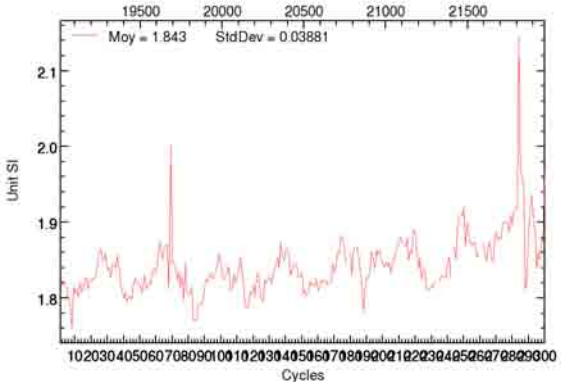

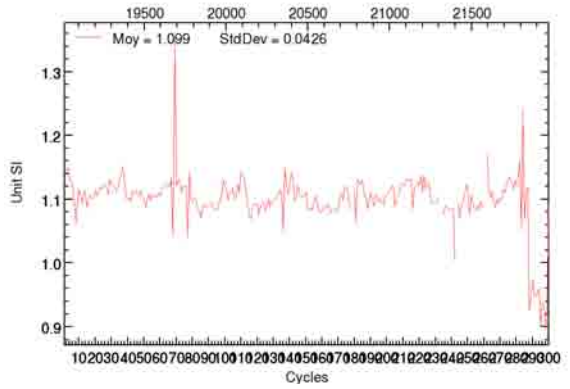

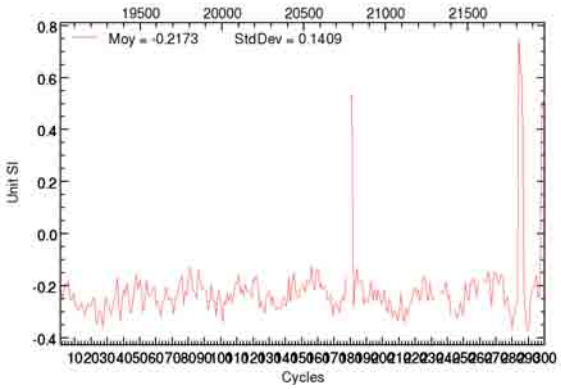

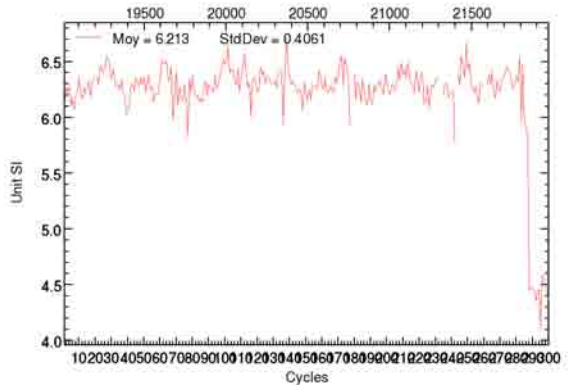

3.5.3. Suivi par cycle du champ SLA_TG_QUAL_NOCORR_VAL_HN

1526 SLA_TG_QUAL_NOCORR_VAL_HN : Anomalie de hauteur de mer validée avec application du contrôle qualité marégraphique, mesurée par le marégraphe (Hémisphère Nord)

Les figures sont rangées dans l'ordre suivant (de gauche à droite et de haut en bas) :
Nombre, Moyenne, Ecart-type, Minimum, Maximum.

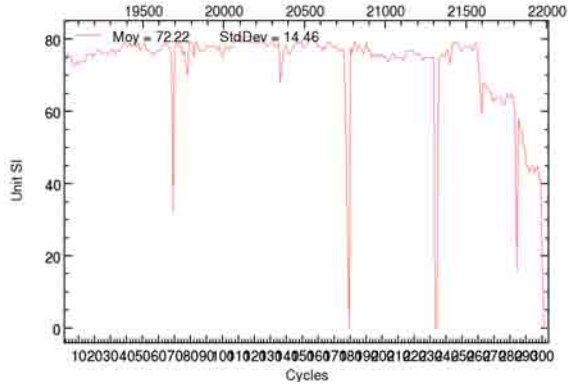

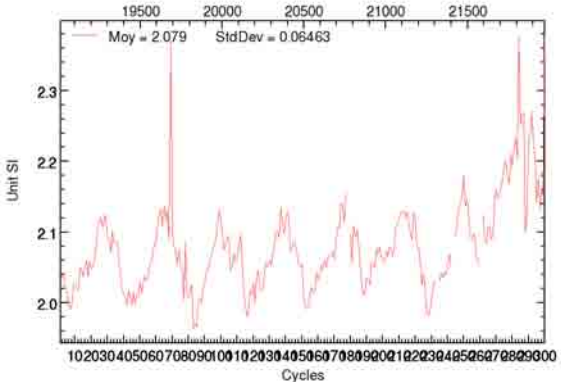

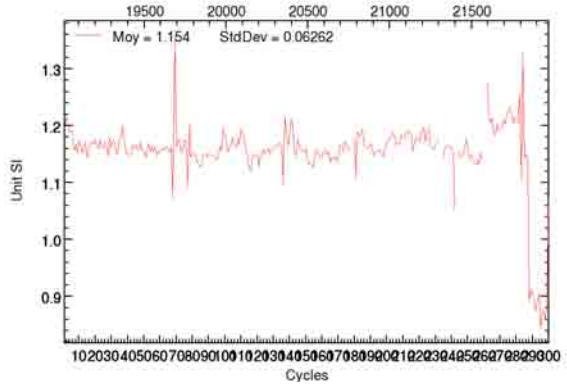

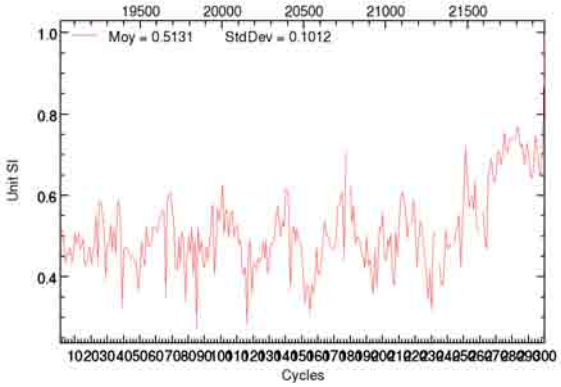

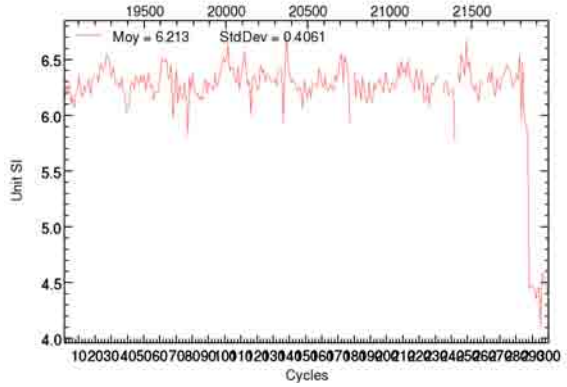

3.5.4. Suivi par cycle du champ SLA_TG_QUAL_NOCORR_VAL_HS

1533 SLA_TG_QUAL_NOCORR_VAL_HS : Anomalie de hauteur de mer validée avec application du contrôle qualité marégraphique, mesurée par le marégraphe (Hémisphère Sud)

Les figures sont rangées dans l'ordre suivant (de gauche à droite et de haut en bas) :
Nombre, Moyenne, Ecart-type, Minimum, Maximum.

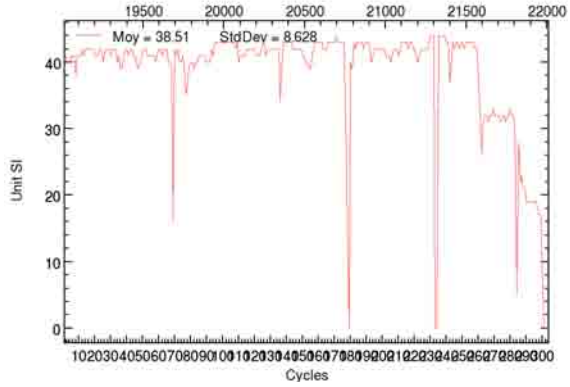

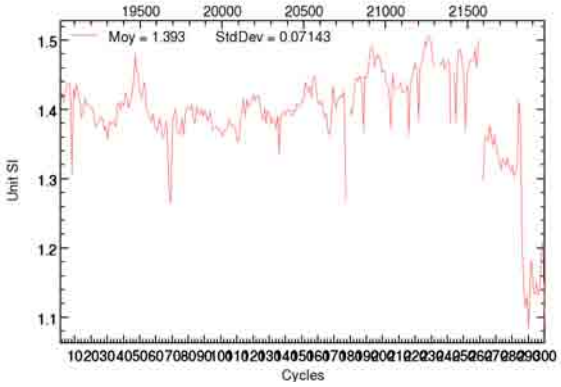

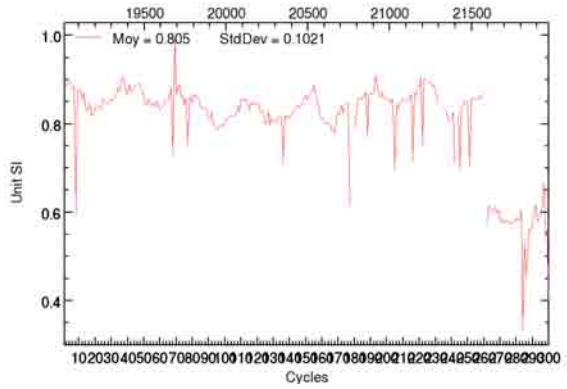

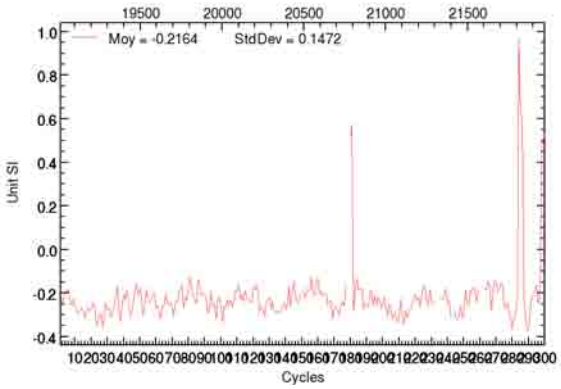

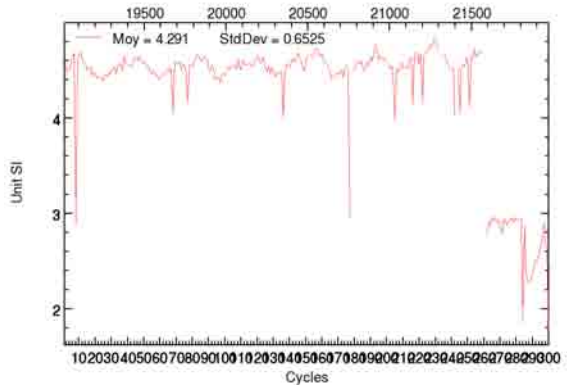

3.5.5. Suivi par cycle du champ SLA_TG_QUAL_NOCORR_VAL_TrP

1540 SLA_TG_QUAL_NOCORR_VAL_TRP : Anomalie de hauteur de mer validée avec application du contrôle qualité marégraphique, mesurée par le marégraphe (Hémisphère Nord)

Les figures sont rangées dans l'ordre suivant (de gauche à droite et de haut en bas) :
Nombre, Moyenne, Ecart-type, Minimum, Maximum.

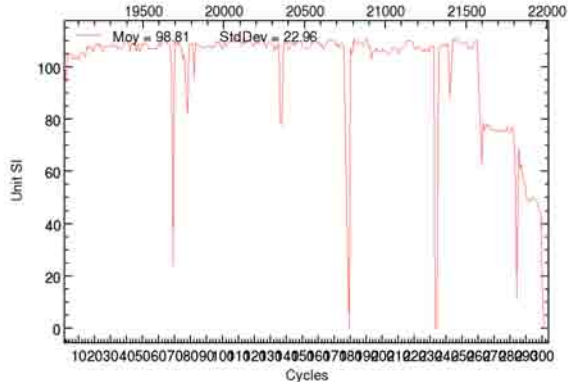

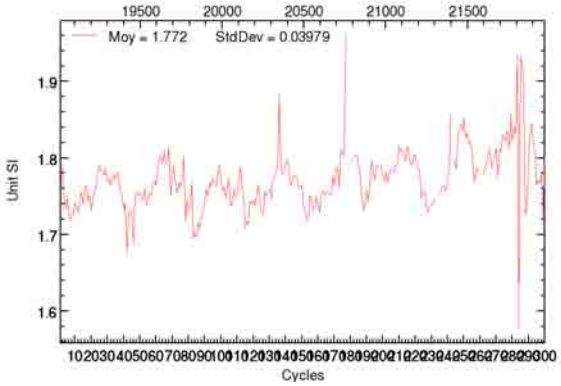

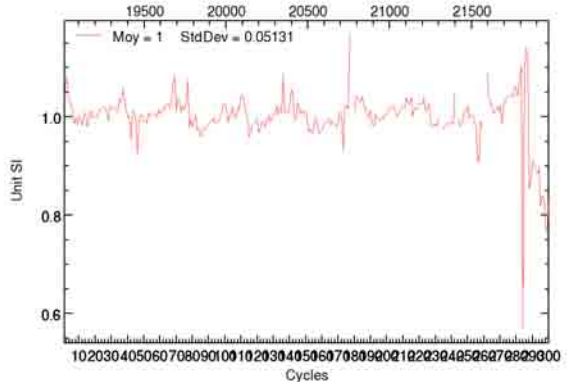

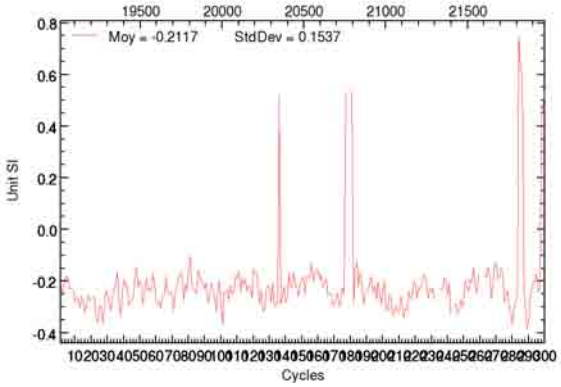

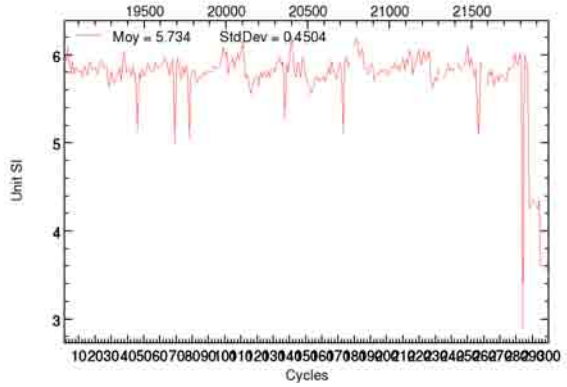

3.5.6. Suivi par cycle du champ SLA_TG_QUAL_NOCORR_VAL_Trl

1547 SLA_TG_QUAL_NOCORR_VAL_TRI : Anomalie de hauteur de mer validée avec application du contrôle qualité marégraphique, mesurée par le marégraphe (Hémisphère Sud)

Les figures sont rangées dans l'ordre suivant (de gauche à droite et de haut en bas) :
Nombre, Moyenne, Ecart-type, Minimum, Maximum.

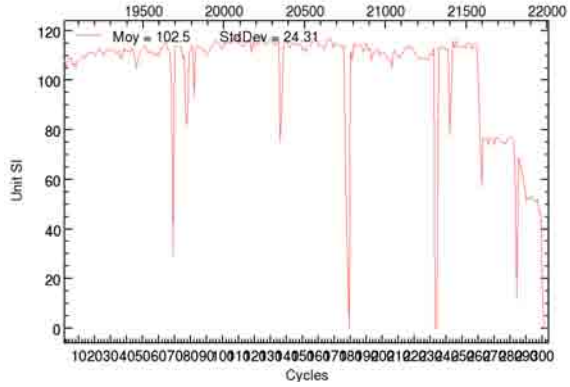

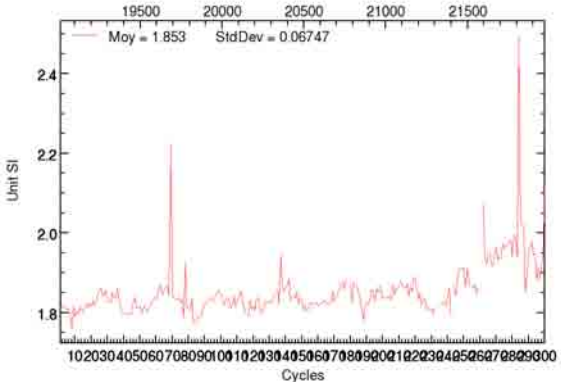

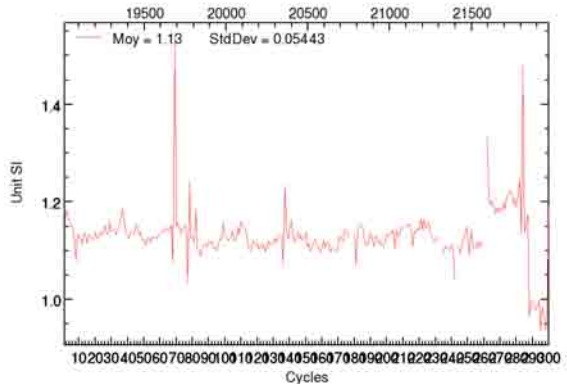

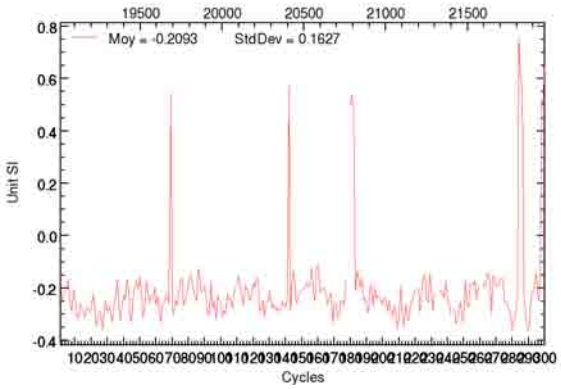

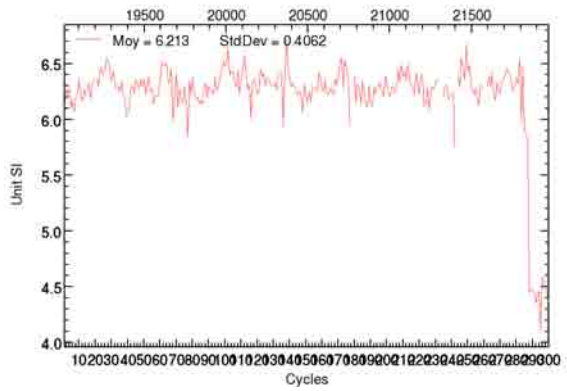

3.5.7. Suivi par cycle du champ SLA_TG_QUAL_BIAIS_BRUTE

1098 SLA_TG_QUAL_BIAIS_BRUTE : Anomalie de hauteur de mer brute avec application du contrôle qualité marégraphique, mesurée par le marégraphe, avec correction du biais

Les figures sont rangées dans l'ordre suivant (de gauche à droite et de haut en bas) :
Nombre, Moyenne, Ecart-type, Minimum, Maximum.

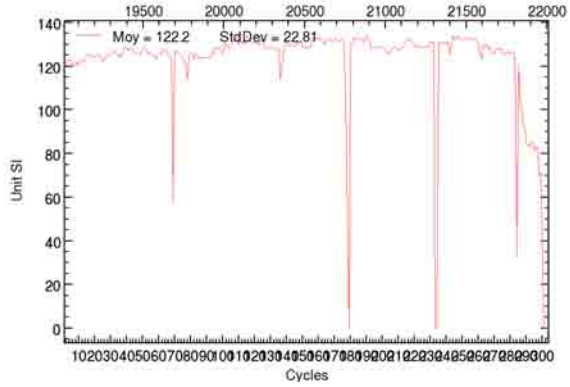

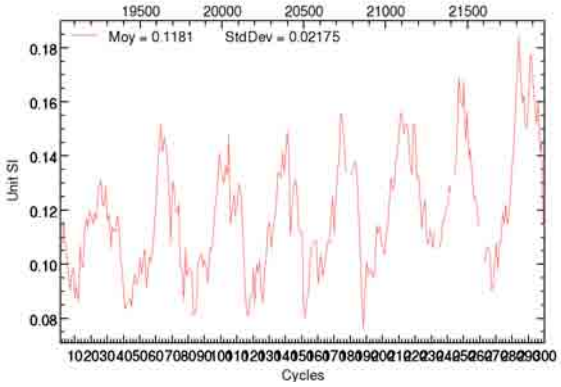

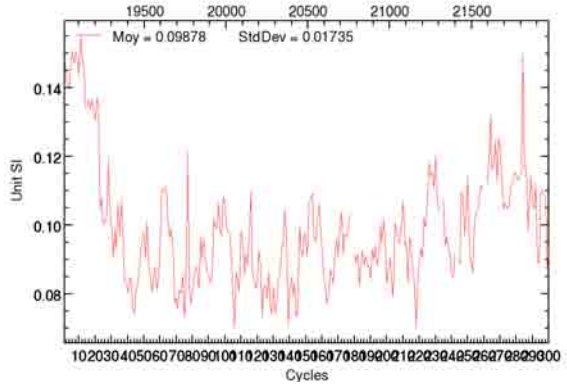

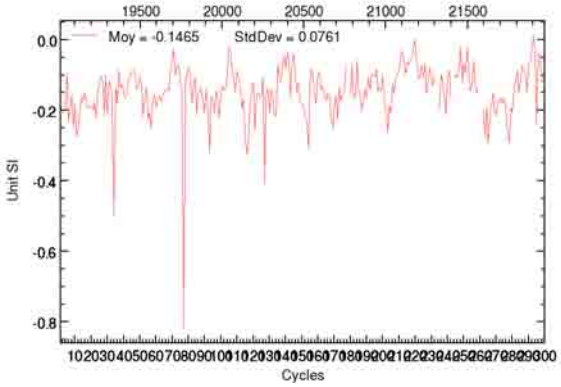

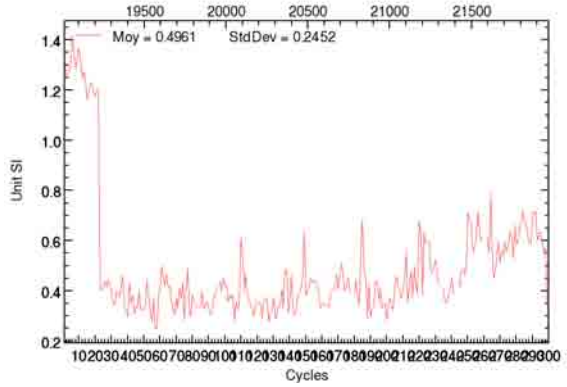

3.5.8. Suivi par cycle du champ SLA_TG_QUAL_BIAIS_VAL

1105 SLA_TG_QUAL_BIAIS_VAL : Anomalie de hauteur de mer validée avec application du contrôle qualité marégraphique, mesurée par le marégraphe, avec correction du biais

Les figures sont rangées dans l'ordre suivant (de gauche à droite et de haut en bas) :
Nombre, Moyenne, Ecart-type, Minimum, Maximum.

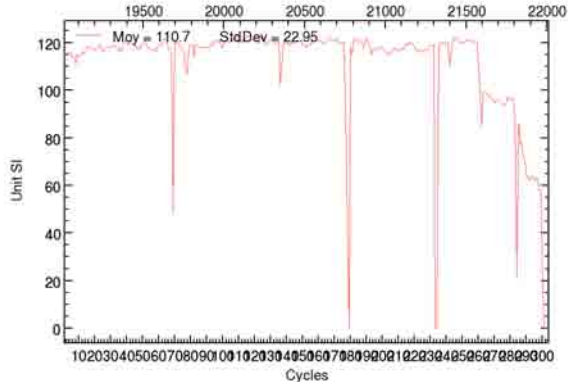

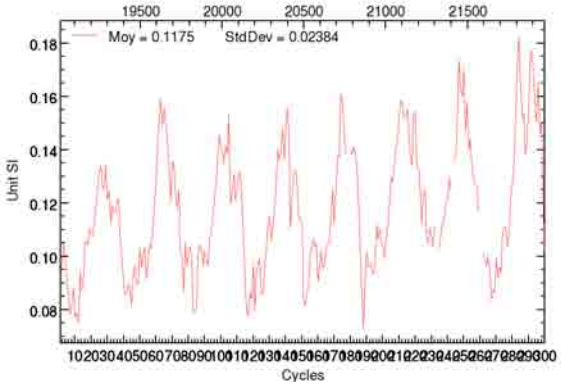

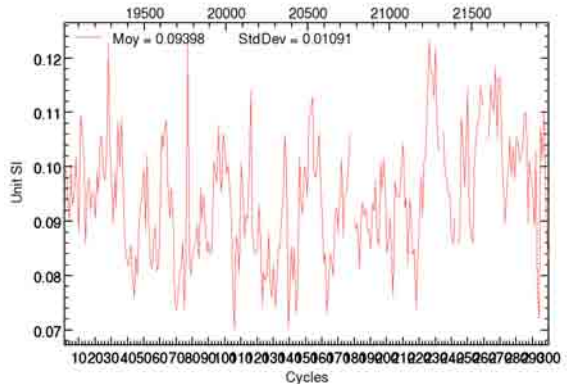

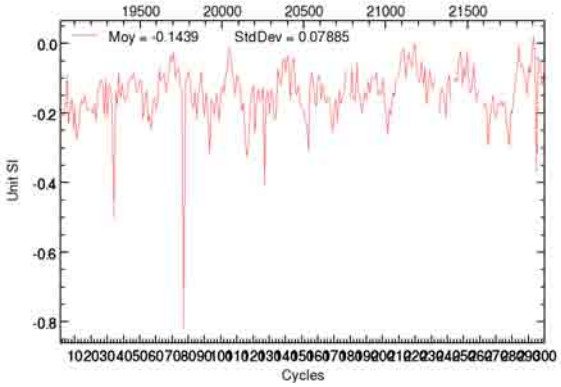

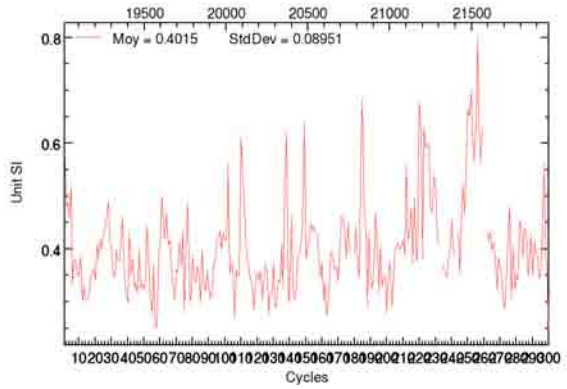

3.5.9. Suivi par cycle du champ SLA_TG_QUAL_BIAIS_VAL_HN

1527 SLA_TG_QUAL_BIAIS_VAL_HN : Anomalie de hauteur de mer validée avec application du contrôle qualité marégraphique, mesurée par le marégraphe, avec correction du biais (Hémisphère Nord)

Les figures sont rangées dans l'ordre suivant (de gauche à droite et de haut en bas) :
Nombre, Moyenne, Ecart-type, Minimum, Maximum.

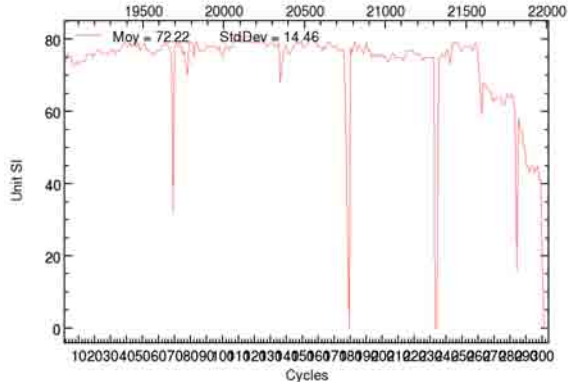

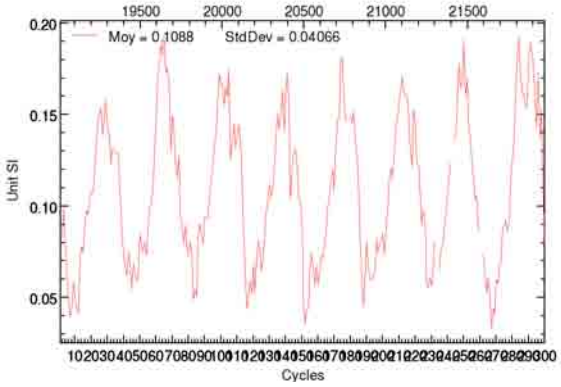

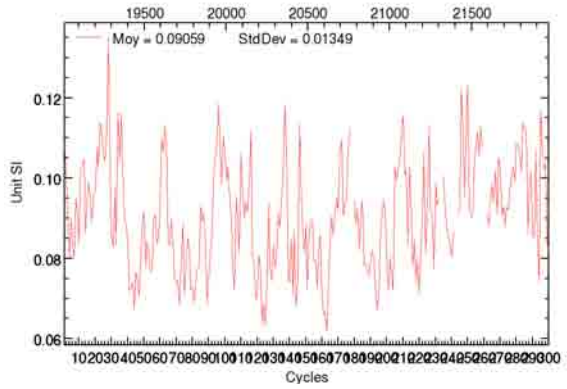

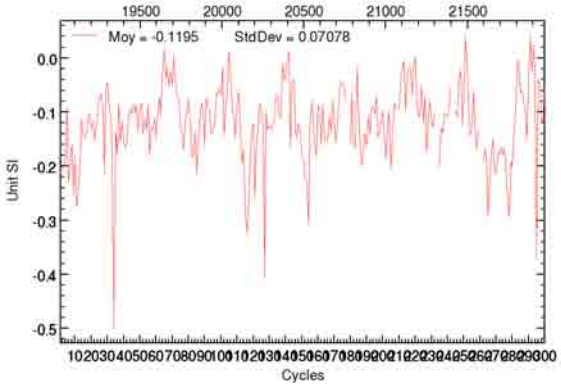

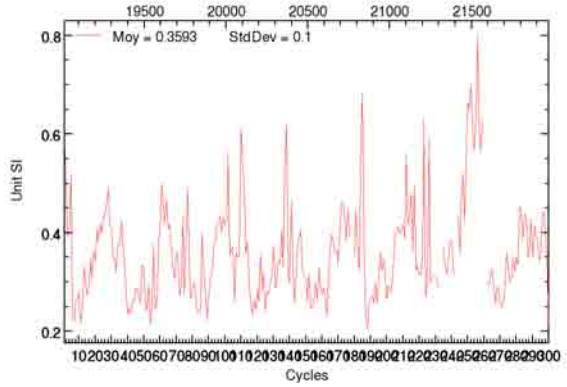

3.5.10. Suivi par cycle du champ SLA_TG_QUAL_BIAIS_VAL_HS

1534 SLA_TG_QUAL_BIAIS_VAL_HS : Anomalie de hauteur de mer validée avec application du contrôle qualité marégraphique, mesurée par le marégraphe, avec correction du biais (Hémisphère Sud)

Les figures sont rangées dans l'ordre suivant (de gauche à droite et de haut en bas) :
Nombre, Moyenne, Ecart-type, Minimum, Maximum.

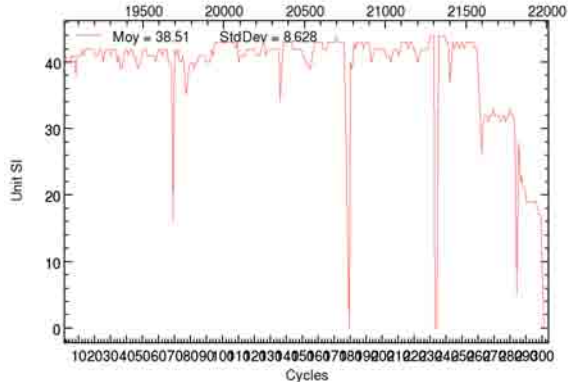

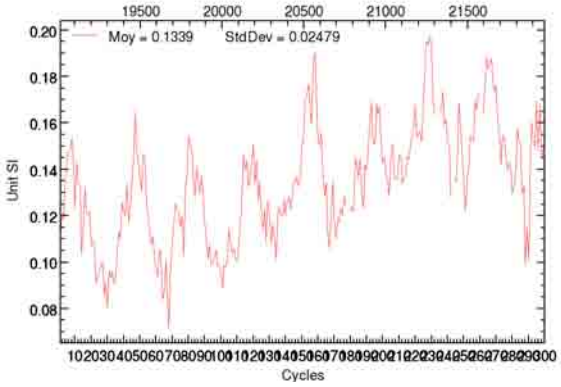

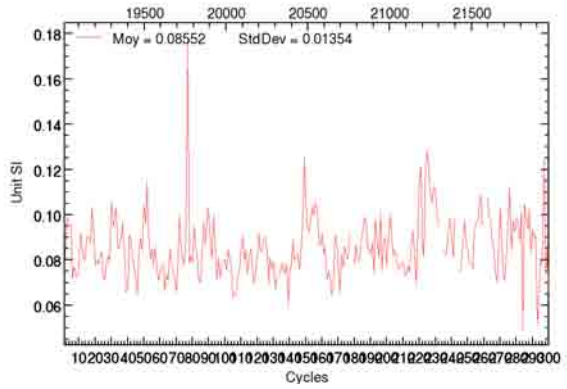

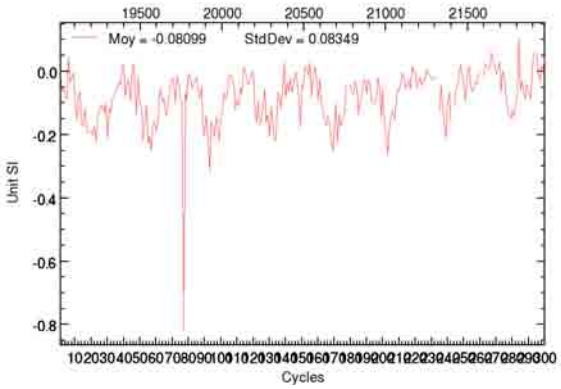

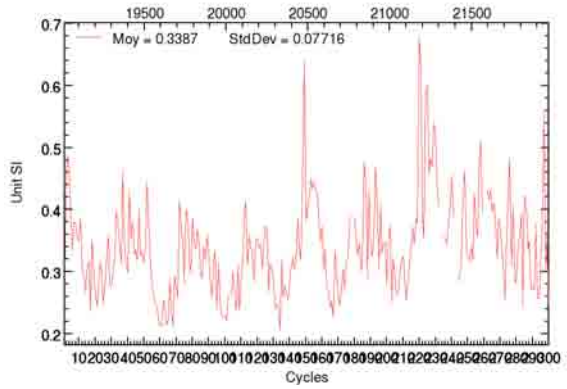

3.5.11. Suivi par cycle du champ SLA_TG_QUAL_BIAIS_VAL_TrP

1541 SLA_TG_QUAL_BIAIS_VAL_TRP : Anomalie de hauteur de mer validée avec application du contrôle qualité marégraphique, mesurée par le marégraphe, avec correction du biais (Hémisphère Nord)

Les figures sont rangées dans l'ordre suivant (de gauche à droite et de haut en bas) :
Nombre, Moyenne, Ecart-type, Minimum, Maximum.

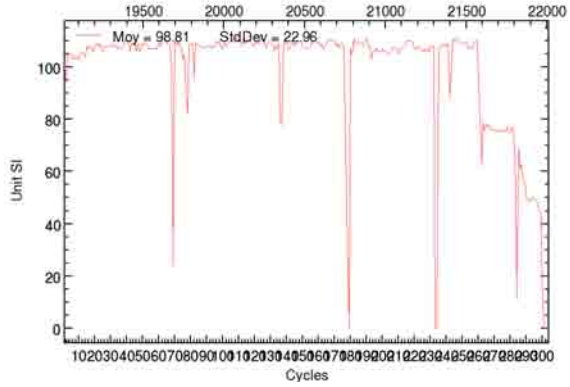

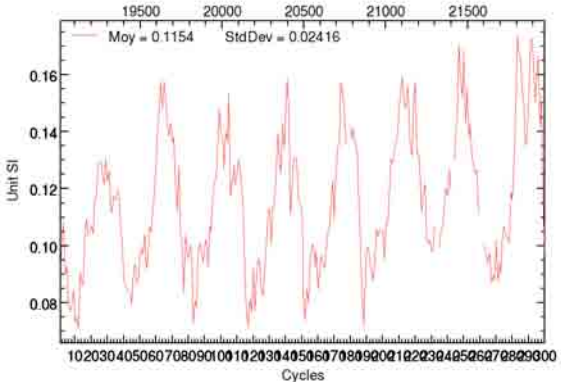

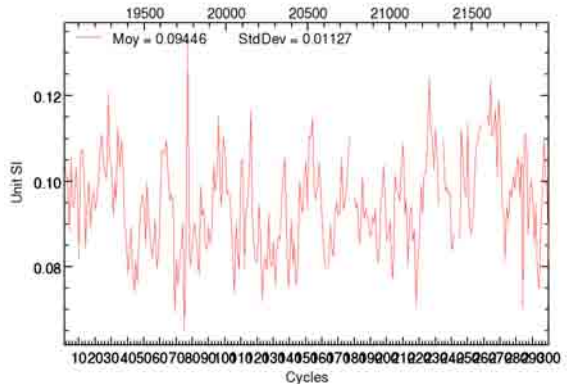

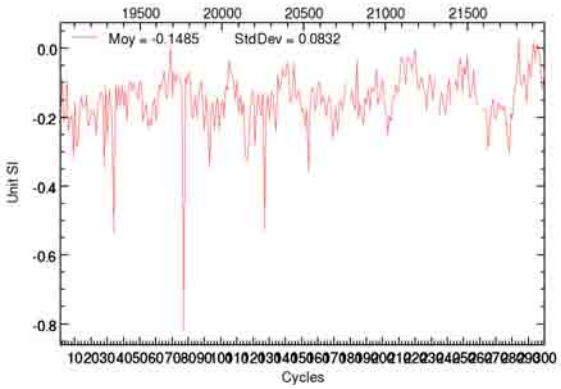

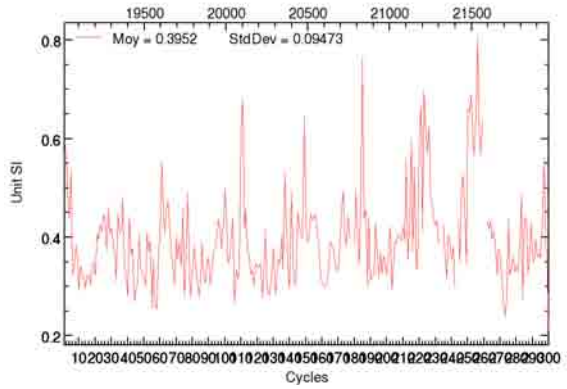

3.5.12. Suivi par cycle du champ SLA_TG_QUAL_BIAIS_VAL_Trl

1548 SLA_TG_QUAL_BIAIS_VAL_TRI : Anomalie de hauteur de mer validée avec application du contrôle qualité marégraphique, mesurée par le marégraphe, avec correction du biais (Hémisphère Sud)

Les figures sont rangées dans l'ordre suivant (de gauche à droite et de haut en bas) :
Nombre, Moyenne, Ecart-type, Minimum, Maximum.

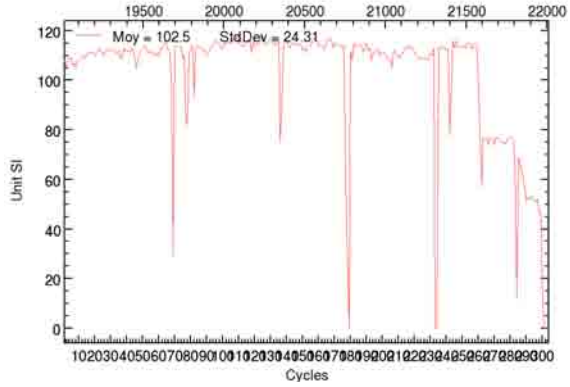

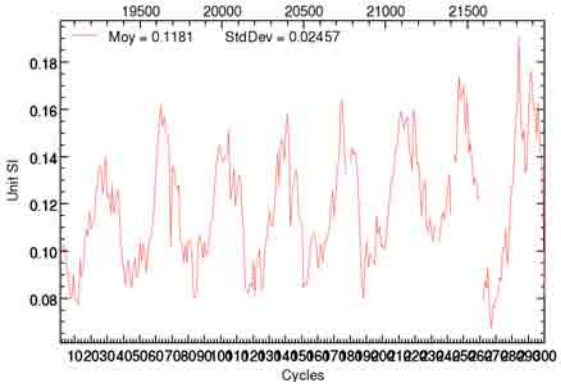

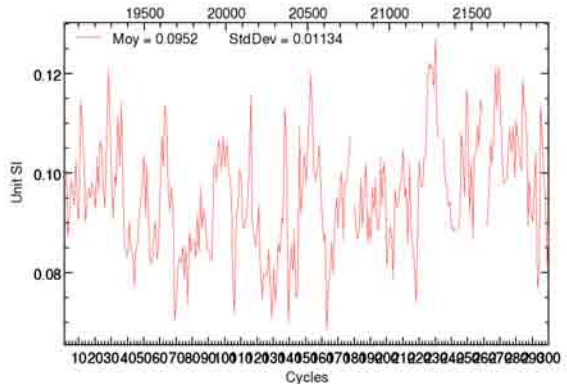

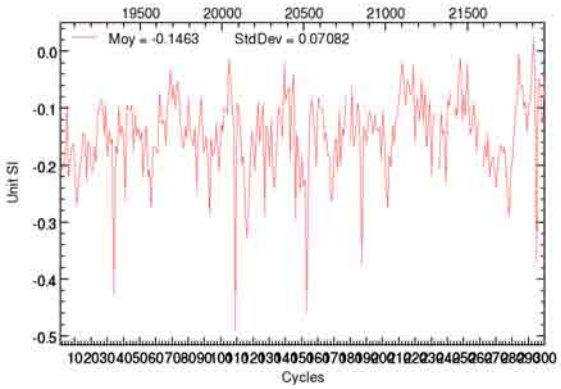

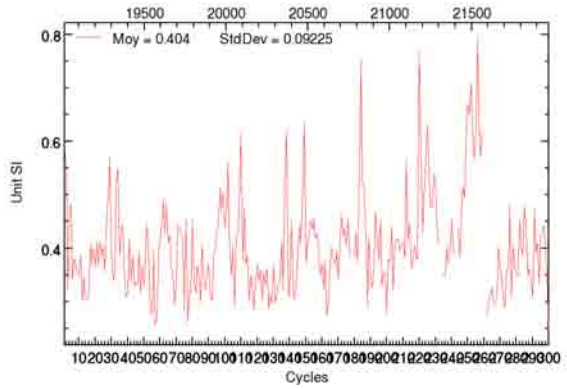

3.5.13. Suivi par cycle du champ SLA_TG_QUAL_BIAIS_DERIVE_BRUTE

1099 SLA_TG_QUAL_BIAIS_DERIVE_BRUTE : Anomalie de hauteur de mer brute avec application du contrôle qualité marégraphique, mesurée par le marégraphe, avec correction du biais et de la dérive

Les figures sont rangées dans l'ordre suivant (de gauche à droite et de haut en bas) :
Nombre, Moyenne, Ecart-type, Minimum, Maximum.

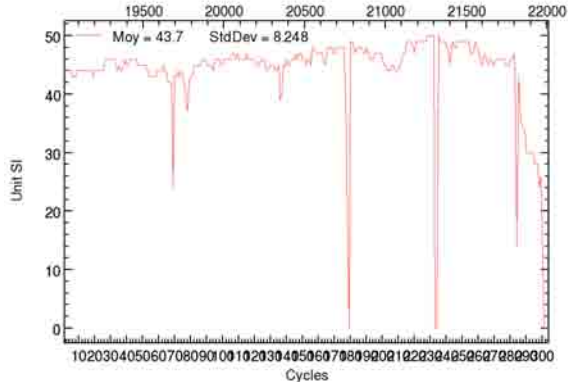

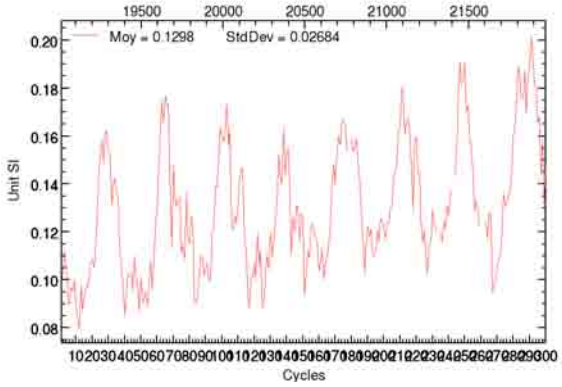

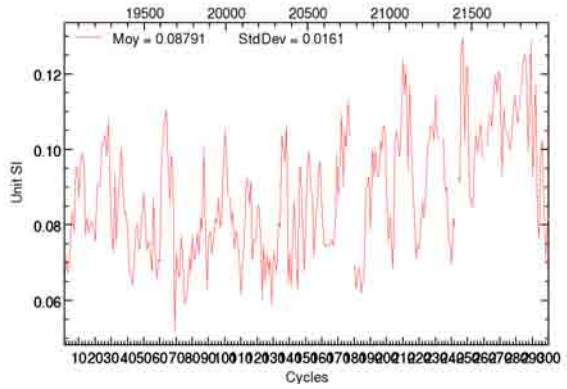

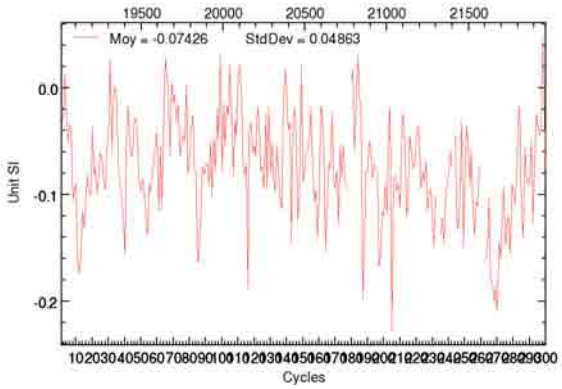

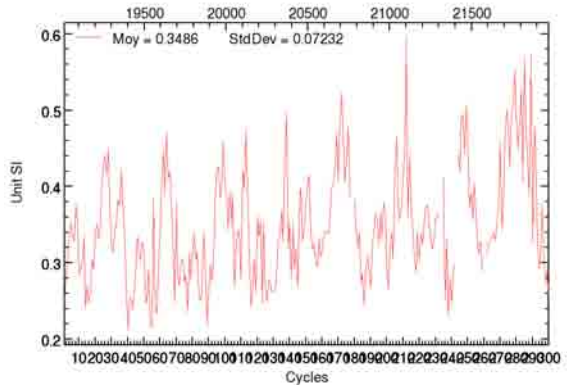

3.5.14. Suivi par cycle du champ SLA_TG_QUAL_BIAIS_DERIVE_VAL

1106 SLA_TG_QUAL_BIAIS_DERIVE_VAL : Anomalie de hauteur de mer validée avec application du contrôle qualité marégraphique, mesurée par le marégraphe, avec correction du biais et de la dérive

Les figures sont rangées dans l'ordre suivant (de gauche à droite et de haut en bas) :
Nombre, Moyenne, Ecart-type, Minimum, Maximum.

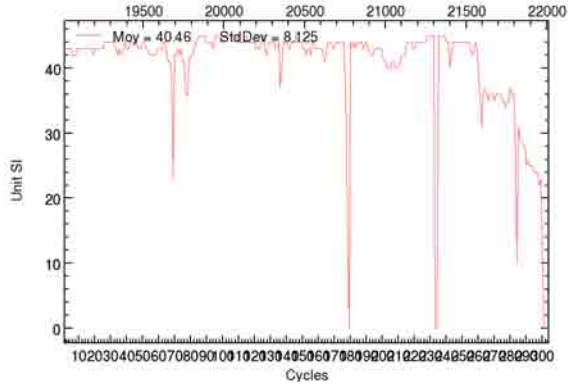

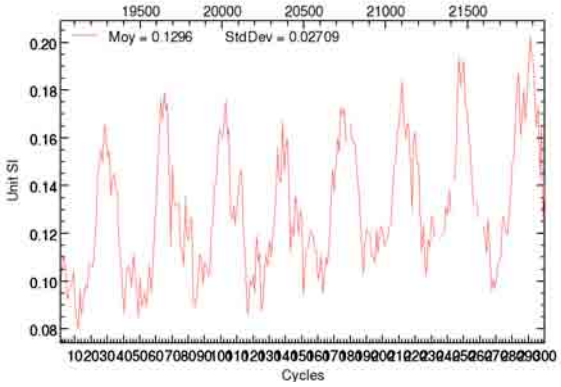

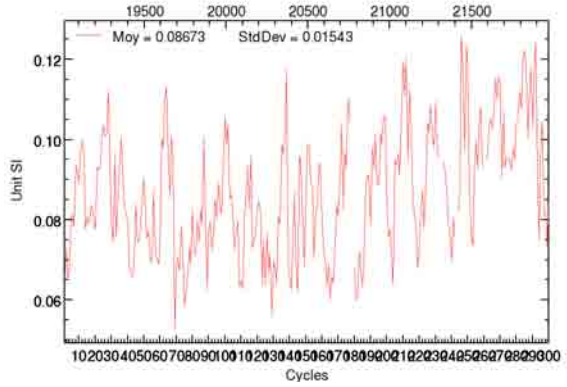

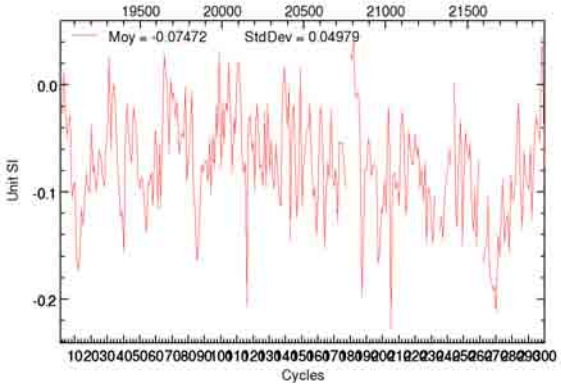

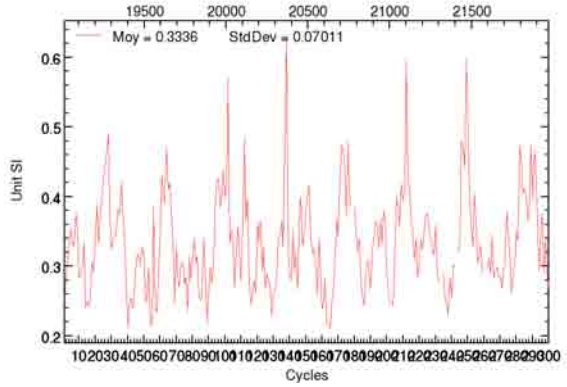

3.5.15. Suivi par cycle du champ SLA_TG_QUAL_BIAIS_DERIVE_VAL_HN

1528 SLA_TG_QUAL_BIAIS_DERIVE_V_HN : Anomalie de hauteur de mer validée avec application du contrôle qualité marégraphique, mesurée par le marégraphe, avec correction du biais et de la dérive (Hémisphère Nord)

Les figures sont rangées dans l'ordre suivant (de gauche à droite et de haut en bas) :
Nombre, Moyenne, Ecart-type, Minimum, Maximum.

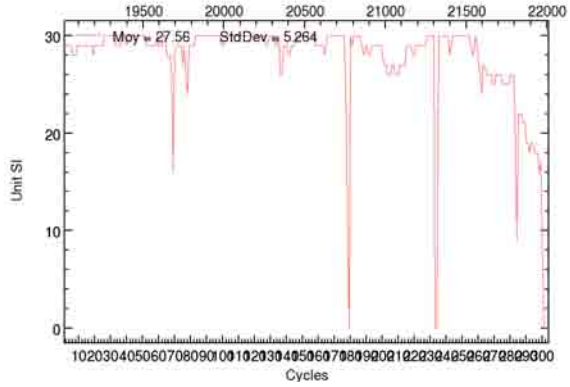

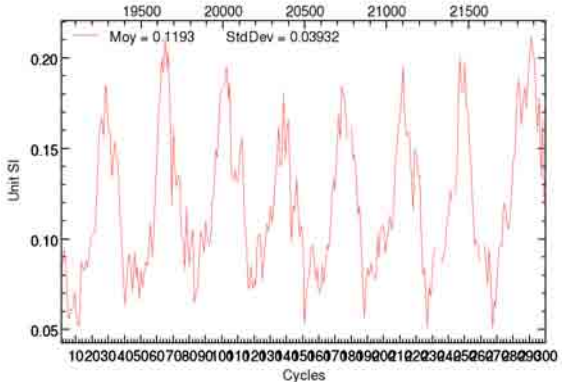

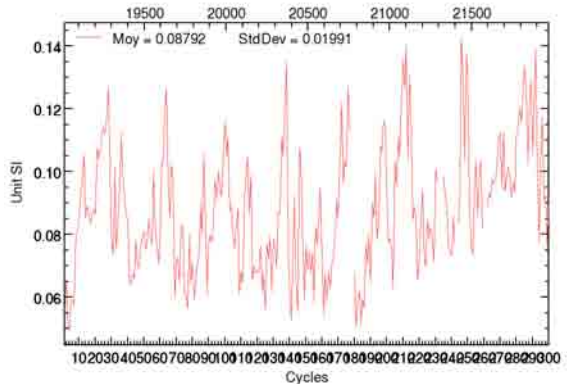

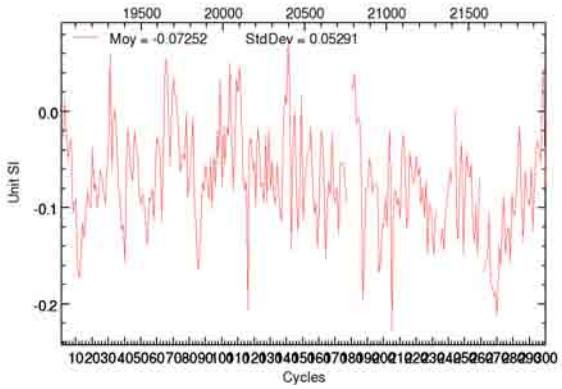

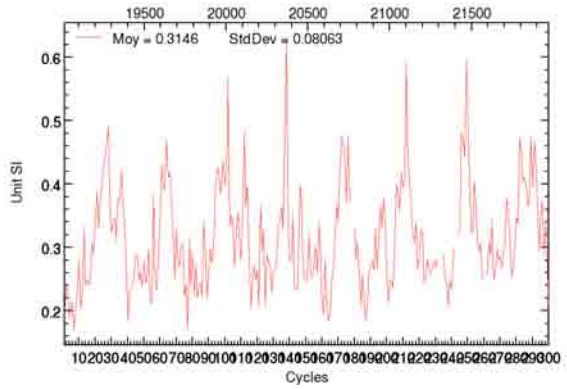

3.5.16. Suivi par cycle du champ SLA_TG_QUAL_BIAIS_DERIVE_VAL_HS

1535 SLA_TG_QUAL_BIAIS_DERIVE_V_HS : Anomalie de hauteur de mer validée avec application du contrôle qualité marégraphique, mesurée par le marégraphe, avec correction du biais et de la dérive (Hémisphère Sud)

Les figures sont rangées dans l'ordre suivant (de gauche à droite et de haut en bas) :
Nombre, Moyenne, Ecart-type, Minimum, Maximum.

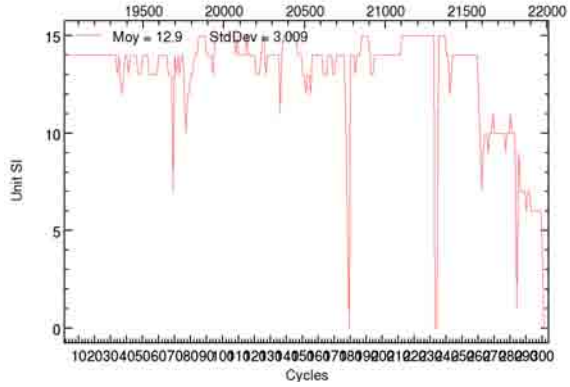

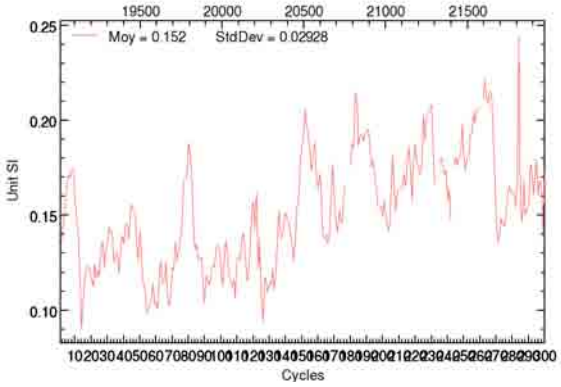

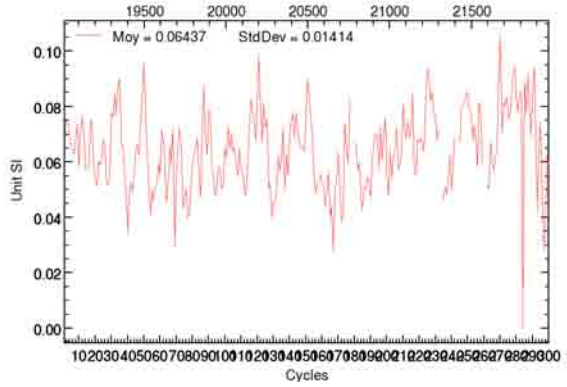

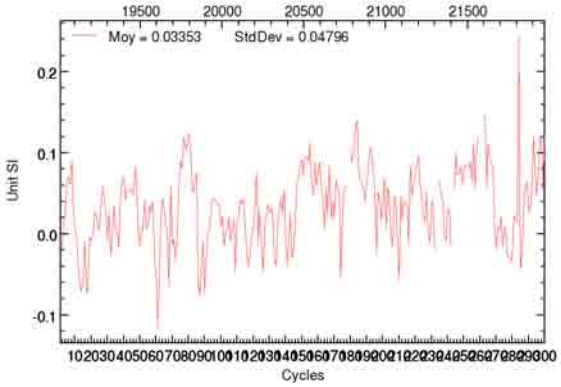

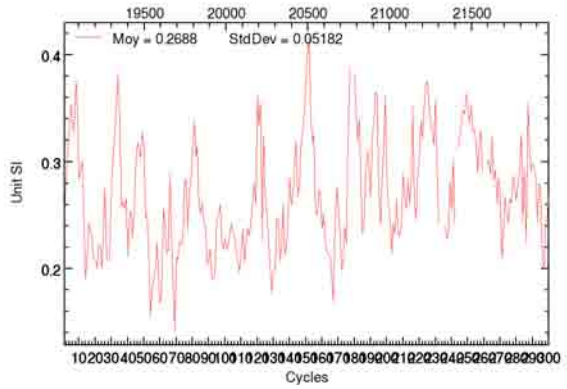

3.5.17. Suivi par cycle du champ SLA_TG_QUAL_BIAIS_DERIVE_VAL_TrP

1542 SLA_TG_QUAL_BIAIS_DERIVE_V_TRP : Anomalie de hauteur de mer validée avec application du contrôle qualité marégraphique, mesurée par le marégraphe, avec correction du biais et de la dérive (Hémisphère Nord)

Les figures sont rangées dans l'ordre suivant (de gauche à droite et de haut en bas) :
Nombre, Moyenne, Ecart-type, Minimum, Maximum.

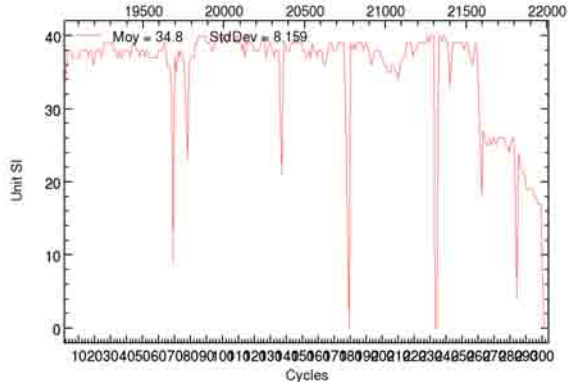

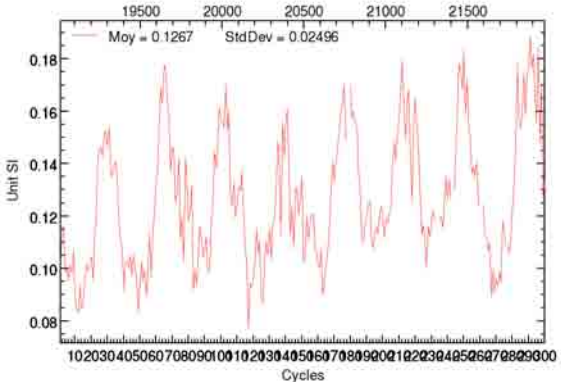

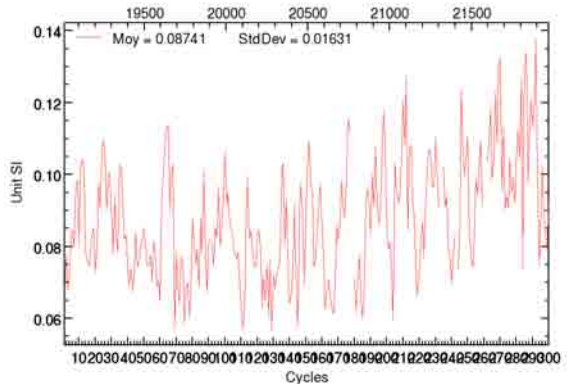

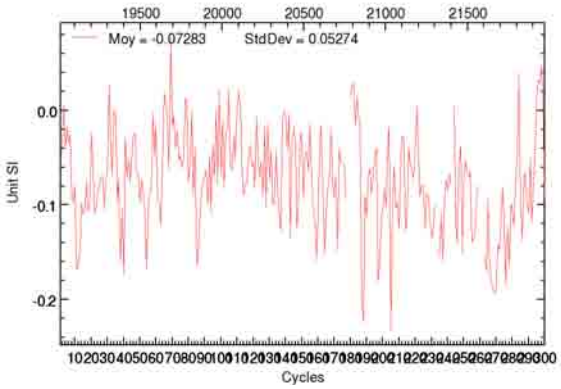

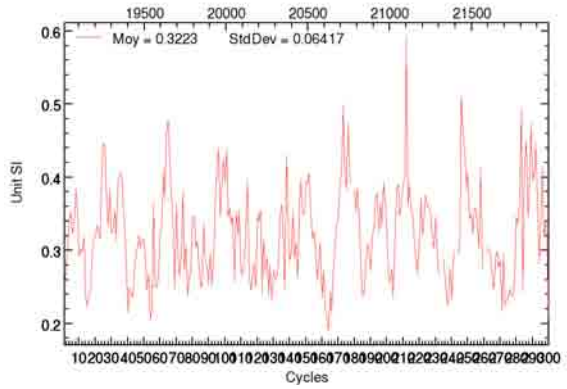

3.5.18. Suivi par cycle du champ SLA_TG_QUAL_BIAIS_DERIVE_VAL_TrI

1549 SLA_TG_QUAL_BIAIS_DERIVE_V_TRI : Anomalie de hauteur de mer validée avec application du contrôle qualité marégraphique, mesurée par le marégraphe, avec correction du biais et de la dérive (Hémisphère Sud)

Les figures sont rangées dans l'ordre suivant (de gauche à droite et de haut en bas) :
Nombre, Moyenne, Ecart-type, Minimum, Maximum.

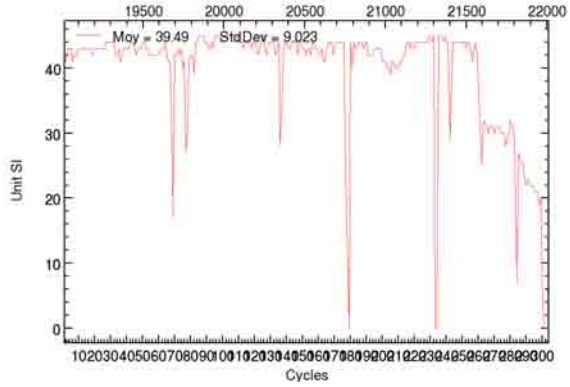

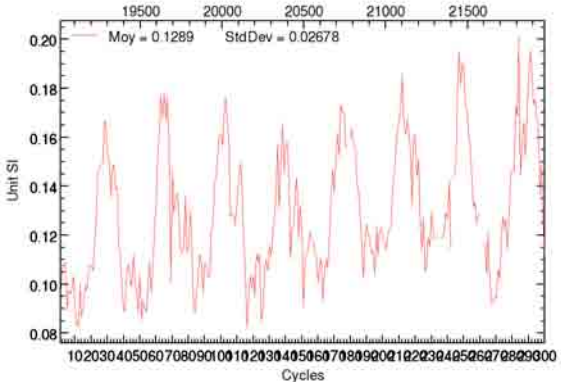

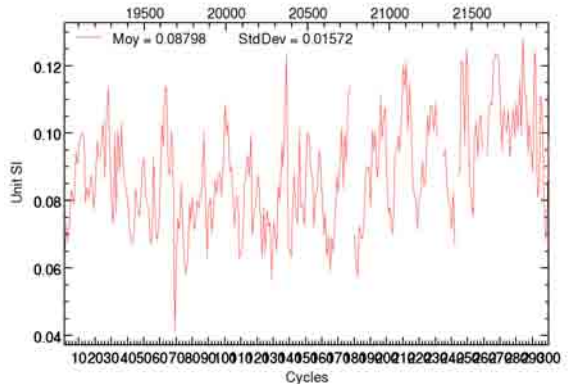

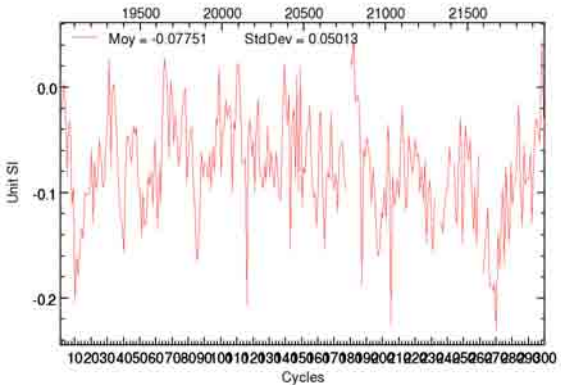

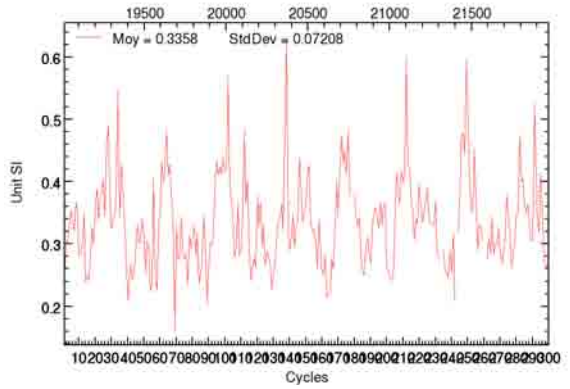

3.6. Suivi de la différence de SLA satellite et marégraphique sans correction du biais entre les marégraphes et sans la dérive crustale

3.6.1. Suivi par cycle du champ D_SLA_QUAL_NOCORR_BRUTE

1100 D_SLA_QUAL_NOCORR_BRUTE : Différence des hauteurs de mer brutes avec application du contrôle qualité marégraphique, altimétrique et marégraphique

Les figures sont rangées dans l'ordre suivant (de gauche à droite et de haut en bas) :
Nombre, Moyenne, Ecart-type, Minimum, Maximum.

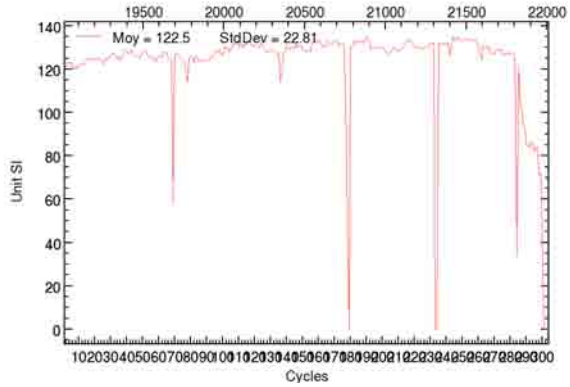

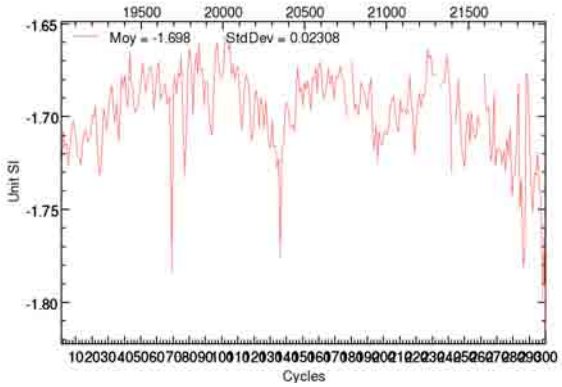

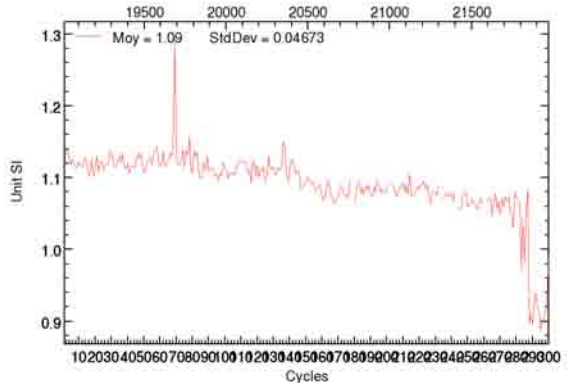

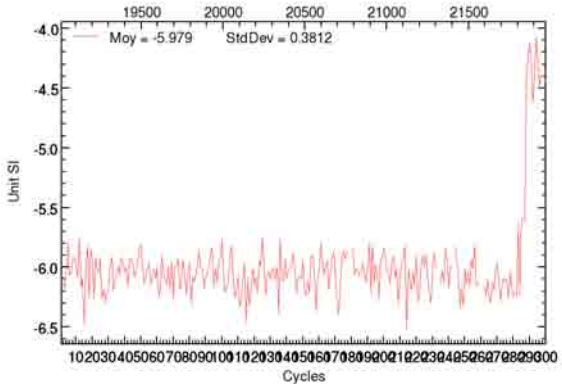

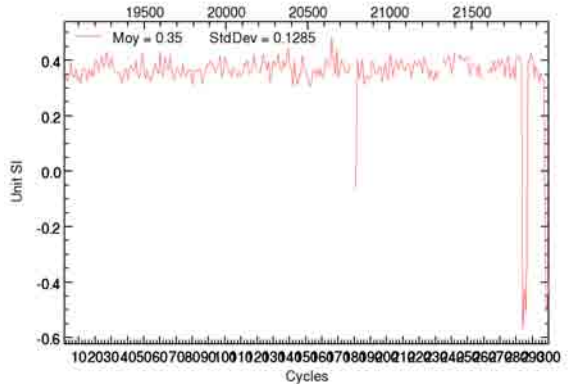

3.6.2. Suivi par cycle du champ D_SLA_QUAL_NOCORR_VAL

1107 D_SLA_QUAL_NOCORR_VAL : Différence des hauteurs de mer validées avec application du contrôle qualité marégraphique,a ltimétrique et marégraphique

Les figures sont rangées dans l'ordre suivant (de gauche à droite et de haut en bas) :
Nombre, Moyenne, Ecart-type, Minimum, Maximum.

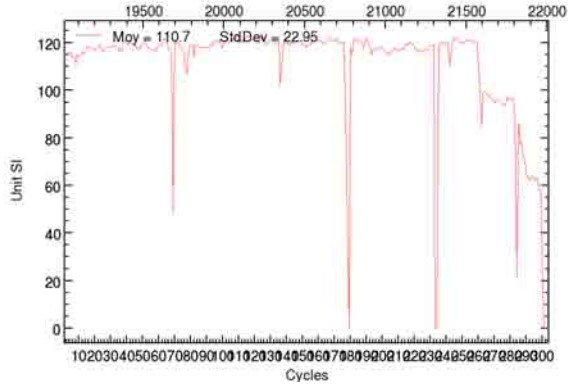

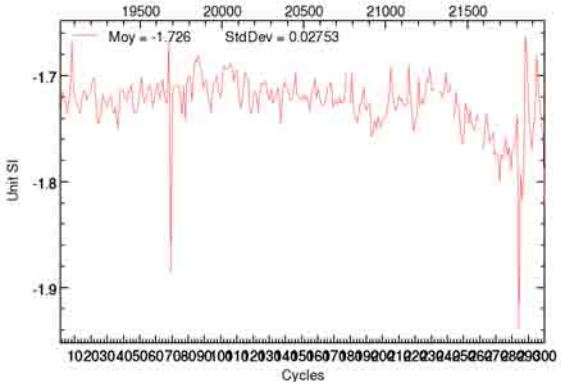

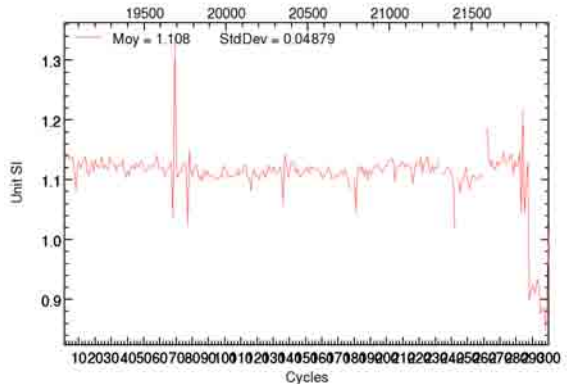

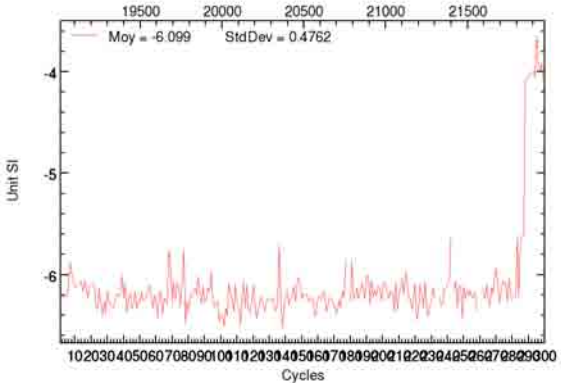

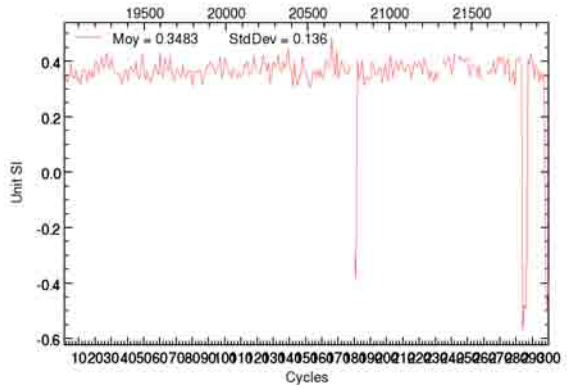

3.6.3. Suivi par cycle du champ D_SLA_QUAL_NOCORR_VAL_HN

1529 D_SLA_QUAL_NOCORR_VAL_HN : Différence des hauteurs de mer alti/TG validées avec application du contrôle qualité marégraphique (Hémisphère Nord)

Les figures sont rangées dans l'ordre suivant (de gauche à droite et de haut en bas) :
Nombre, Moyenne, Ecart-type, Minimum, Maximum.

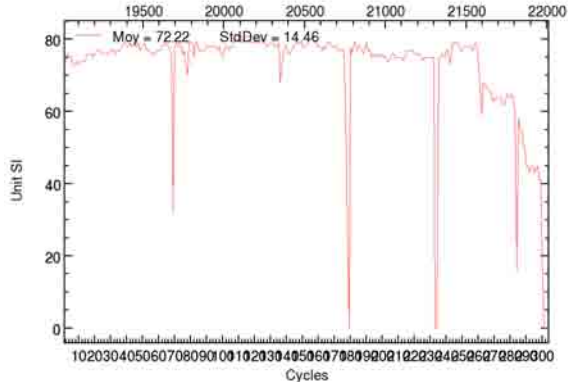

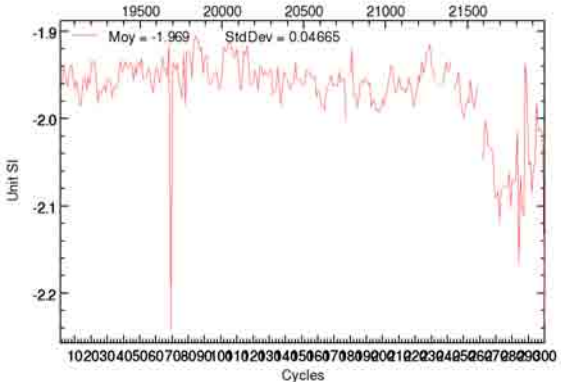

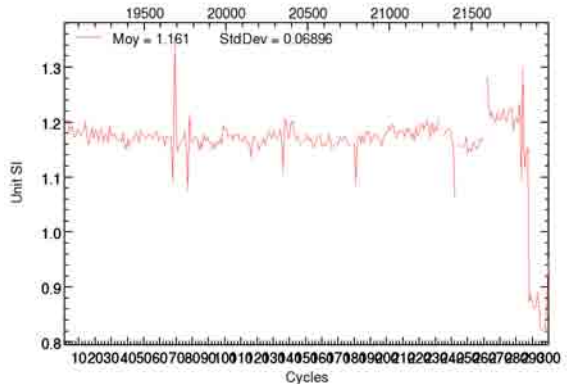

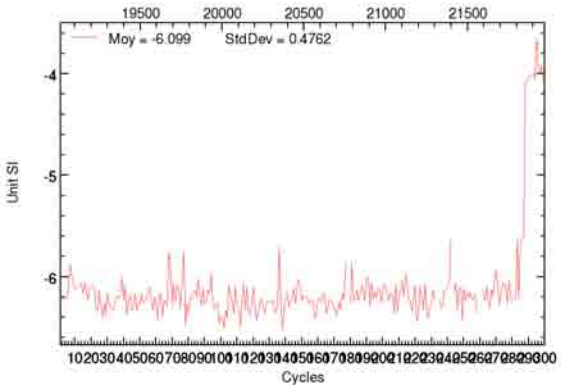

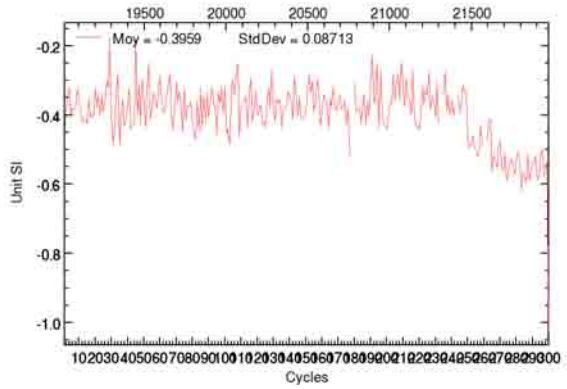

3.6.4. Suivi par cycle du champ D_SLA_QUAL_NOCORR_VAL_HS

1536 D_SLA_QUAL_NOCORR_VAL_HS : Différence des hauteurs de mer alti/TG validées avec application du contrôle qualité marégraphique (Hémisphère Sud)

Les figures sont rangées dans l'ordre suivant (de gauche à droite et de haut en bas) :
Nombre, Moyenne, Ecart-type, Minimum, Maximum.

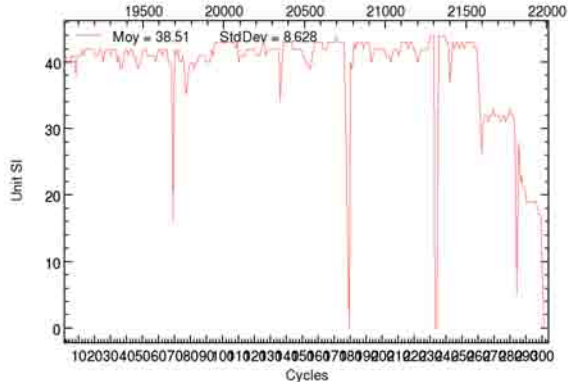

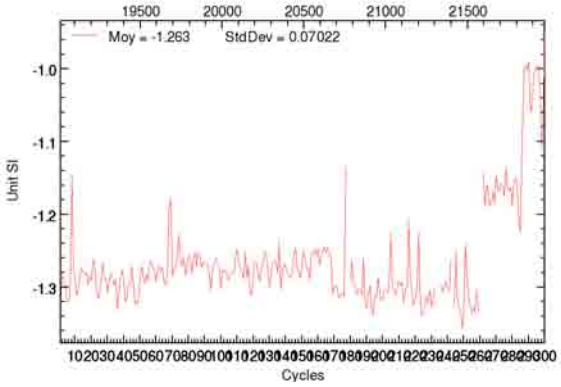

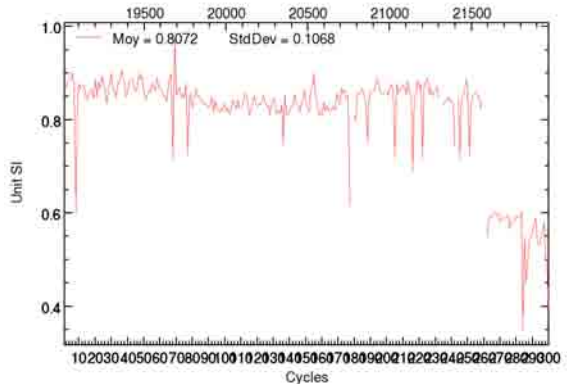

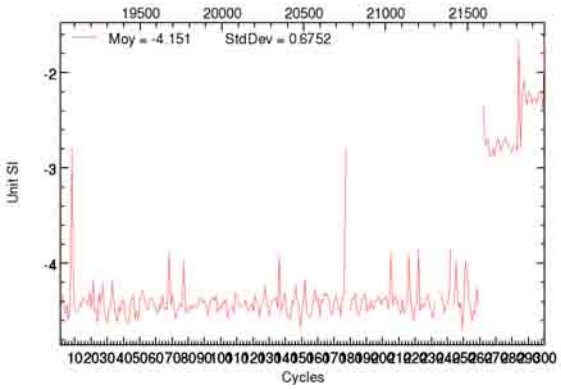

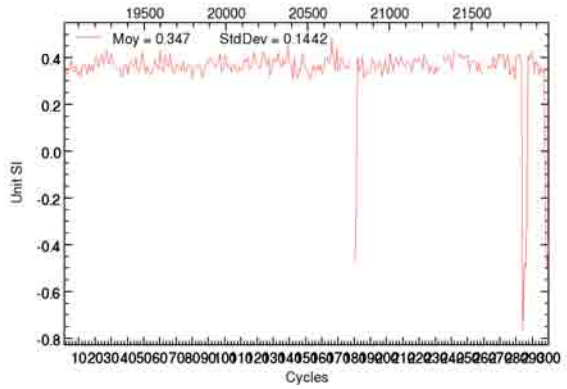

3.6.5. Suivi par cycle du champ D_SLA_QUAL_NOCORR_VAL_TrP

1543 D_SLA_QUAL_NOCORR_VAL_TRP : Différence des hauteurs de mer alti/TG validées avec application du contrôle qualité marégraphique (Hémisphère Nord)

Les figures sont rangées dans l'ordre suivant (de gauche à droite et de haut en bas) :
Nombre, Moyenne, Ecart-type, Minimum, Maximum.

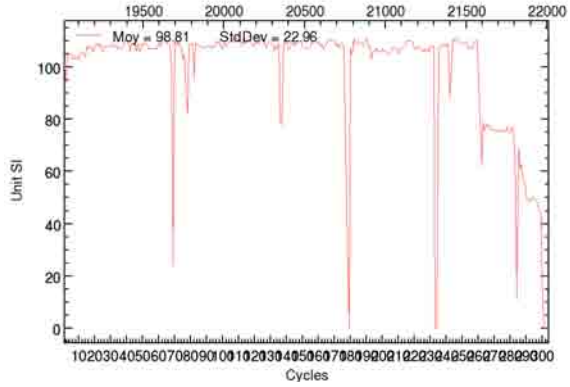

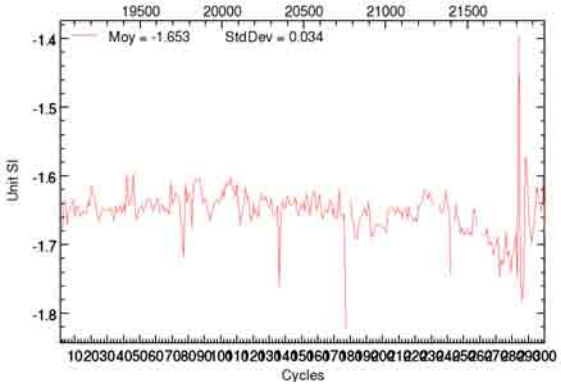

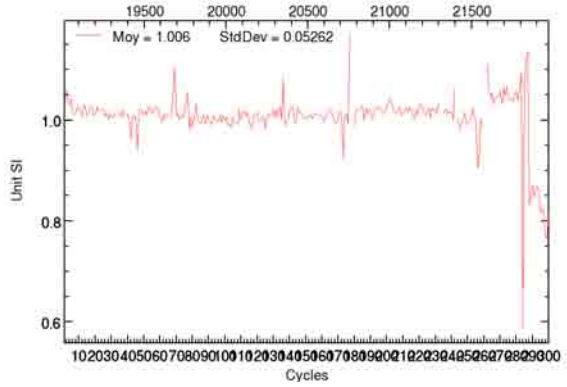

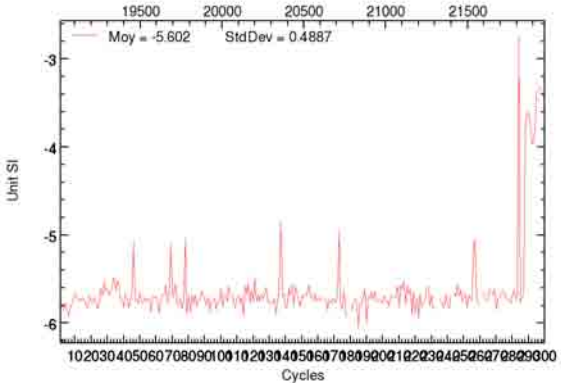

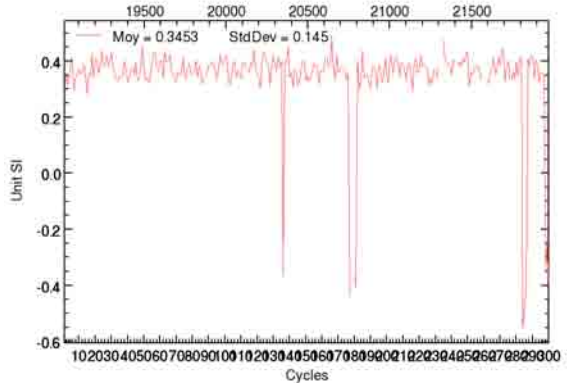

3.6.6. Suivi par cycle du champ D_SLA_QUAL_NOCORR_VAL_TrI

1550 D_SLA_QUAL_NOCORR_VAL_TRI : Différence des hauteurs de mer alti/TG validées avec application du contrôle qualité marégraphique (Hémisphère Sud)

Les figures sont rangées dans l'ordre suivant (de gauche à droite et de haut en bas) :
Nombre, Moyenne, Ecart-type, Minimum, Maximum.

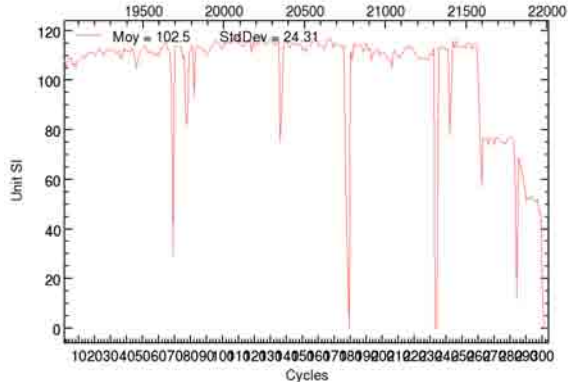

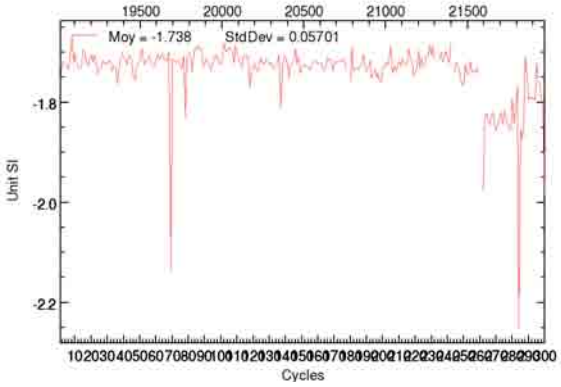

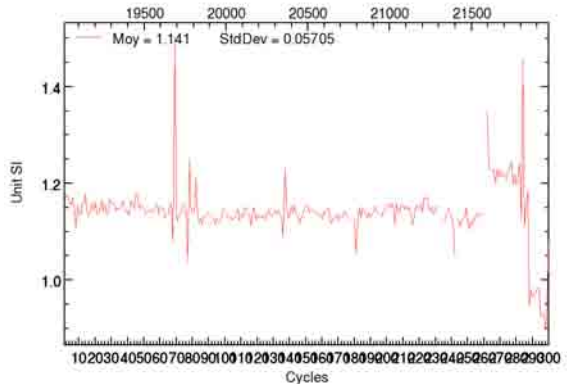

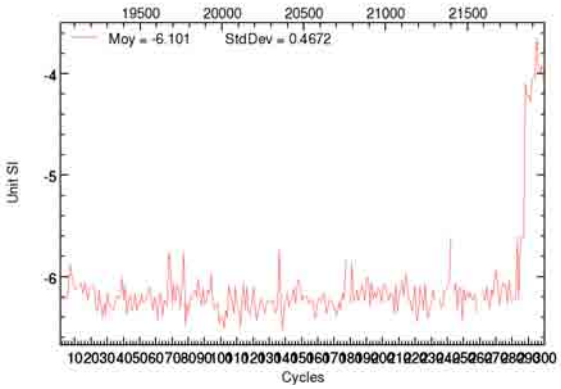

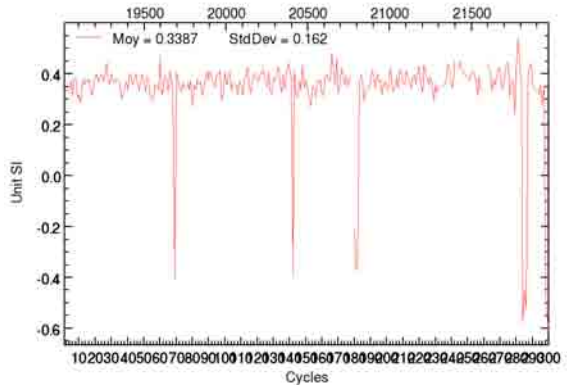

3.6.7. Suivi par cycle du champ D_SLA_QUAL_BIAIS_BRUTE

1101 D_SLA_QUAL_BIAIS_BRUTE : Différence des hauteurs de mer brutes avec application du contrôle qualité marégraphique, altimétrique et marégraphique, avec correction du biais

Les figures sont rangées dans l'ordre suivant (de gauche à droite et de haut en bas) :
Nombre, Moyenne, Ecart-type, Minimum, Maximum.

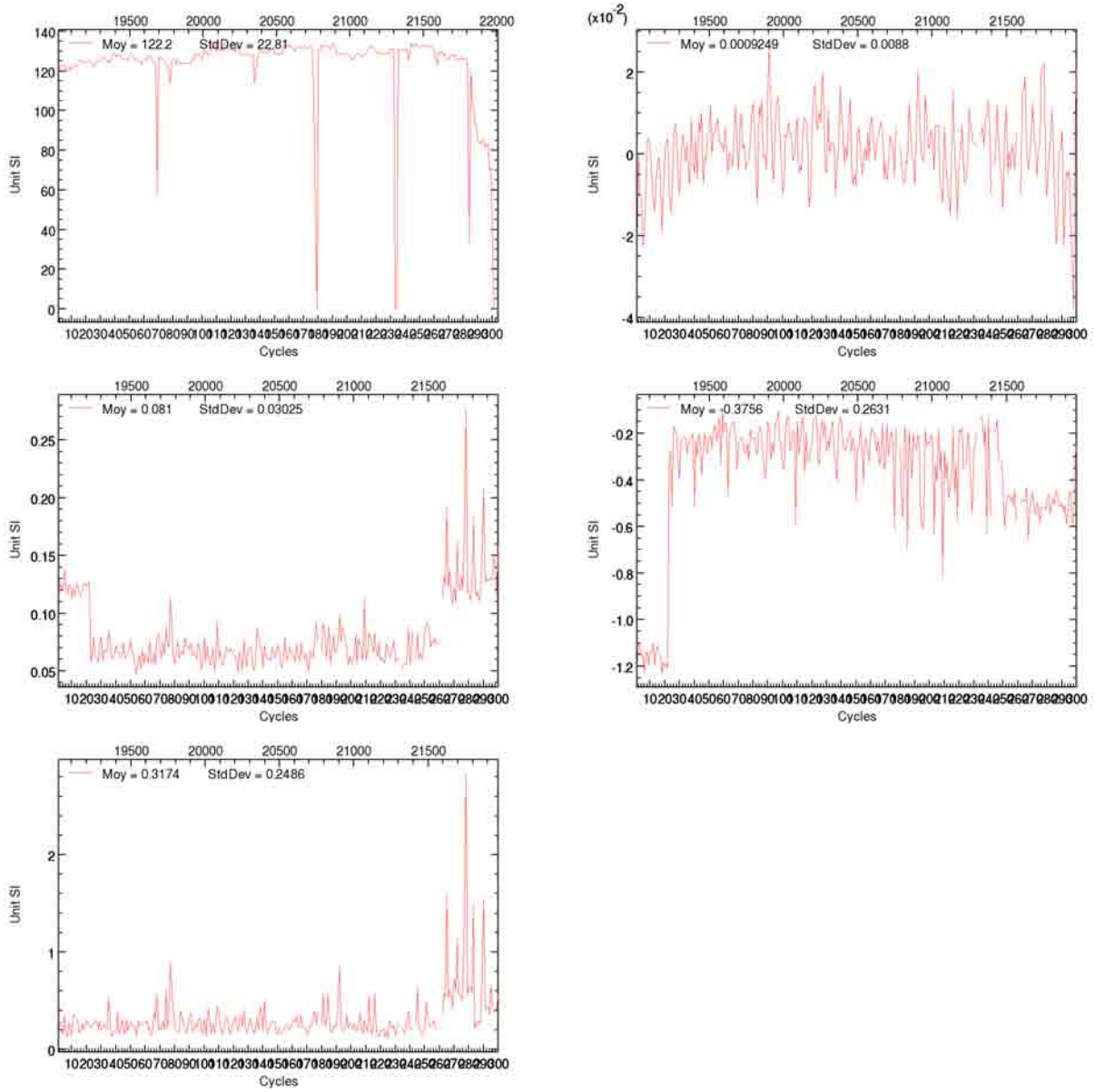

3.6.8. Suivi par cycle du champ D_SLA_QUAL_BIAIS_VAL

1108 D_SLA_QUAL_BIAIS_VAL : Différence des hauteurs de mer validées avec application du contrôle qualité marégraphique, altimétrique et marégraphique, avec correction du biais

Les figures sont rangées dans l'ordre suivant (de gauche à droite et de haut en bas) :
Nombre, Moyenne, Ecart-type, Minimum, Maximum.

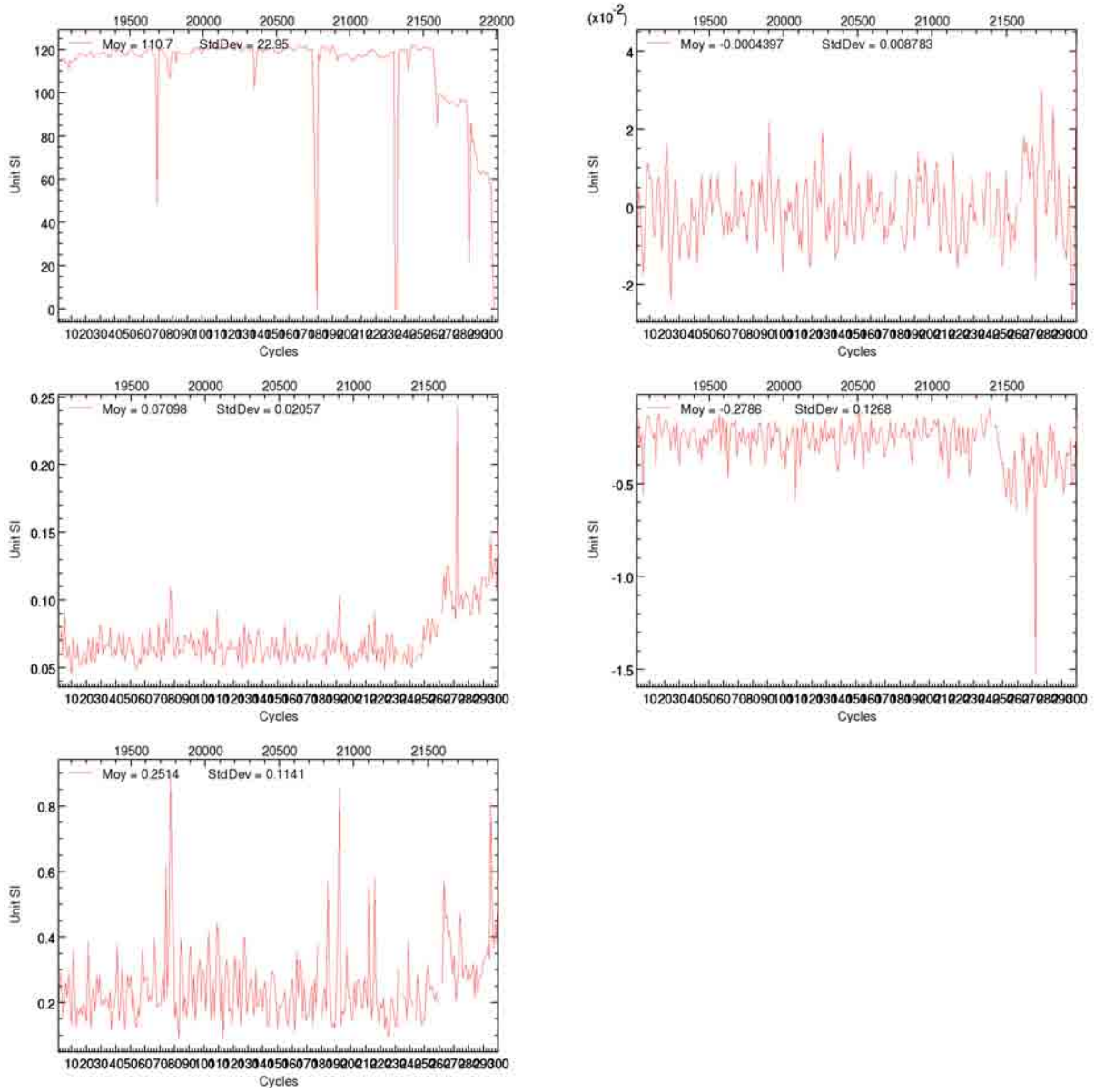

3.6.9. Suivi par cycle du champ D_SLA_QUAL_BIAIS_VAL_HN

1530 D_SLA_QUAL_BIAIS_VAL_HN : Différence des hauteurs de mer alti/TG validées avec application du contrôle qualité marégraphique et correction du biais (Hémisphère Nord)

Les figures sont rangées dans l'ordre suivant (de gauche à droite et de haut en bas) :
Nombre, Moyenne, Ecart-type, Minimum, Maximum.

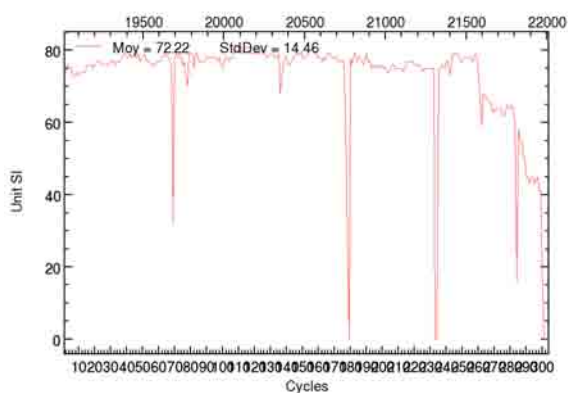

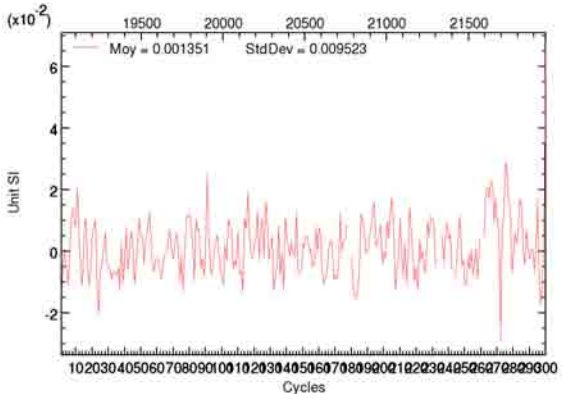

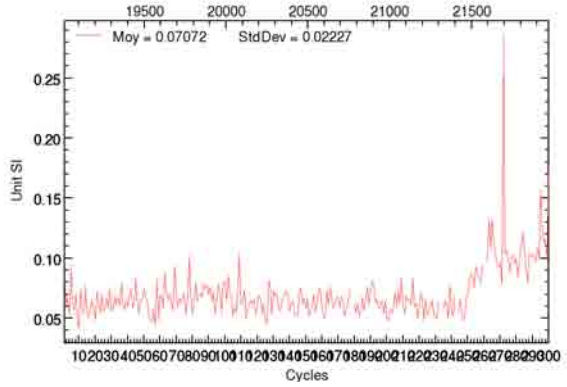

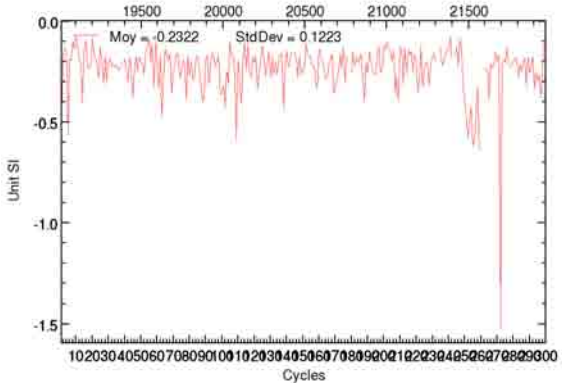

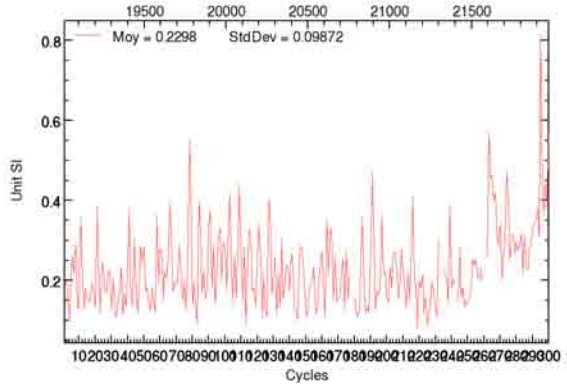

3.6.10. Suivi par cycle du champ D_SLA_QUAL_BIAIS_VAL_HS

1537 D_SLA_QUAL_BIAIS_VAL_HS : Différence des hauteurs de mer alti/TG validées avec application du contrôle qualité marégraphique et correction du biais (Hémisphère Sud)

Les figures sont rangées dans l'ordre suivant (de gauche à droite et de haut en bas) :
Nombre, Moyenne, Ecart-type, Minimum, Maximum.

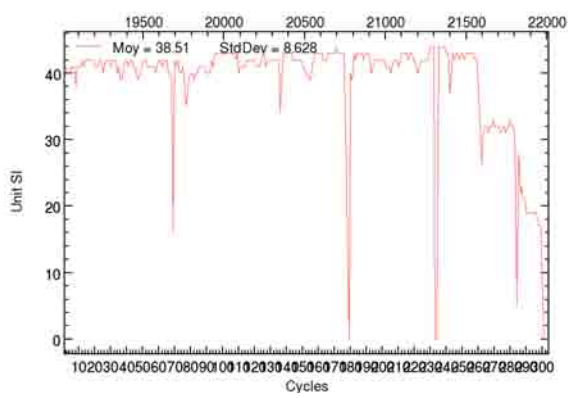

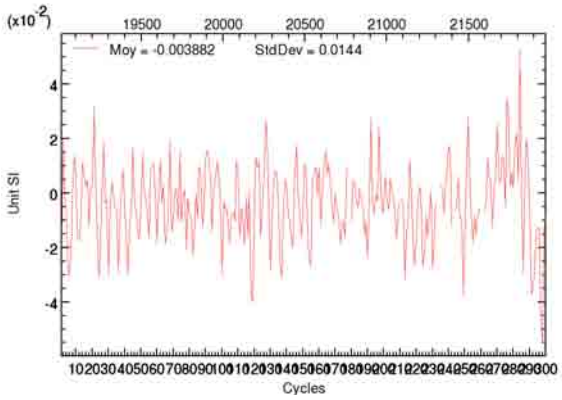

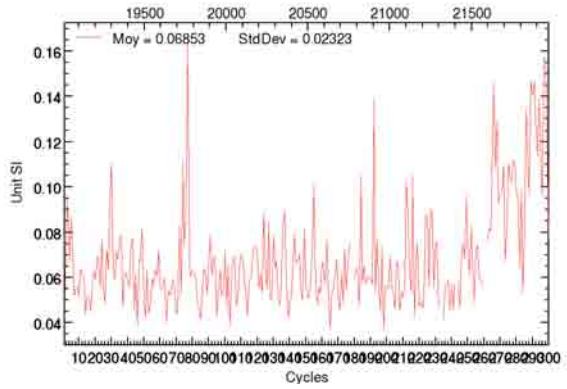

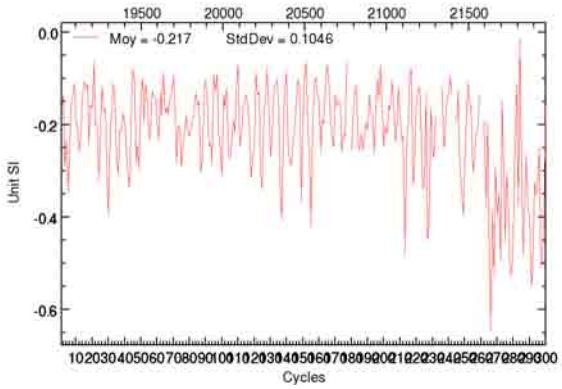

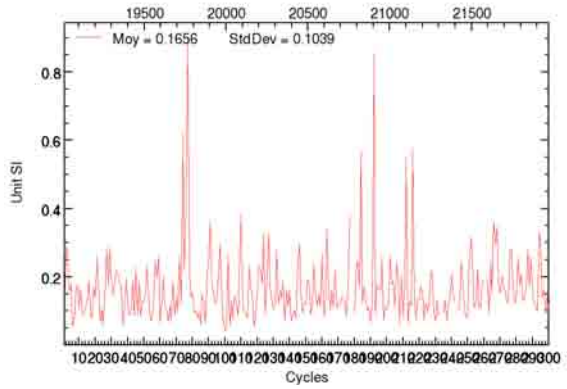

3.6.11. Suivi par cycle du champ D_SLA_QUAL_BIAIS_VAL_TrP

1544 D_SLA_QUAL_BIAIS_VAL_TRP : Différence des hauteurs de mer alti/TG validées avec application du contrôle qualité marégraphique et correction du biais (Hémisphère Nord)

Les figures sont rangées dans l'ordre suivant (de gauche à droite et de haut en bas) :
Nombre, Moyenne, Ecart-type, Minimum, Maximum.

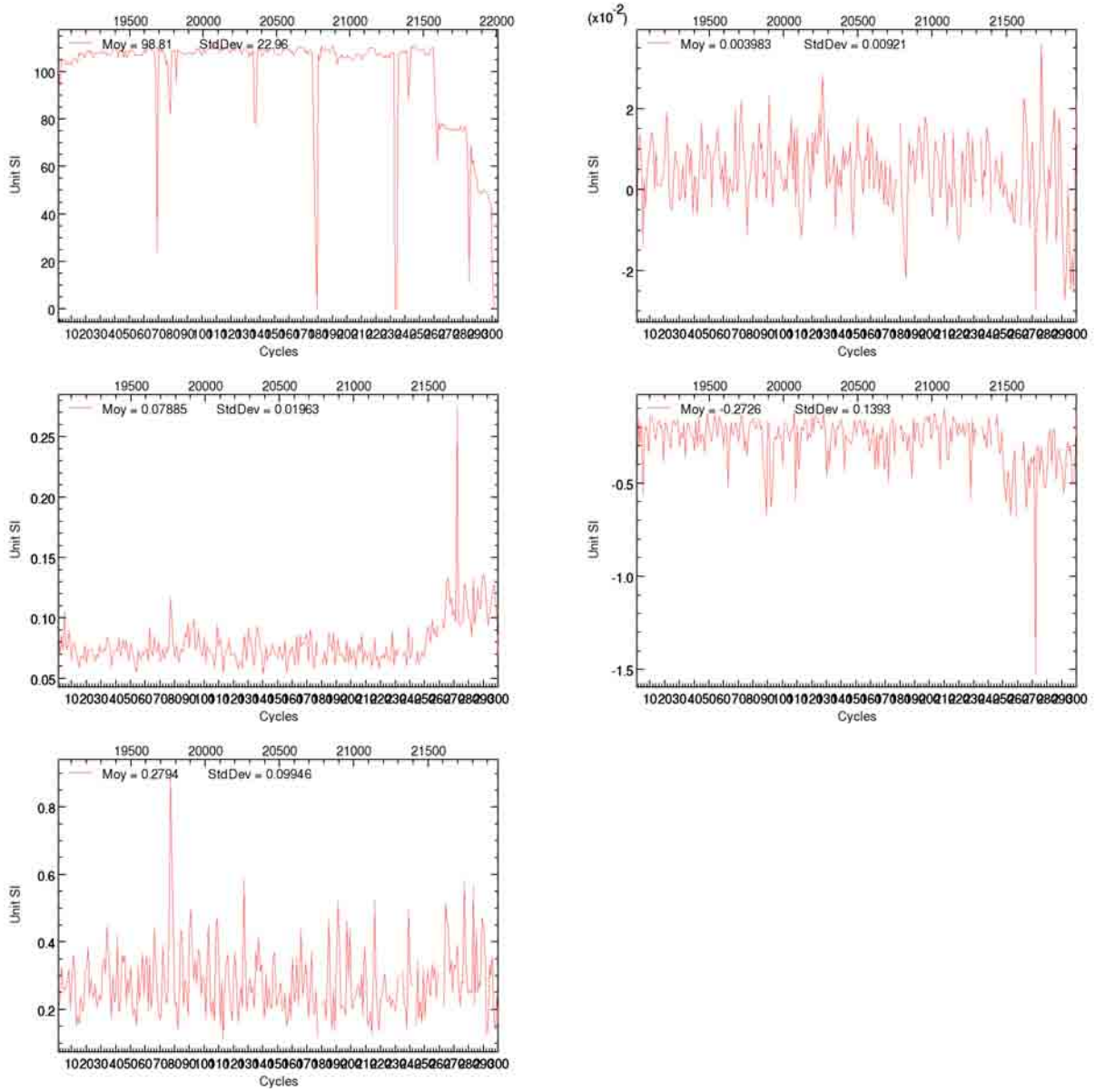

3.6.12. Suivi par cycle du champ D_SLA_QUAL_BIAIS_VAL_TrI

1551 D_SLA_QUAL_BIAIS_VAL_TRI : Différence des hauteurs de mer alti/TG validées avec application du contrôle qualité marégraphique et correction du biais (Hémisphère Sud)

Les figures sont rangées dans l'ordre suivant (de gauche à droite et de haut en bas) :
Nombre, Moyenne, Ecart-type, Minimum, Maximum.

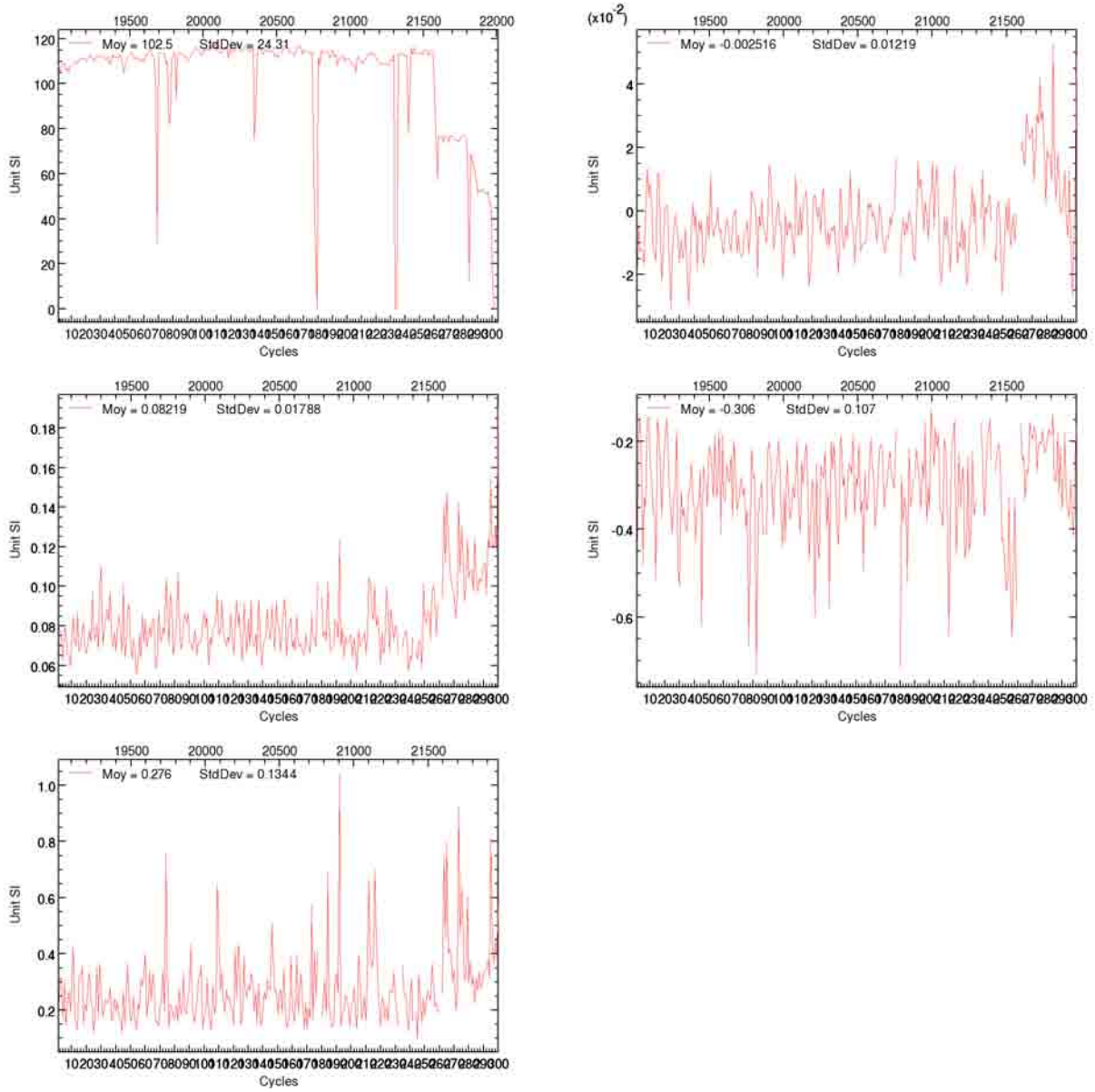

3.6.13. Suivi par cycle du champ D_SLA_QUAL_BIAIS_DERIVE_BRUTE

1102 D_SLA_QUAL_BIAIS_DERIVE_BRUTE : Différence des hauteurs de mer brutes avec application du contrôle qualité marégraphique, altimétrique et marégraphique, avec correction du biais et de la dérive

Les figures sont rangées dans l'ordre suivant (de gauche à droite et de haut en bas) :
Nombre, Moyenne, Ecart-type, Minimum, Maximum.

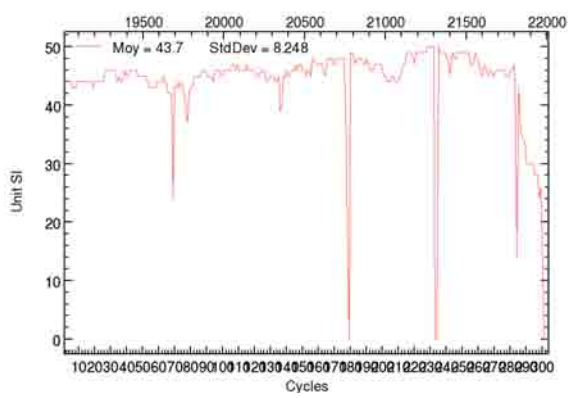

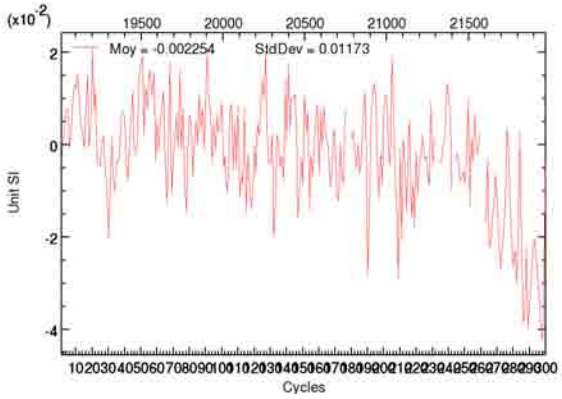

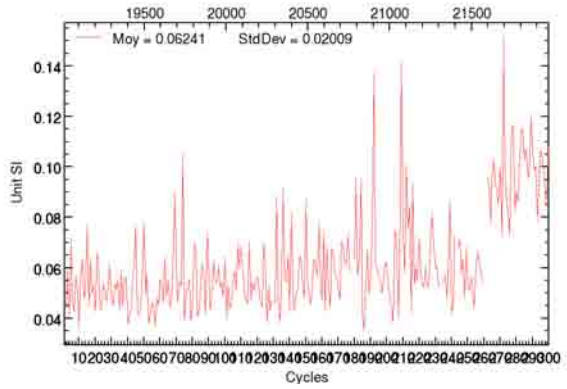

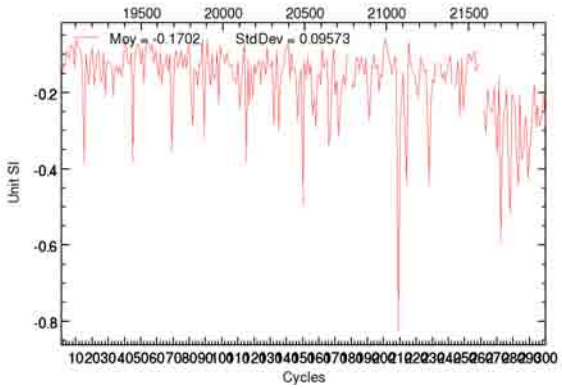

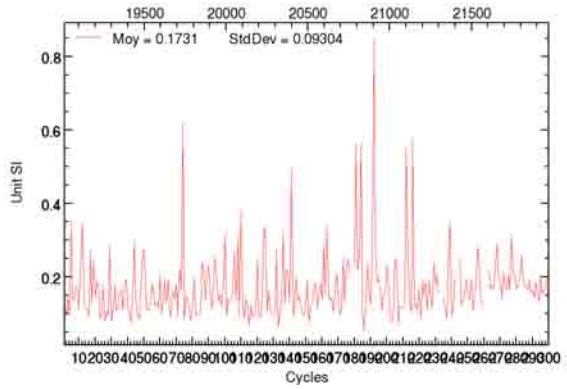

3.6.14. Suivi par cycle du champ D_SLA_QUAL_BIAIS_DERIVE_VAL

1109 D_SLA_QUAL_BIAIS_DERIVE_VAL : Différence des hauteurs de mer validées avec application du contrôle qualité marégraphique, altimétrique et marégraphique, avec correction du biais et de la dérive

Les figures sont rangées dans l'ordre suivant (de gauche à droite et de haut en bas) :
Nombre, Moyenne, Ecart-type, Minimum, Maximum.

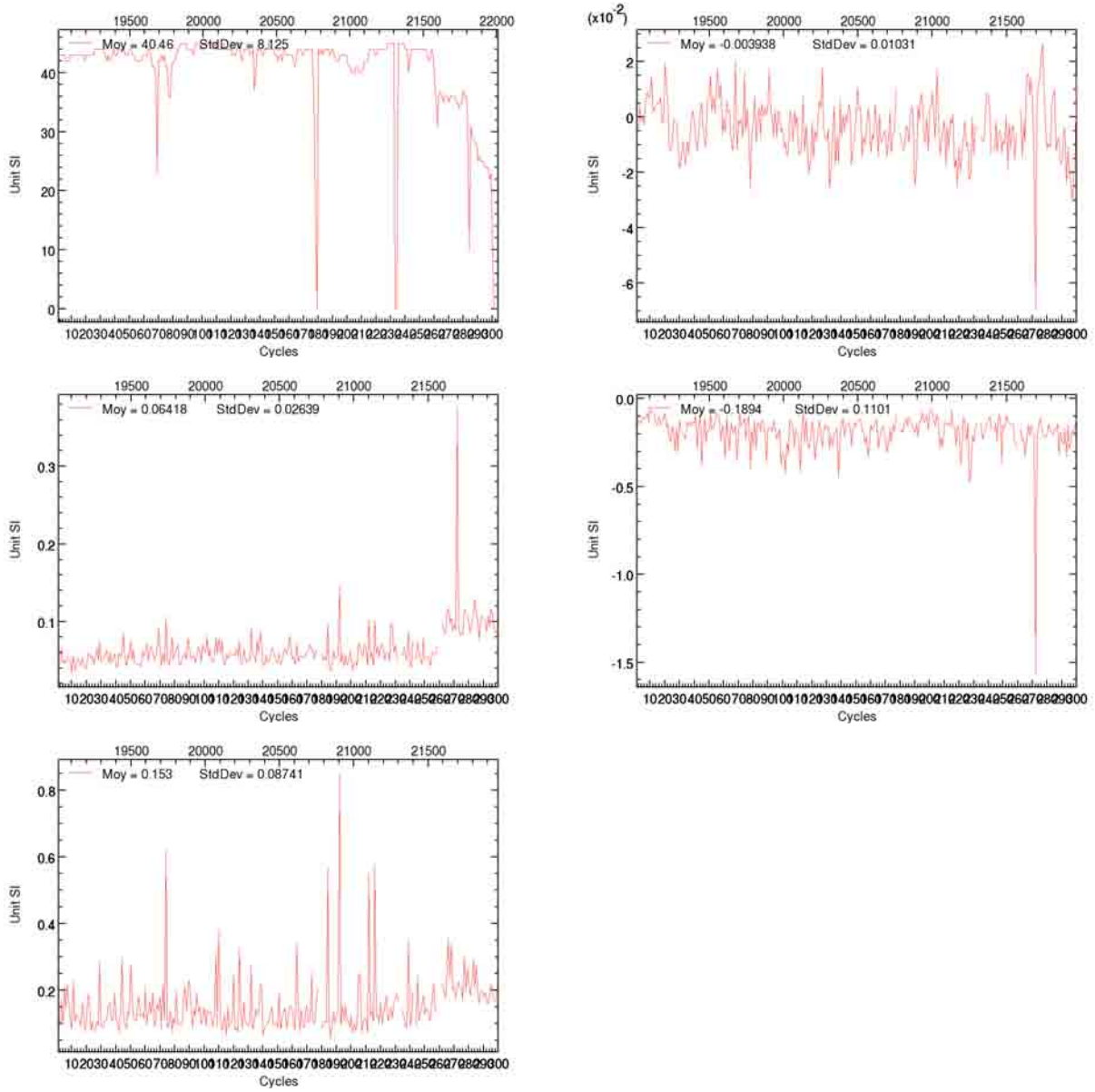

3.6.15. Suivi par cycle du champ D_SLA_QUAL_BIAIS_DERIVE_V_HN

1531 D_SLA_QUAL_BIAIS_DERIVE_V_HN : Différence des hauteurs de mer alti/TG validées avec application du contrôle qualité marégraphique et correction du biais et de la dérive (Hémisphère Nord)

Les figures sont rangées dans l'ordre suivant (de gauche à droite et de haut en bas) :
Nombre, Moyenne, Ecart-type, Minimum, Maximum.

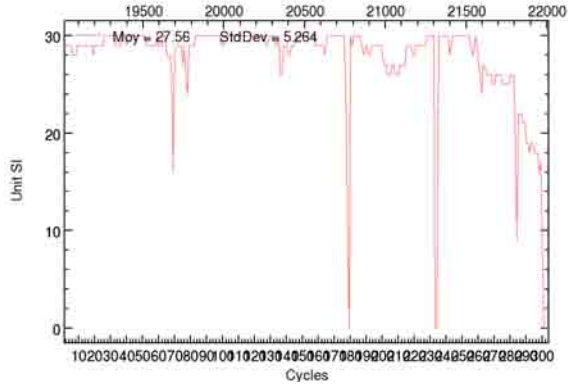

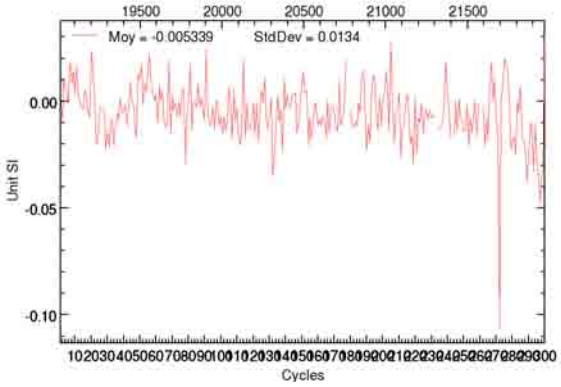

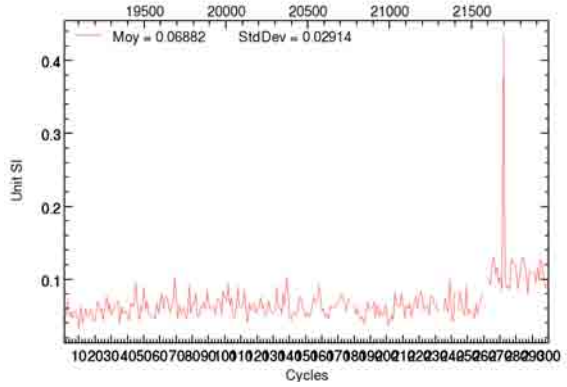

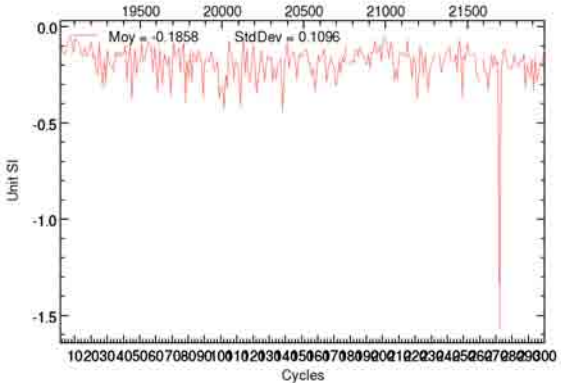

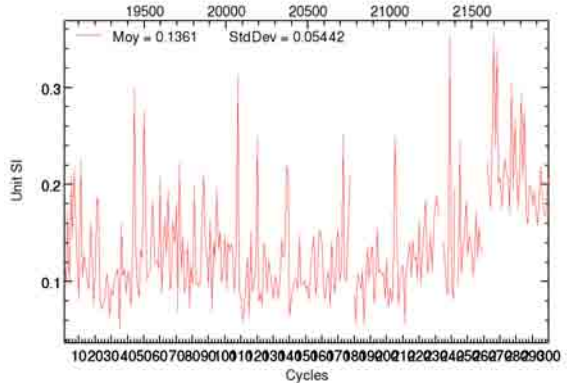

3.6.16. Suivi par cycle du champ D_SLA_QUAL_BIAIS_DERIVE_V_HS

1538 D_SLA_QUAL_BIAIS_DERIVE_V_HS : Différence des hauteurs de mer alti/TG validées avec application du contrôle qualité marégraphique et correction du biais et de la dérive (Hémisphère Sud)

Les figures sont rangées dans l'ordre suivant (de gauche à droite et de haut en bas) :
Nombre, Moyenne, Ecart-type, Minimum, Maximum.

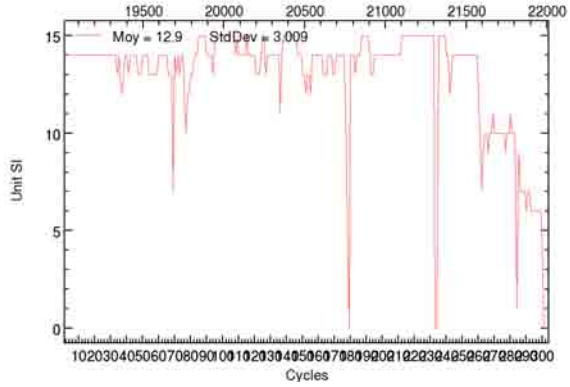

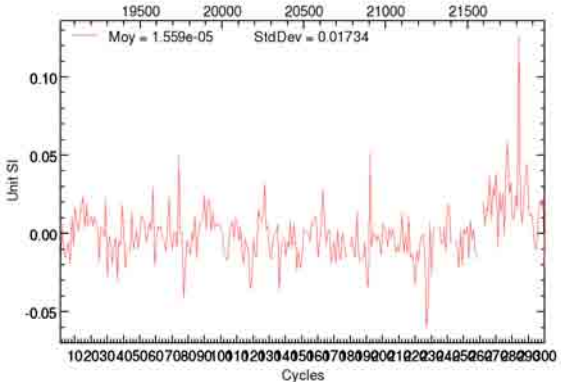

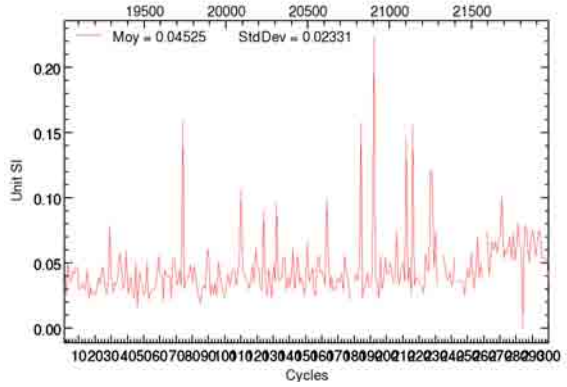

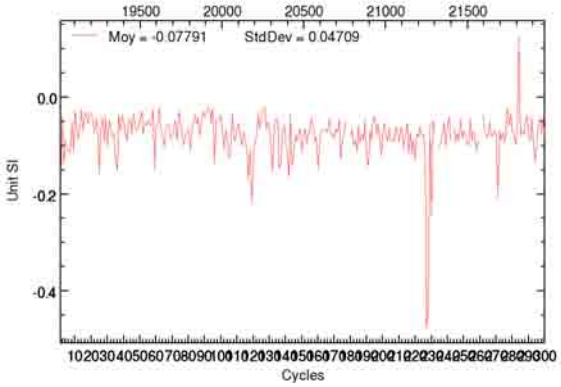

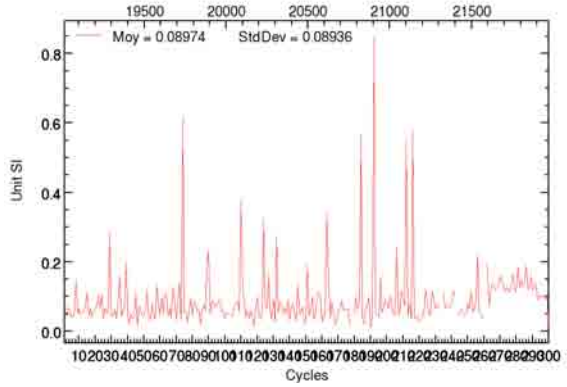

3.6.17. Suivi par cycle du champ D_SLA_QUAL_BIAIS_DERIVE_V_TrP

1545 D_SLA_QUAL_BIAIS_DERIVE_V_TRP : Différence des hauteurs de mer alti/TG validées avec application du contrôle qualité marégraphique et correction du biais et de la dérive (Hémisphère Nord)

Les figures sont rangées dans l'ordre suivant (de gauche à droite et de haut en bas) :
Nombre, Moyenne, Ecart-type, Minimum, Maximum.

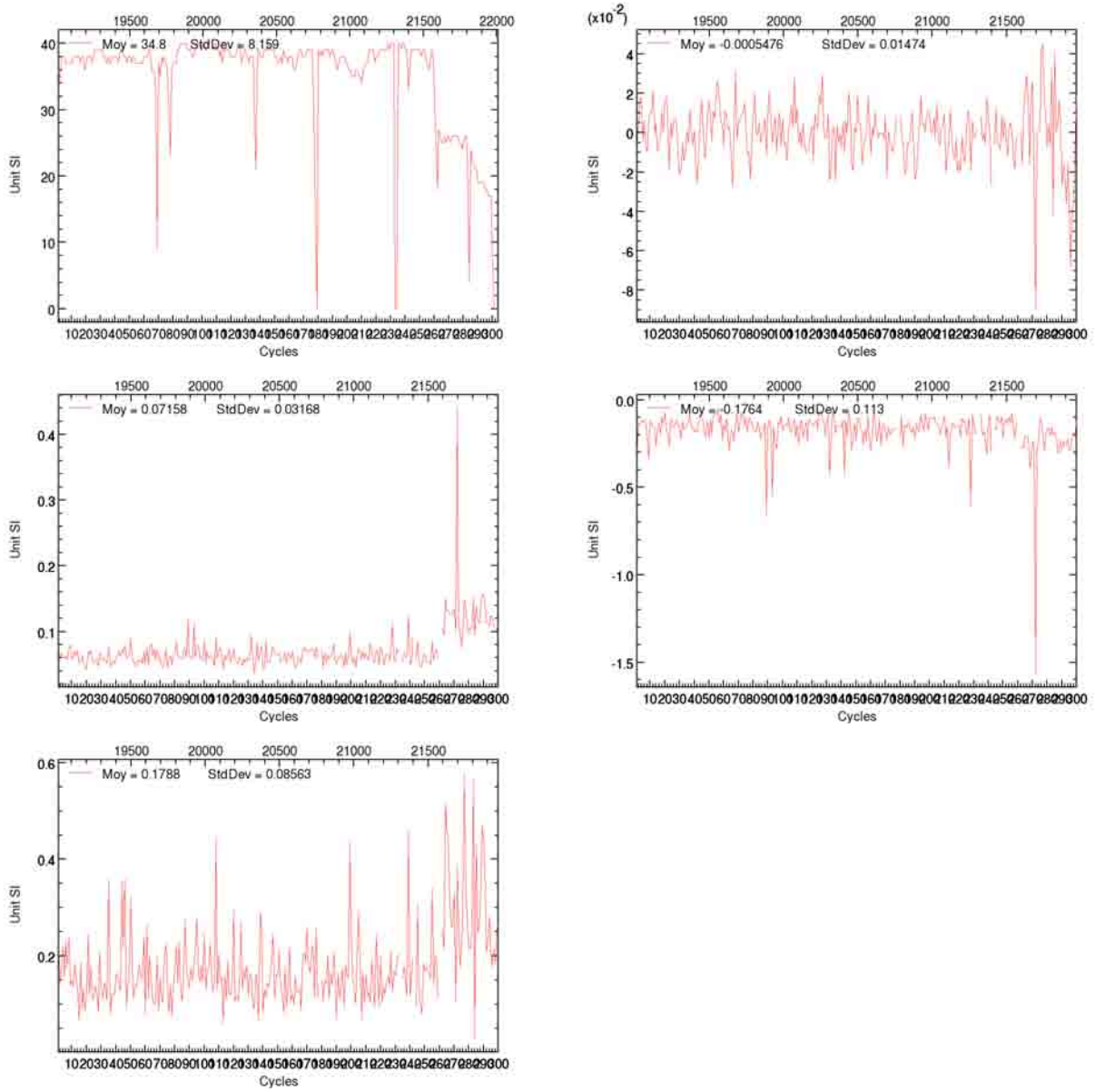

3.6.18. Suivi par cycle du champ D_SLA_QUAL_BIAIS_DERIVE_V_TrI

1552 D_SLA_QUAL_BIAIS_DERIVE_V_TRI : Différence des hauteurs de mer alti/TG validées avec application du contrôle qualité marégraphique et correction du biais et de la dérive (Hémisphère Sud)

Les figures sont rangées dans l'ordre suivant (de gauche à droite et de haut en bas) :
Nombre, Moyenne, Ecart-type, Minimum, Maximum.

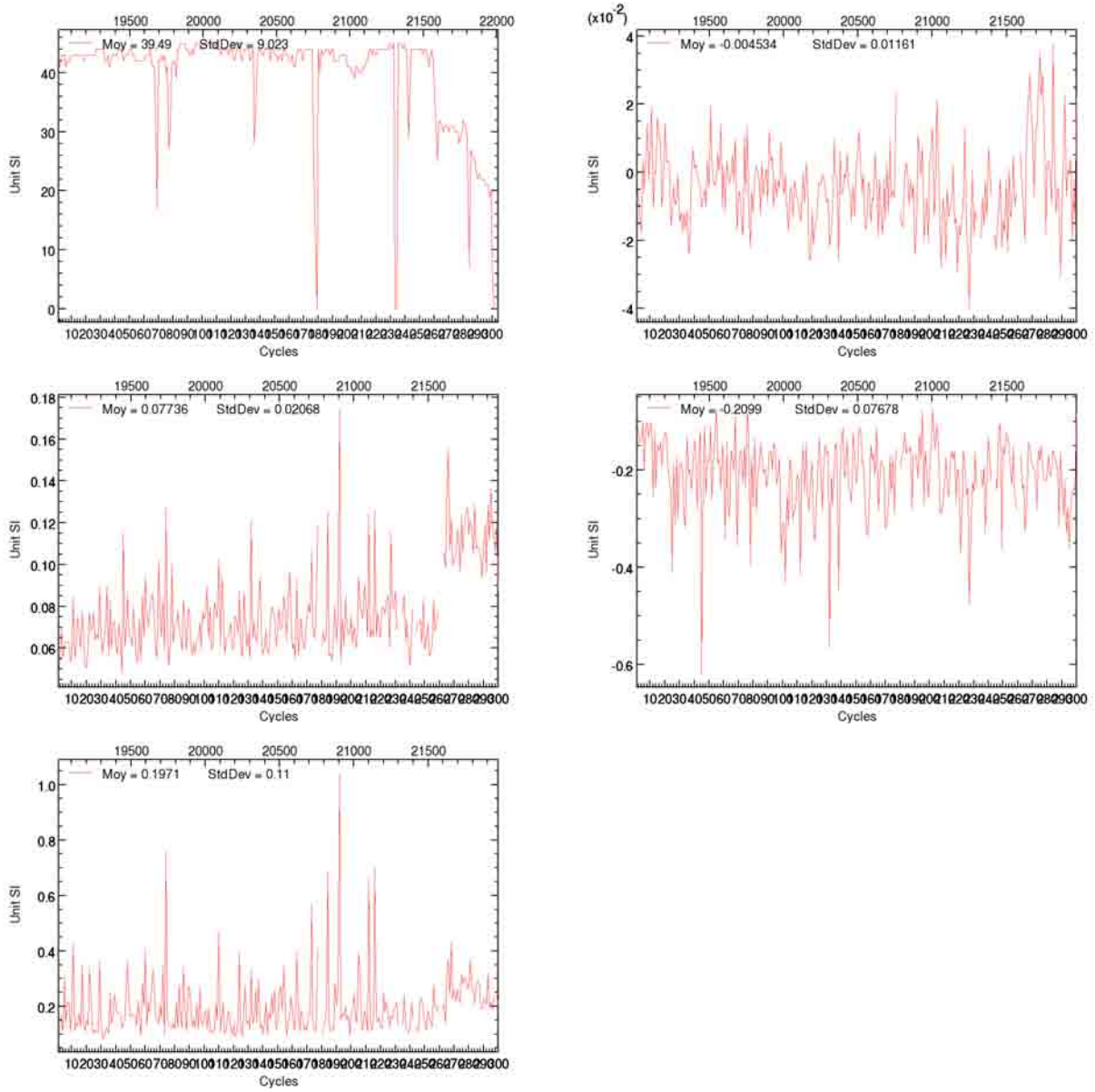

3.7. Suivi de la dérive liée aux mouvements verticaux

3.7.1. Suivi par cycle du champ DERIVE_TG

1095 DERIVE_TG : Corrections des mouvements verticaux (effets atmosphériques, surcharges hydrologiques, mouvements crustaux ...)

Les figures sont rangées dans l'ordre suivant (de gauche à droite et de haut en bas) :
Moyenne.

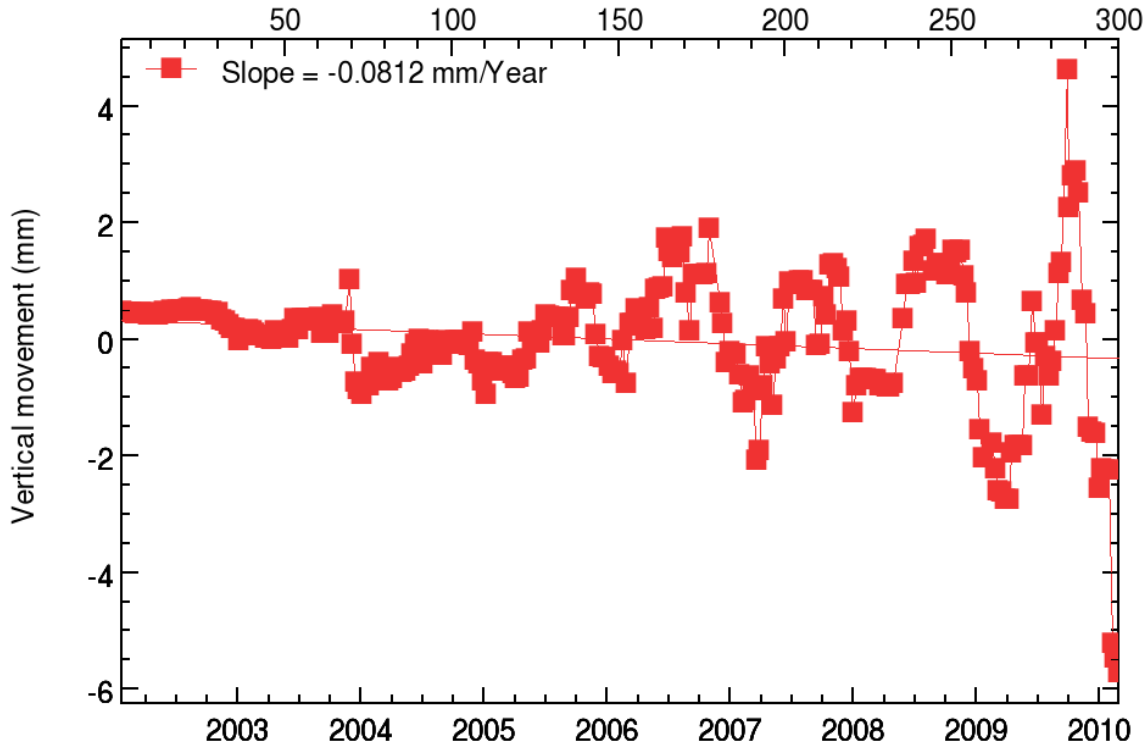

3.8. Suivi de la différence de SLA satellite et marégraphique avec application du contrôle qualité marégraphique et correction du biais entre les marégraphes et sans la dérive crustale (après filtrage et ajustement)

3.8.1. Suivi par cycle du champ SMOY_D_SLA_QUAL_BIAIS_VAL_F

11110 SMOY_D_SLA_QUAL_BIAIS_VAL_F : Moyenne : Différence des hauteurs de mer validées et filtrées, altimétrique et marégraphique, avec application du contrôle qualité marégraphique et correction du biais

Les figures sont rangées dans l'ordre suivant :
Moyenne.

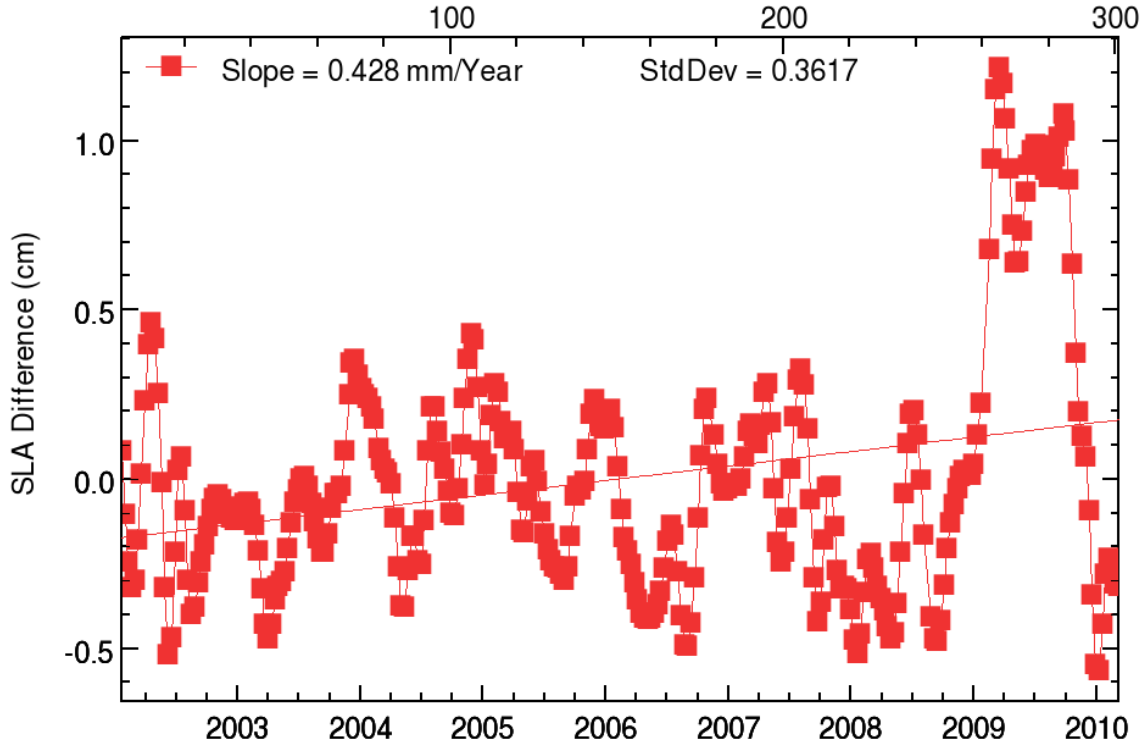

3.9. Suivi de la différence de SLA satellite et marégraphique avec application du contrôle qualité marégraphique et correction du biais entre les marégraphes et de la dérive crustale (après filtrage et ajustement)

3.9.1. Suivi par cycle du champ SMOY_D_SLA_QUAL_BIAIS_DERIVE_VAL_F

11111 SMOY_D_SLA_QUAL_BIAIS_DERIVE_VAL_F : Moyenne : Différence des hauteurs de mer validées et filtrées, altimétrique et marégraphique, avec application du contrôle qualité marégraphique et correction du biais et de la dérive
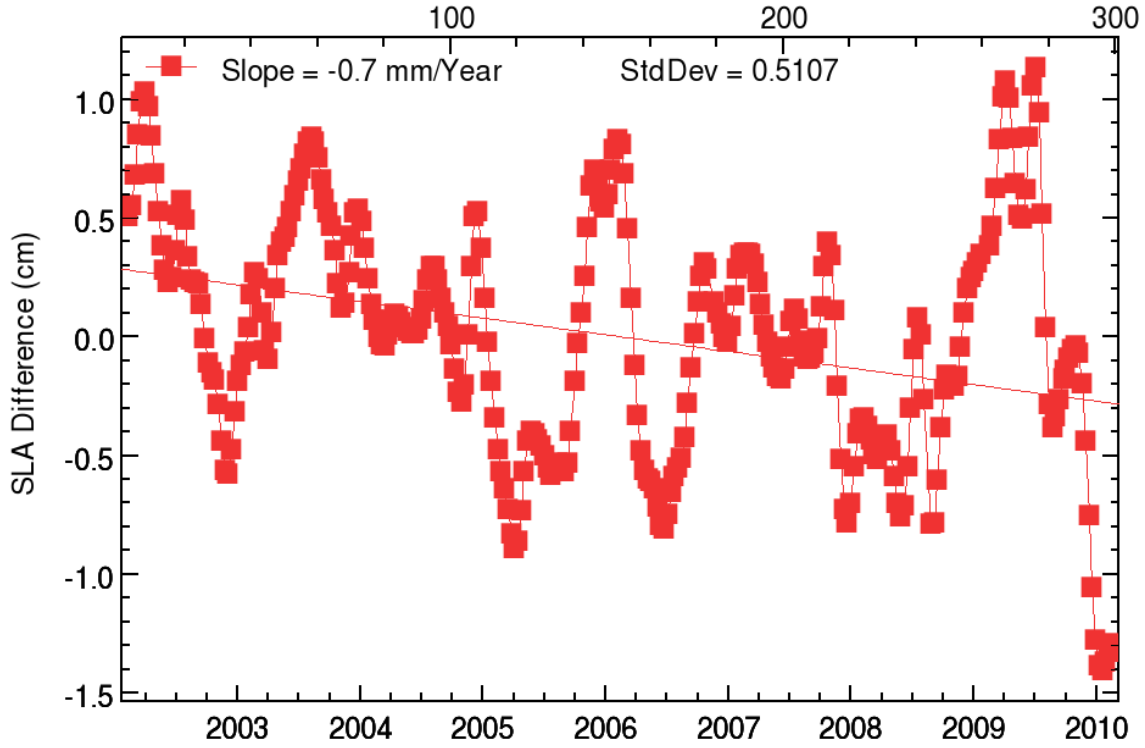
Les figures sont rangées dans l'ordre suivant :
Moyenne.